PhD Thesis

STUDY OF THE PATHOPHYSIOLOGICAL ROLE OF NITRIC OXIDE ON THE AMYLOID-INDUCED TOXICITY ATTENDING TO THE BIOCHEMICAL MODIFICATIONS AND CELLULAR DAMAGES

FRANCESC XAVIER GUIX RÀFOLS

Barcelona, 2008

MEMÒRIA PRESENTADA PER OPTAR AL GRAU DE
DOCTOR PER LA UNIVERSITAT POMPEU FABRA

Programa de doctorat en Ciències de la Salut i de la Vida

Facultat de Ciències de la Salut i de la Vida
Departament de Ciències Experimentals i de la Salut
Grup de Canalopaties i Fisiologia Molecular

FRANCESC XAVIER GUIX RÀFOLS

L'interessat,

Francesc Xavier Guix Ràfols

DIRECTORS
Francisco José Muñoz López
Miguel Ángel Valverde de Castro

Barcelona, 2008

Dr. Francisco José Muñoz López, Professor Lector de la Universitat Pompeu Fabra i Dr. Miguel Angel Valverde de Castro, Catedràtic de la Universitat Pompeu Fabra,

CERTIFIQUEN:

Que la següent Tesi Doctoral titulada “study of the pathophysiological role of nitric oxide on the amyloid-induced toxicity attending to the biochemical modifications and cellular damages”, presentada per Francesc Xavier Guix Ràfols, Llicenciat en Biologia per la Universitat Pompeu Fabra, ha estat realitzada sota la seva direcció i reuneix tots els requisits necessaris per ser jutjada, autoritzant la seva presentació per optar al grau de Doctor per la Universitat Pompeu Fabra.

Francisco José Muñoz López Miguel Angel Valverde de Castro

Barcelona, 28 de Novembre de 2008

Als meus pares, Gabriel i Natàlia,

i a la meva germana Natàlia

Voldria agrair de forma molt breu però de tot cor a tota la gent que, d'una forma o una altra, m'ha donat el seu suport durant aquests últims anys, en moments bons i no tan bons. Molt especialment a en Paco i a en Miguel per la seva ajuda i recolzament constant, sense els quals m'hagués estat ben difícil tirar endavant.

També m'agradaria donar un càlid agraïment a tota la gent del laboratori, tant als presents com a aquells qui hi han passat, perquè més que companys de feina han estat i són autèntics amics, i per la paciència que moltes vagades han hagut de mostrar envers a mi. Aquestes línies d'agraïment també van dirigides a tots els meus amics i amigues de Poblenou i de les Pobles, que d'una forma o altra sempre estan presents.

Per acabar voldria donar les gràcies molt especialment als meus pares i a la meva germana, així com als meus cosins, oncles, i a tota la meva família, sense els quals jo avui no estaria escrivint aquestes línies.

A tots i a totes, moltes gràcies!

Index

Abbreviations

Aβ	Amyloid-β-peptide
AcCoA	Acetyl coenzyme A
ACh	Acetylcholine
AD	Alzheimer's disease
ADAMs	A desintegrin and metalloproteases
AGEs	Advanced glycation end products
ALS	Amyotrophic lateral sclerosis
APH-1	Anterior pharynx defective 1
Apo E	Apolipoprotein-E
APP	Amyloid precursor protein
BACE1	β-site APP clearing enzyme 1
CAA	Cerebral amyloid angiopathy
CDC2	Cell division cycle 2
CDK5	Cyclin-dependent kinase 5
CNS	Central nervous system
CSF	Cerebrospinal fluid
DHAP	Dihydroxyacetone phosphate
ER	Endoplasmic reticulum
eNOS	Endothelial NOS
FAD	Familiar AD
GAP	Glyceraldehyde 3-phosphate
GS	Glutamina synthase
GSK-3β	Glycogen synthase kinase 3β
HoloPS	Holoprotein PS

InsP3R	Inositol 1,4,5-trisphosphate receptor
IRP-1	Iron regulatory protein-1
JNK	c-Jun N-terminal kinase
KO	Knock out
LRP	Low-density-lipoprotein receptor-related protein-1
MAP	Microtubule-associated protein
MAPKs	Mitogen-activated protein kinases
MnSOD	Manganese SOD
MtHSP75	Mitochondrial heat shock protein 75
NCT	Nicastrin
NF-κβ	Nuclear factor-κβ
NFT	Neurofibrillary tangles
NMDA	N-methyl-D-aspartate
NO	Nitric oxide
nNOS	Neuronal NOS
PDZ	Post-synaptic density-95/Dlg/ZO-1
PEN-2	Presenilin enhancer-2
PHF	Pair helical filaments
PKC	Protein kinase C
PS	Presenilin
PS1-CTF	C-terminal fragment of presenilin 1
PS1-NTF	N-terminal fragment of presenilin 1
RAGE	Receptor for advanced glycation end products
ROS	Reactive oxygen species
SOD	Superoxide dismutase

SSAO	Semicarbazide-sensitive amine oxidase
TBI	Traumatic brain injury
TCP1	T-complex protein 1
TPI	Triosephosphate isomerase
TRPM	Transient receptor potential ion channels – melastatin

Molecular formula

H_2O_2	Hydrogen peroxide
O_2	Oxygen
$O_2^{\cdot -}$	Superoxide anion
$OH^{\cdot}$	Hydroxyl radical
$ONOO^-$	Peroxynitrite
ONOOH	Peroxynitrous acid
$ONOOCO_2^-$	Nitrosoperoxycarbonate
$^{\cdot}NO_2$	Nitrogen dioxide
NO	Nitric oxide

Preface

This thesis demonstrates that amyloid ß-peptide (Aß)-induced peroxynitrite contributes to the switch of the $A\beta_{42}/A\beta_{40}$ ratio that occurs in Alzheimer's disease (AD). Since $A\beta_{42}$ is more toxic due to its higher aggregation and stability, it contributes to the trigger of the disease. In addition the aggregation of $A\beta_{42}$ in form of the highly toxic oligomers is incremented by the presence of peroxynitrite. Moreover, these nitro-$A\beta_{42}$ oligomers are more toxic than those non-nitrated. All these results support the important role of peroxynitrite in AD etiology.

Furthermore, since the identification of Aß accumulation and the subsequent formation of neurofibrillary tangles (NFT) as the two defining pathological hallmarks of AD, a fair amount of research on AD has been driven by the need to find the molecular mechanism linking Aß and NFT. This thesis shows the Aß-induced peroxynitrite, and the consequent nitrotyrosination of proteins, promotes *tau* fibrillization. Thus triosephosphate isomerase (TPI) nitrotyrosination could be the link between Aß-induced toxicity and *tau* pathology. Therefore, TPI nitrotyrosination may explain the temporal progression from Aß toxicity to NFT formation in AD brain. The work presented in this thesis could open a novel angle in the research of the pathophysiology of AD and could also have an impact to the research in other neurodegenerative diseases involving oxidative stress and protein misfolding.

I. INTRODUCTION

1. INTRODUCTION TO ALZHEIMER'S DISEASE

After Auguste D's death on 1906, Alois Alzheimer examined her brain and described it as "consistently atrophic" being the first reported case of Alzheimer's disease (AD) (Alzheimer A., 1906). Silver preparations revealed "peculiar changes of the neurofibrils, clustering together in thick bundles". Moreover, he also found several "miliary foci, distinguishable by the deposit in the cerebral cortex of a peculiar substance". To date, we still use these two pathological changes to make the proper diagnoses for AD. At the present, they are named senile plaques and neurofibrillary tangles (NFT), and represent the two pathological hallmarks of the disease (Figure 1). Nowadays, AD is the most common form of human dementia, affecting around 20 million people worldwide (Antony Bayer and Jan Reban, 2004). Initially, short-term memory and learning are the major affected skills both related with the neuronal damage in the hippocampal formation (Antony Bayer and Jan Reban, 2004;Gluck et al., 2006). In advanced stages of the disease, speech and comprehension are strongly impaired due to severe dysfunction of the prefrontal cortex when the dementia is appearing (Antony Bayer and Jan Reban, 2004). The symptoms progressively worsen over 5 to 10 years (Antony Bayer and Jan Reban, 2004).

Depending on the onset time of the symptoms, we can classify AD into two different types: Familiar AD (FAD) and sporadic AD. FAD accounts for less than 3% of all the AD cases, and it is an early-onset form of the disease, appearing before the age of 65 years old (Vetrivel et al., 2006). It is caused by mutations in the genes of the amyloid precursor protein (APP) or presenilins (PS) (Levy-Lahad et al., 1995;Rogaev et al.,

1995;Sherrington et al., 1995;Bayer et al., 1999). Nevertheless, the most common form of the disease is the sporadic AD, which accounts for more than 97% of all the AD cases. It is a late-onset form of AD, appearing after the age of 65 years old (Lambert and Amouyel, 2007;Bertram and Tanzi, 2004). The ultimate cause of sporadic AD remains unknown, though there are few confirmed polimorphisms which increase the probability to develop AD, mainly the APOE4 allele (Sando et al., 2008;Bird, 2008;Li and Grupe, 2007).

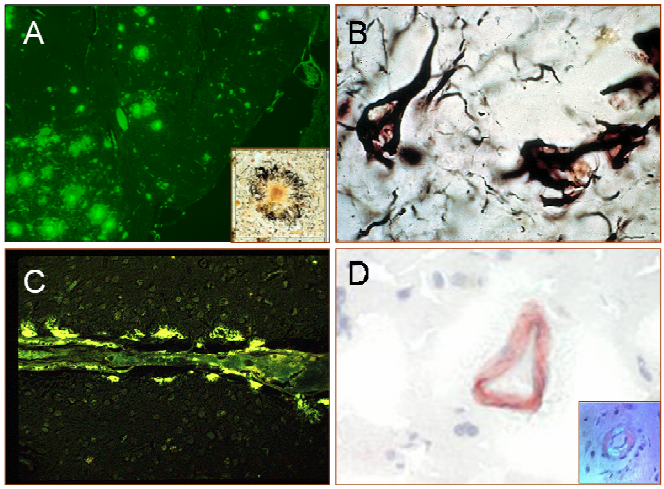

Figure 1. The pathological hallmarks of AD. (A) Aß deposits in the brain parenchyma of 3xTg mice overexpressing APP. The inset shows a core of senile plaque surrounded by dystrophic neurites with NFT. **(B)** NFTs in the brain parenchyma. (**C, D**) Aß deposits in cerebral blood vessels are visulaized with (**C**) thioflavine T staining and (**D**) Congo red dye (inset visualized under polarized light)**.**

2. THE AMYLOID PRODUCTION

2.1. The amyloid precursor protein

Senile plaques and brain vascular amyloid deposits are mainly composed of amyloid β-peptide (Aβ) (Zhang, 2004). Aβ is produced from the proteolysis of a type I transmembrane glycoprotein called Amyloid Precursor Protein (APP). APP is expressed in many tissues (Figure 2), but the strongest expression is found in the brain and the kidney. Its function has been related with adhesion to matrix and interactions cell-to-cell interactions (Del Toro D et al., 2005).

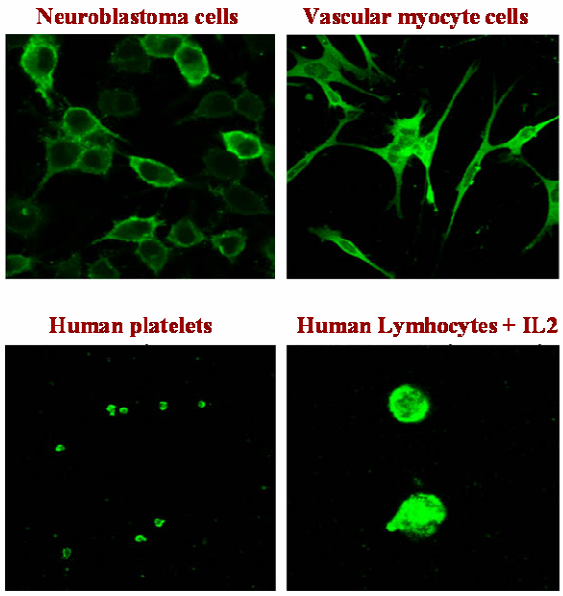

Figure 2. APP is expressed ubiquitously in many tissues constitutively such as in the case of neuroblastoma, myocytes and platelets, and also in an inducible way such as in lymphocytes.

APP can be found in many isoforms that differ in the length. Thus, in the brain the most common isoforms are APP_{695} and APP_{714}, while in other locations APP_{770} and APP_{751} are the most commonly found isoforms (Kang and Muller-Hill, 1990). APP contains several independent domains. The extracellular region, much larger than the intracellular region, is divided into the E1 and E2 domains; E1 contains several subdomains including a growth factor-like domain (GFLD), a metal-binding motif, and a serine protease inhibitor. The last domain is absent in the APP isoform expressed in the brain (Sisodia et al., 1993). The E2 domain contains a dimerization motif that may bind proteoglycans in the extracellular matriz (Wang and Ha, 2004). APP undergoes extensive post-translational modifications including glycosylation, phosphorylation and tyrosine sulfation (De and Annaert, 2000).

APP can be processed by a non-amyloidogenic pathway (Figure 3) due to the consecutive cleavage of an α-secretase activity that cut APP at the amino acid 660, refereed to the APP_{770}, followed by the action of γ-secretase that cut APP at the amino acids 711 or 713, refereed to the APP_{770} (Del Toro D et al., 2005). As a result of the non-amyloidogenic pathway, a non-pathological p3 peptide (≈ 3 kDa) is released.

The non-amyloidogenic pathway is predominant in peripheral cells and also in neurons. However, the proportion of APP cleaved by the amyloidogenic pathway increases with age and under pathological conditions such as AD (Basha et al., 2005;Wu et al., 2008;Zhang, 2004). In the pathological amyloidogenic pathway (Figure 3), APP suffers two consecutive cleavages by the β-secretase and the γ-secretase. Thus β-secretase activity cut APP at the amino acid 672 refereed to the APP_{770} followed by the action of γ-secretase that cut APP at the amino acids 711 or 713, refereed to the APP_{770} (Del Toro D et al., 2005). The final product is the Aβ, mostly with 40 aa ($A\beta_{40}$). Species with 42 aa ($A\beta_{42}$) are released but at low rate. Shorter and larger forms (38, 39

and 43 aa) are also produced but their contribution to senile plaques or aggregative processes is considered very low (Tabaton and Gambetti, 2006). All the above suggests that a dysregulation in the APP processing occurs early in the disease process, resulting in increasing production of $A\beta_{42}$ peptide and the aggregation of the whole amyloid in brain to form senile plaques.

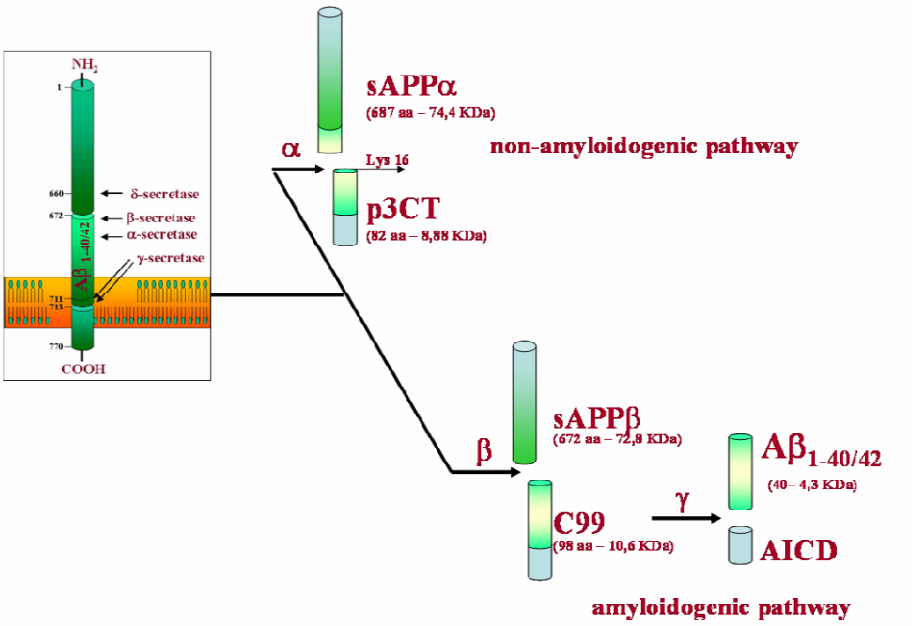

Figure 3. APP processing cleavage. The non amylodiogenic pathway is performed by the α-secretase producing sAPPα and C83. C83 can be proteolysed by γ-secretase to render the p3 peptide. The amyloidogenic pathway is carried out by ß-secretase which produces sAPPß and C99. C99 is proteolysed by the γ-secretase to render Aß.

2.2. The Aβ-peptide

The Aβ-peptide is the major component of senile plaques in AD**.** There is considerable evidence that the size, structural features, and morphology of the aggregated species are the key determinants of toxicity (Ward et al., 2000). Numerous efforts have been directed to identify the aggregate forms of the peptide that are the most neurotoxic.

It has been reported that intermediates of the aggregation pathway, rather than the mature Aβ fibrils, are the most toxic forms (Figure 4). In fact, a recent article is showing that dimmers isolated from AD brains are inducing neurodegeneration by their toxic effect on synapses affecting mainly to learning and memory (Shankar et al., 2008). As in several degenerative diseases concur with the formation of oligomeric structures, this means that they must share a common pathogenic mechanism, probably due to the oligomeric structure itself. Amyloid oligomers display a common structural motif that is distinct from fibrils based on the observation that a conformation dependent antibody specifically recognizes a common epitope on amyloid oligomers, but not fibrils, monomers or natively folded proteins for many different types of proteins (Kayed et al., 2003). Aβ oligomers appears as small spherical aggregates of approximately 5 nm in diameter with molar masses of 25-50 kDa (Lambert et al., 1998), as well as large spherical oligomers with diameters around 15 nm and molar masses approaching 1 million Da (Huang et al., 2000). These spherical oligomers appear to represent intermediates in the pathway of fibril formation (Figure 4). The mechanisms to induce cell damage by oligomers are the same than those used by mature fibrils: reactive oxygen species (ROS) production (Schubert et al., 1995), altered signalling pathways (Mattson, 1995) and mitochondrial dysfunction (Shoffner, 1997).

Protofibrills (Figure 4) are formed at longer aggregation times, which are linear (as opposed to globular) aggregates that appear early in the amyloid pathway, probably by coalescence of the spherical subunits (Harper et al., 1997). Protofibrils may share structural epitopes with oligomers, and may be highly toxic (Kayed et al., 2003). Aβ protofibrils detected by atomic force microscopy are 4 nm in height, with a periodicity of about 20 nm, and lengths of 20 nm to 200 nm or longer (Harper et al., 1999), whereas Aβ protofibrils imaged by TEM are described as "curvilinear structures of 4–11 nm diameter and < 200 nm length (Hartley et al., 1999).

Aβ can also give bigger aggregates called protofilaments and filaments. They are linear aggregates that can reach 100 nm (Serpell et al., 2000). Their structural characteristics are closer to those of fully mature fibrils.

Fibrils appear at later stages of the aggregative process (Figure 4). Amyloid fibrils have a "cross-β" structure, which indicates that the backbone hydrogen bonding is parallel to the fibril axis (Eanes and Glenner, 1968;Kirschner et al., 1986;Kirschner et al., 1987). They are typically 7-12 nm in diameter and can reach 1 μm or more in length. Amyloids also bind characteristic dyes, like Congo red and thioflavin dyes, which may be a reflection of their common cross-β structure (LeVine, III, 1993). Spectroscopic structural analysis of several different amyloids indicates that the polypeptide is commonly arranged as parallel-β strands (Torok et al., 2002). The notion of structural polymorphism has surfaced recently, as it becomes clear that there may be multiple alternative fibril morphologies (e.g., twisted or not, branched, even circular) (Paravastu et al., 2006;Petkova et al., 2005). Fibrils tend to associate further into bundles (Ward et al., 2000). Mature fibrils are the insoluble end product of amyloidogenesis.

Finally, the primary sequence of the protein determines its tendency to aggregate. The hydrophobicity in the primary sequence of the peptide is a key feature in its

tendency to fibrillate (Soto et al., 1994). For example, the Aβ synthetic mutant with the V18A mutation does not aggregate (Muñoz and Inestrosa, 1999), whereas the familiar Dutch mutation (E22Q) (Levy et al., 1990) increases the formation of fibrils. In addition it is known that the Aβ from mice, which has a different sequence from human, does not aggregate (De et al., 1995). But when rodent hippocampal neurons overexpress the mutated forms of the human APP665, they show senile plaques (De et al., 1995). On the other hand the Aβ from *Octodon degu*, which share 97.5% homology with the human Aβ, aggregates and triggers a AD pathology in wild type aged *Octodon degu* (Inestrosa et al., 2005).

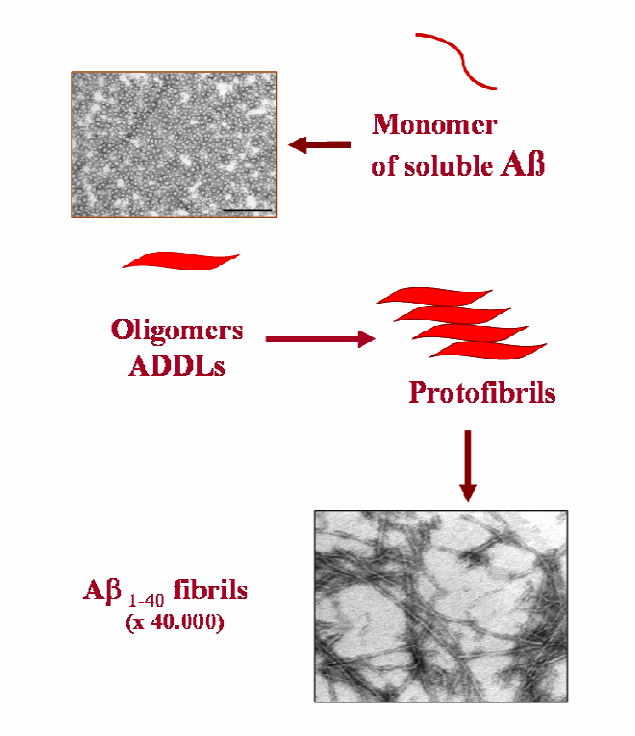

Figure 4. Aβ aggregation states. Aβ oligomers appears as small spherical aggregates. Protofibrills are formed at longer aggregation times, which are linear (as opposed to globular) aggregates that appear early in the amyloid pathway probably by coalescence of the spherical subunits. Fibrils are at the later state of the aggregative process.

2.3. The α-secretase activity

Although the major APP proteolytic pathway is the non-amyloidogenic pathway, the identity of the α-secretase has remained controversial (Sisodia, 1992). The emerging view is that there is a group of metalloproteases capable of cleaving APP at the α-secretase site. The main candidates are three members of the adamalysin or ADAMs family proteins, ADAM9/meltrin γ (Koike et al., 1999), ADAM 10 (Lammich et al., 1999) and ADAM17, also called TACE (TNF-α converting enzyme) due to its first identification for the shedding of proTNF-α (Buxbaum et al., 1998;Slack et al., 2001). Probably the three members contribute to a greater or less extent to the α-secretase cleavage of APP, due to the fact that cell cultures from either Knock Out (KO) mice for ADAM9, ADAM10 and ADAM17 still show α-secretase activity (Hartmann et al., 2002;Weskamp et al., 2002). But ADAM 10 is the most widely expressed in neurons and seems to be the most active alpha secretase (Del Toro et al., 2005).

ADAMs are members of type I integral proteins with common characteristic domains. It has an N-terminal signal peptide followed by a prodomain and the catalytic domain in which some ADAMs have a consensus HEXXH zinc-binding motif (X represents any amino acid) which is involved in the proteolytic activity. This prodomain contains an odd cysteine, which inhibits the catalytic site of the enzyme by its interaction with zinc. The predomain is removed intracellularly during transport to the cell surface by furin-type pro-protein concertase being a prerequisite for the protease activity (Peiretti et al., 2003). In addition it has a cysteine-rich, desintegrin-/EGF-like domain involved in cell adhesion, a transmembrane domain and a short cytoplasmic domain (Allinson et al., 2003). The role of the α-helical conformation and the distance (12-13 residues) of the hydrolyzed bond from the membrane are two main determinants for the non-amyloidogenic cleavage (Sisodia, 1992;Sahasrabudhe et al., 1992).

ADAMs are widely expressed and play a role in diverse biological processes such as control of growth factors, cytokines shedding, membrane fusion, cell migration, fertilization, myogenesis and neurogenesis (Primakoff and Myles, 2000;Kojro and Fahrenholz, 2005).

2.4. The β-secretase activity

β-secretase is the first activity to cleavage APP in the amyloidogenic pathway. An aspartyl protease called β–site APP cleaving enzyme type I (BACE1) is the β-secretase (Vassar et al., 1999). BACE1 is a type I integral membrane protein highly expressed in the brain (Tamagno et al., 2002;Vassar et al., 1999). It is synthesized as a proprotein called pro-BACE1, which contains a 24-amino-acid prodomain necessary for the proper folding in the Endoplasmic Reticulum (ER) and its posterior trafficking (Shi et al., 2001). The activity of BACE1 depends on the previously cleavage of the prodomain by members of the furin family of convertases at the trans-Golgi network and the number of these glygosylations (Charlwood et al., 2001).

BACE1 gene expression is strongly regulated and the maximal activity is seen in the central nervous system (CNS) (Sinha et al., 1999;Knops et al., 1995;Sambamurti et al., 2004). Oxidative stress has been reported to increase the transcription of BACE1 (Tong et al., 2005). AD patients show an increased of the β-secretase activity in the cerebral cortex (Evin et al., 2003). The Swedish mutation, consisting of Lys to Asn and Met to Leu amino acid substitutions at codons 670 and 671 of the APP transcript, has an enhanced β-secretase activity associated (Mullan et al., 1992). Curiously there are not mutations in BACE1 associated with AD. However, PS1 is directly involved in the maturation of BACE1, thus regulating the β-secretase activity (Kuzuya et al., 2007) and PS1 mutations trigger FAD. Recently oxidative stress has been proposed as a molecular

mechanisms linking γ-secretase to β-secretase activity (Tabaton and Tamagno, 2007). This hypothesis comes from the fact that PS1 mutations increase the production of Aβ, which enhances the oxidative stress. Then oxidative stress would increment the β-secretase activity.

2.5. The γ-secretase activity

γ–secretase is a high molecular complex composed of PS1 or PS2, nicastrin (Nct), anterior pharynx-defective phenotype 1 (Aph1) and PS enhancer 2 (Pen2) (Sato et al., 2007) (Figure 5). The catalytic activity of the complex resides on PS, a protein with 9 transmembrane domains, since PS1 and PS2 knock-out (KO) mice do not have Aβ production (De et al., 1998). Moreover, more than 150 mutations in PS1 and 10 mutations in PS2 have been associated with AD (Wakabayashi and De, 2008). Mutation of two conserved intramembranous aspartate residues (Asp-257 and Asp-385) of PS1 abolishes the γ–secretase activity supporting the hypothesis that they constitute the catalytic site of the enzyme (Wolfe et al., 1999).

To be fully functional, the components that form the γ–secretase complex must assembly in the ER (Kim et al., 2004;Capell et al., 2005), and then can be transported to the plasma membrane. After the assembly of all the components, PS1 undergoes an endocatalytical cleavage within a loop encoded by exon 9 of the corresponding gene (Knappenberger et al., 2004), releasing a C-terminal fragment (CTF-PS1) and an N-terminal fragment (NTF-PS1) (Hebert et al., 2003). Both of them must heterodimerize to confer the catalytic properties to the complex (Hebert et al., 2003).

The substrate for γ–secretase is the C-terminal fragment of APP resulted from the β-secretase activity. As a result of the γ–secretase cleavage, different Aβ types are rendered, but mostly $A\beta_{40}$ and $A\beta_{42}$, both species involved in AD (Iijima et al.,

2004;Levites et al., 2006;Kawarabayashi et al., 2001). $A\beta_{40}$ contains 40 aminoacids and it is the highest species produced and the major component of the senile plaques (Sinha and Lieberburg, 1999). However, sometimes the gamma-secretase complex cuts two aminoacids more at the carboxyl terminus of APP giving rise to $A\beta_{42}$, a longer and more toxic form of Aβ. The higher toxicity of the $A\beta_{42}$ peptide resides on its major tendency to fibrillate, forming the core of the senile plaques and facilitating the posterior deposition of $A\beta_{40}$ around this initial "seed"(Dolev and Michaelson, 2006). Although the γ–secretase complex produces normally $A\beta_{40}$, the production of $A\beta_{42}$ can increase under some pathological conditions like in AD (Gorman et al., 2008;Kumar-Singh et al., 2006;Lewczuk et al., 2004;Zhuo et al., 2008) or by some mutations in PS1 (Kauwe et al., 2008;Findeis, 2007;Czech et al., 2000). In sporadic AD, the mechanism ruling this switch in the $A\beta_{42}$ production is unknown. Although oxidative stress has been already involved in the increase of γ–secretase activity found in AD (Tabaton and Tamagno, 2007), to date there is no experimental data on the biochemical mechanisms linking the oxidative stress with the increase in $A\beta_{42}/A\beta_{40}$ ratio. Nonetheless, there are some evidences pointing out to oxidative stress as a causal factor. These evidences come from pathological processes that course with inflammatory processes and high levels of radical oxygen species (ROS) production. It is the case of Traumatic Brain Injury (TBI) (DeKosky et al., 2007;ng-Bryant et al., 2008;Singh et al., 2006) or *in vitro* H_2O_2 treatments (Coma et al., 2008). In both cases high levels of $A\beta_{42}$ has been reported (DeKosky et al., 2007;Coma et al., 2008).

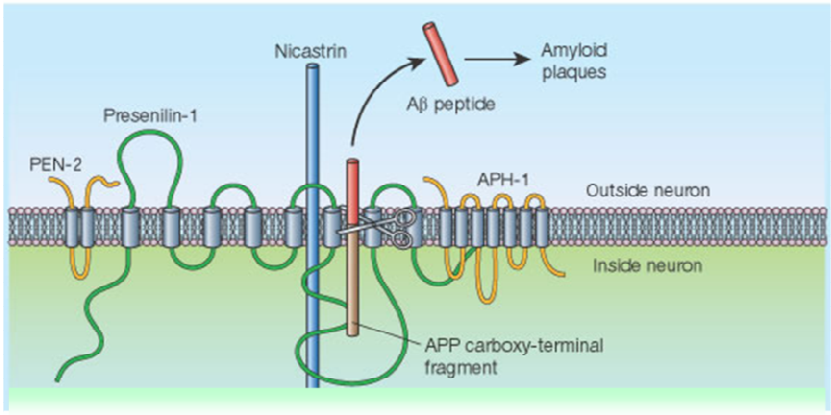

Figure 5. The γ–secretase complex. γ–secretase is a high molecular complex composed of PS1 or PS2, nicastrin (Nct), anterior pharynx-defective phenotype 1 (Aph1) and PS enhancer 2 (Pen2). The catalytic activity of the complex resides on PS, a protein with 9 transmembrane domains (taken from De strooper and Woodget, 2003).

2.6. The NFT

Together with senile plaques, NFT are one of the main hallmarks of AD. NFT are intraneuronal fibrillar deposits composed mainly by a microtubule-associated protein called tau (Ding and Johnson, 2008). Tau belongs to the emerging class of natively unfolded proteins containing a low content of hydrophobic aminoacids. Tau is expressed in the nervous system and localized mostly in the axons of neurons and their cytosol (Drubin and Kirschner, 1986). In the human CNS there are 6 different isoforms generated by alternative splicing of exons 2, 3 and 10 (Goedert et al., 1989b;Goedert et al., 1989a). In the foetal brain, the smallest isoform ht23 lacking exons 2, 3 and 10, is the predominat one, whereas in adult brain all isoforms can be found in roughly equal amounts. Tau contains four tau/MAP repeat sequences, which bind to microtubules (Eliezer et al., 2005). Depending on number of repeats into the tau/MAP domain, we can classify tau isoforms into type I, which only have 3 repeats in the tau/MAP domain,

or type II, containing 4 repeats (Goedert et al., 1989b). The difference between type I and II is the presence or absence of exon 10 (Goedert et al., 1989b).

The function of tau seems to be involved in the assembly and stability of microtubules, allowing in this way the establishment and the maintenance of neuronal polarity (Eliezer et al., 2005). While the C-terminus binds axonal microtubules, the N-terminus binds neural plasma membrane components, suggesting that tau functions as a linker protein between both (Eliezer et al., 2005). The short isoforms allow plasticity of the cytoskeleton whereas the longer isoforms may preferentially play a role in its stabilization (Eliezer et al., 2005). The protein has been reported to be phosphorylated at serine and threonine by proline-directed protein kinases CDC2, CDK5, GSK-3β and MAPK (Imahori and Uchida, 1997;Liu et al., 2004;Pei et al., 2002;Puig et al., 2004;Hanger et al., 2007). The phosphorylation occurs only at 2-3 sites during interphase and seems to weaken the interaction between tau and microtubules or plasma membrane components when it is found within the repeated domain or flanking regions (Preuss et al., 1995). In AD the neural cytoskeleton is progressively disrupted and replaced by tangles of β-sheet rich paired helical filaments (PHF), which are regular and stable structures formed by a pair of twisted filaments composed of tau protein that is hyperphosphorylated (Mandelkow et al., 2007). PHFs are the base for the formation of characteristic neurofibrillary tangles.

2.7. The relationship between Aβ and PHFs

Some authors argue that NFT formation is a key step to develop dementia since intraneuronal NFT correlates with the degree of dementia and memory loss (Goedert and Spillantini, 2006). On the other hand, tau mutations result in fronto-temporal

dementia (Heutink, 2000), since the mutated tau show reduced ability to bind microtubules and high self-aggregation.

In AD, the NFT formation is a consequence of the increased Aβ production. This assessment comes from several observations: i) mutations in tau give rise to tau inclusions but not senile plaques, whereas mutations in APP or presenilin genes give rise to both senile plaques and NFT (Heutink, 2000;Lewis et al., 2001); ii) the double mutant mice for APP and tau protein (overexpressing tau protein and producing more Aβ peptide) present more NFT than the mice with only tau mutated (Mudher and Lovestone, 2002); iii) in a parallel experiment another group showed that injection of amyloid into the cerebrum of tau mutant transgenic mice exacerbated tangle pathology in another brain region from where neurons project the neurites to the injection site (Gotz et al., 2001). Altogether, the previous data strongly suggest that Aβ aggregation is a previous step which triggers NFT formation.

The molecular link between plaques and tangles remains unknown. The process of tau aggregation in the absence of mutations is unknown but might result from increased phosphorylation (Mandelkow et al., 2007), protease action of caspases (Guo et al., 2004;Ramalho et al., 2008) or exposure to polyanions, such as glycosaminoglycans (Sibille et al., 2006). However, tau hyperphosphorylation affects its binding to microtubules instead of triggering its aggregation (Lovestone and Reynolds, 1997). It would help to the aggregative process by providing more free tau. On the other hand, it has been suggested that tau phosphorylation occurs after its aggregation (Mena et al., 1996), or even inhibits filament formation (Schneider et al., 1999). Moreover the concentration used to aggregate tau *in vitro* in all the above conditions was from 1 to 10 μM, clearly over the physiological ranges (Kuret et al., 2005).

3. THE NITRO-OXIDATIVE STRESS IN AD

3.1. The oxidative stress in AD

The neurotoxic properties of Aβ are mainly due to the production of ROS by the Aβ fibrils (Behl et al., 1994), then oxidative stress is the major damaging mechanism in AD (Miranda et al., 2000) (Figure 6). Micromolar concentrations of Aβ peptide increases H_2O_2 in cells in culture (Behl et al., 1994) and catalase, an enzyme that converts H_2O_2 to O_2 and H_2O, blocks Aβ toxicity. Oxidized protein, lipid and nucleic acid are present in AD brains (Miranda et al., 2000). Aβ induces lipoperoxidation of membranes (Koppal et al., 1998;Mark et al., 1999) which will modify all the membrane fluid properties and the movement and activity of the proteins such as receptors or ATPases. Moreover, antioxidants treatment such as vitamine E or trolox have demonstrated neuroprotective effects against Aβ cytotoxicity (Munoz et al., 2002;Coma et al., 2005).

Transition metals have been reported to highly contribute to Aβ induced toxicity (Multhaup et al., 1996). AD brains showed high content in aluminum (Good et al., 1992) and iron (Connor et al., 1992;Richardson, 1993) compared to brains from non demented individuals. In particular, copper, iron and zinc are highly concentrated within the core and periphery of senile plaques (Lovell et al., 1998). In fact, these ions can generate ROS due to Fenton reaction, and Aβ peptide has been shown to produce H_2O_2 through the reduction of iron and copper *in vitro* (Huang et al., 1999). Then transition metals found in senile plaques are considered a source of ROS that increase the oxidative stress observed in AD (Smith et al., 2007).

Another mechanism proposed for Aβ-mediated ROS production is the activation of NMDA receptors by $A\beta_{42}$ oligomers, which increases the calcium influx yielding to the activation of NADPH oxidase (NOX) (Shelat et al., 2008;Brechard and Tschirhart,

2008). It induces excitotoxicity and damages the synaptic plasticity and learning and memory processes (Kishida et al., 2005;Kishida and Klann, 2007). The demonstration of increased NOX activity in AD brain further supports the role of ROS in the progression of the disease (Zekry et al., 2003).

On the other hand, Unzeta M. et al. found an increased expression of the enzyme semicarbazide-sensitive amine oxidase (SSAO) in cerebrovascular tissues of patients with AD coupled with vascular damage (Unzeta et al., 2007). SSAO is a multifunctional enzyme present mainly in adipocytes, endothelial and smooth muscle cells that catalyses the oxidative deamination of primary aromatic and aliphatic amines, producing ammonia, hydrogen peroxide (H_2O_2) and the corresponding aldehyde (Unzeta et al., 2007). Aminoacetone and methylamine are considered the physiological SSAO substrates (Precious et al., 1988;Lyles and Chalmers, 1995), and their oxidation generates methylglioxal and formaldehyde, respectively (Dar et al., 1985). In turn, the products generated by SSAO can yield AGEs and more oxidation of biomolecules. In this way, the overexpression of SSAO can contribute to the oxidative damage in AD.

Moreover, senile plaques are normally surrounded by reactive glia (microglia and astroglia) which are increasing the tissue damage due to its inflammatory and oxidative response (Dickson et al., 1988). These immune reactive cells have several receptors capable of recognizing oxidized proteins, lipoproteins, but also the Aβ (El et al., 1996;Coraci et al., 2002;Laporte et al., 2004). After the activation, they have a respiratory burst due to the action of NOX generating ROS. This activation by Aβ binding has been demonstrated through the receptor for advanced glycation end products (RAGE), the low-density lipoprotein receptor-related protein (LRP) and the scavenger receptor. All of them have been demonstrated to bind Aβ and mediate its

internalization by glial cells (El et al., 1996;Coraci et al., 2002;Laporte et al., 2004;Deane et al., 2008).

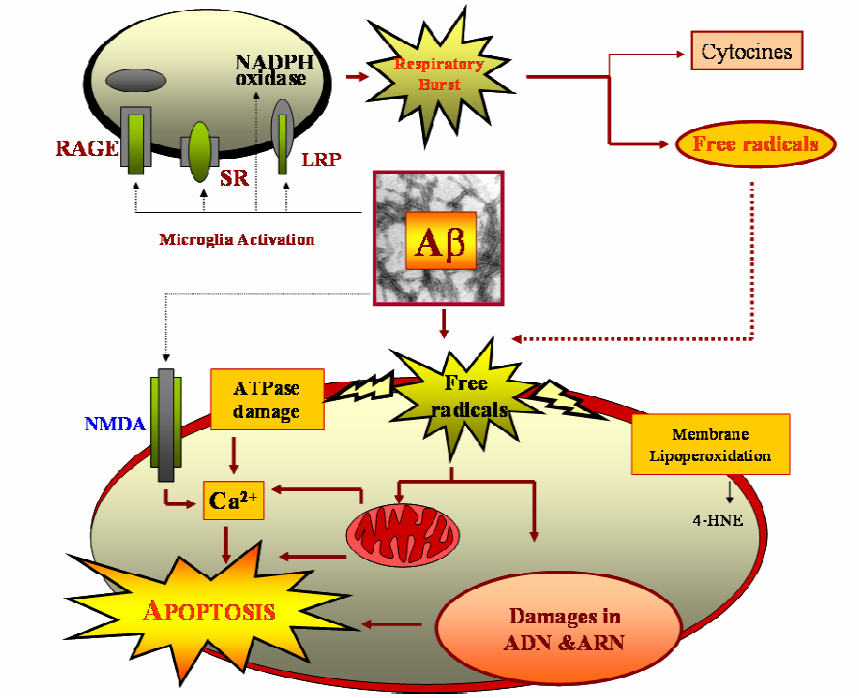

Figure 6. Amyloid fibrils neurotoxicity is mediated by oxidative stress. Aβ fibrils are producing hydrogen peroxide. It induces the membrane lipoperoxidation, which leads to its functional impairment and 4-HNE production. There is also an oxidative damage of the membrane proteins which impairs the ATPases function and consequently the calcium homeostasis is lost. The intracellular increment in the calcium levels would trigger the apoptotic pathway. Moreover, the Aβ has been demonstrated to activate NMDA receptors yielding to glutamatergic-mediated excitotoxicity. The mitochondria damage leads to a dysfunction of the respiratory chain what causes an energetic failure and a calcium efflux from this organelle to the cytosol, contributing to trigger apoptosis. On the other hand, microglia can be activated after the binding of Aβ to several receptors (RAGE, SR or LRP), producing a respiratory burst as a consequence of NOX activation. Activated microglia releases several interleucines and cytokines as well as free radicals that will contribute to the oxidative stress of the neurons in the cerebral parenchyma.

The role of ROS in AD goes further than the neurotoxicity of Aβ fibrils. ROS has been demonstrated to increase the Aβ production due to their action on the Oxidative stress could be behind this increase, since it has been reported to enhance

both the β-secretase activity (Borghi et al., 2006) and Aβ production (Coma et al., 2008;Jo et al., 2008;Borghi et al., 2006).

3.2. Glycation and AD

The amino groups of proteins can be modified by non-enzymatic reactions with monosaccharides, such as the Maillard reaction (the carbonyl group of the sugar reacts with the amino group of the protein giving rise to N-substitute glycosylamine and water) (Figure 7). This initial glycation can subsequently give an Amadori product, which consist of a re-arrangement from the initial Schiff base wherein the hydrogen atom from the hydroxyl group adjacent to the carbon-nitrogen double bond moves to bond to the nitrogen, leaving a ketone (Figure 7). This recently formed Amadori product can then be oxidized, most often by transition metal catalysis, forming the advanced glycation end-products (AGEs) (Munch et al., 1997). The relevance of AGEs formation resides in the fact that, while the first two steps are reversible (Maillard reaction and Amadori products formation), the last step (the oxidation of the Amadori products to AGEs) is irreversible.

One of the most important AGE-inducing compounds is methylglyoxal (MG). MG is a dicarbonyl triose formed as a side-product of several metabolic pathways, the most important of them is glycolysis (Figure 8). In fact, MG is found increased in AD patients (Munch et al., 1997;Takeuchi and Yamagishi, 2008) and could participate in the NFT formation by accelerating the oligomerization of tau (Kuhla et al., 2007). Due to the high toxicity of MG, mammalian cells and most microorganisms possesses a detoxifying system that consists of two GSH-dependent enzymatic activities called glyoxalase I (GLXI) and II (GLXII) respectively (Mannervik, 2008). The glyoxalase system turns MG into D-lactate (Figure 9). In AD, GLXI is found up-regulated,

probably as a compensatory mechanism for the increase of intraneuronal MG accumulation (Kuhla et al., 2007;Kuhla et al., 2005). MG could also be detoxified by other activities such as the NADPH-dependent aldose reductase, the aldehyde dehydrogenase or the 2-oxoaldehyde dehydrogenase (Grillo and Colombatto, 2008). Although there are several hypotheses trying to explain the increase of MG in aged and AD brains, the molecular mechanism behind its synthesis remains poorly understood. It is known that the activity of GLX1 is decreased during the aging process, what might contribute to accumulate MG intracellualary (Thornalley, 2003).

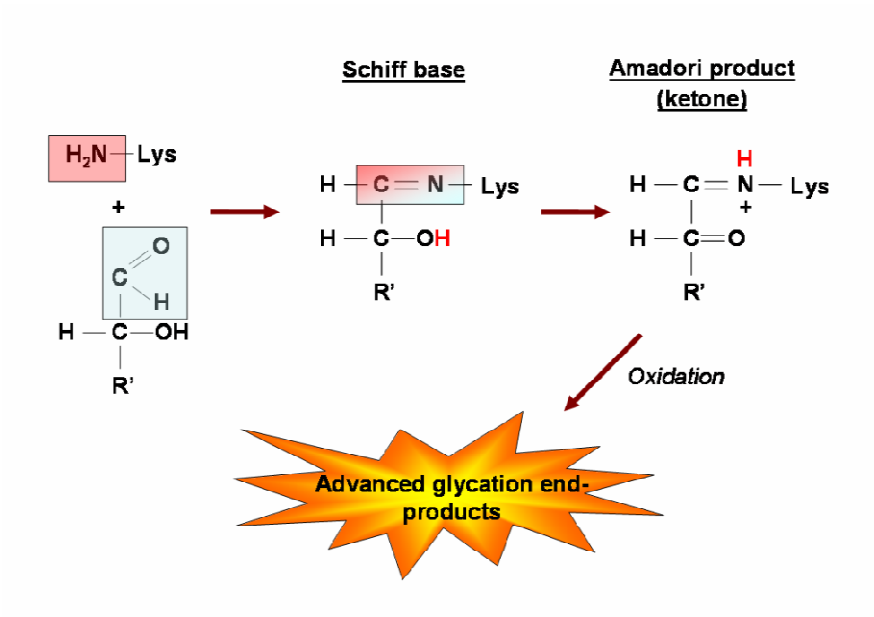

Figure 7. AGEs formation. The carbonyl group of the sugars (i.e. glucose) reacts with the amino group of the protein (i.e. lysine), forming the Schiff base. The ketone is formed after an internal re-arrangement. Finally AGEs appears by the oxidation of the ketone in an irreversible process.

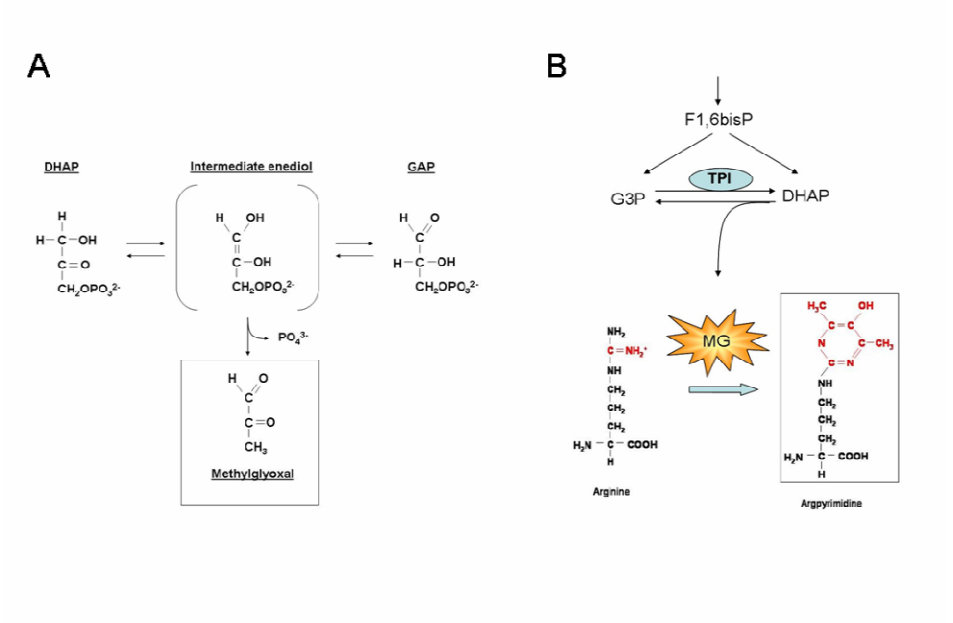

Figure 8. **MG production and effects.** (**A**) MG is a dicarbonyl triose formed in the catalytic centre of TPI as an intermediate of the isomerisation of DHAP and GAP. (**B**) MG released from the catalytic centre of TPI can cause damage to proteins by modifying covalently some amino-acids. MG converts arginines to argpyrimidines.

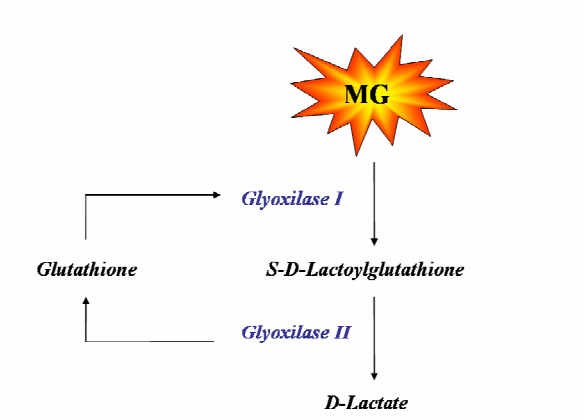

Figure 9. MG detoxification. Mammalian cells and the most microorganisms possess a detoxifying system that consists of two GSH-dependent enzymatic activities called glyoxalase I (GLXI) and II (GLXII) respectively. The glyoxalase system turns MG into D-lactate.

AGE modification of proteins can lead to alterations of normal function by binding to intracellular or extracellular components, or through the binding to different receptors (Gasser and Forbes, 2008). They are also able to modify the quaternary structure of proteins by the induction of cross-linking between proteins (Vasan et al., 2003).

During the normal aging of an individual, AGEs are increasing their activities (Peppa et al., 2008). However in pathological conditions, such as AD, the formation of AGEs is highly incremented (Takeuchi and Yamagishi, 2008). AGE-type modifications and the resulting crosslinking of protein have been demonstrated in both senile plaques and neurofibrillary tangles in AD (Harrington and Colaco, 1994;Munch et al., 1997). Moreover, polymerization of Aβ is accelerated by crosslinking due to AGE action *in vitro* (Munch et al., 1997). This AGE-modified Aβ serves as a "seed" for further aggregation of soluble Aβ peptide (Vitek et al., 1994).

3.3. Nitrative stress

3.3.1. Physiological role of NO in the CNS

NO is a gas produced by a group of enzymes denominated nitric oxide (NO) synthases (NOS). There are four members of the NOS family: neuronal NOS (nNOS), endothelial NOS (eNOS), inducible NOS (iNOS) and mitochondrial NOS (mtNOS). nNOS and eNOS are Ca^{2+}-calmodulin-dependent enzymes constitutively expressed in mammalian cells (Mungrue et al., 2003) that generate increments of NO lasting a few minutes. In contrast, iNOS is Ca^{2+}-calmodulin-independent and its regulation depends on de novo synthesis (Ebadi and Sharma, 2003).

L-Arg is used by NOS to produce NO and citrulline in a process requiring NADPH and O_2 (Figure 10). L-Arg is a semi-essential amino acid since it can be synthesized from glutamate (Wu and Morris, Jr., 1998) or produced by recycling citrulline in the citrulline-NO cycle with argininosuccinate synthetase (AS) and argininosuccinate lyase (AL) (Wiesinger, 2001). The main NO cellular signaling pathway is the guanylate cyclase (GC) activation with the subsequent production of cyclic guanosine-3′,5′-monophosphate (cGMP) (Gold et al., 1990) and protein phosphorylation, but NO also exerts other cellular effects independent of the GC activation.

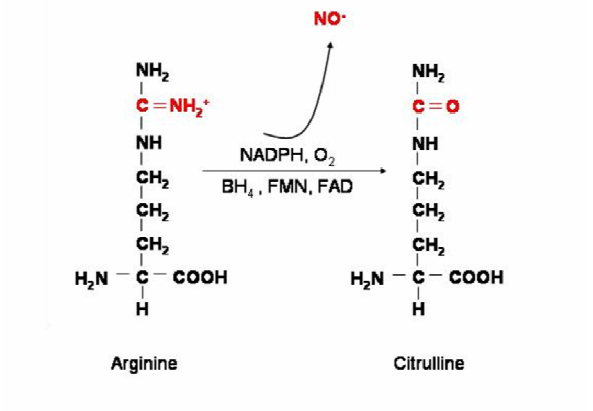

Figure 10. **Synthesis of NO by NOS.** L-Arg in the presence of NADPH and O_2 is oxidized to citrulline producing NO.

The NO produced by the eNOS contained in the endothelial cells acts as a powerful vasorelaxant. Moreover, NO plays an important role as a defence mechanism against pathogens when this is produced by the iNOS expressed in cells of the immune system. NO is also a neurotransmitter and/or neuromodulator in both central and peripheral nervous systems by cGMP-dependent mechanisms (Bredt and Snyder,

1994;Prast and Philippu, 2001;Lewko and Stepinski, 2002;Trabace and Kendrick, 2000). nNOS actions in CNS have been associated with pain perception, especially at the spinal cord level (Yamamoto et al., 1993), and with control of sleep, appetite, thermoregulation (Monti and Jantos, 2004), neural development (Cheng et al., 2003) and synaptic plasticity associated to learning and memory (Dinerman et al., 1994). It plays an important role in the establishment of the Long Term Potentiation (LTP), a mechanism behind the formation of memory that consists of the continuous synaptic activation in some parts of the hippocampus, and started by the NMDA receptors. nNOS is mechanically and functionally coupled to the postsynaptic NMDA receptors via a PDZ domain. Thus, when glutamate is released from the presynaptic terminal, NMDA receptors are activated allowing an influx of calcium. At the same time this cation activates the nNOS enzyme, and in this way, the production of NO. Because of the close proximity of nNOS to NMDA receptors, NO can modify a critical cysteine thiol of this glutamatergic receptor by a chemical reaction called S-nytrosylation. S-nytrosylation exerts a negative effect on NMDA receptors, preventing their excessive activity and consequently avoiding the induced excitotoxicity. However NO also plays an active role in the induction of LTP. In order to maintain the postsynaptic activation, some retrograde communication with the presynaptic component must exist. NO is the retrograde neurotransmitter that activates the glutamate release from the presynaptic component in a cGMP-dependent pathway (Nowicky and Bindman, 1993).

3.3.2. Nitrotyrosination

NO is a molecule with 11 valence electrons, 6 from oxygen and 5 from nitrogen, with an unpaired electron in the last orbital, making NO a free radical (·NO). NO can

also exist as the nitrosonium ion (NO^+) depending on the cellular redox status (Stamler et al., 1992). For this reason it is thermodynamically unstable and tends to react with other molecules.

In a pro-oxidant environment, like in the case of AD, NO is harmful because it reacts with $O_2\cdot^-$ quickly enough to avoid the action of antioxidant systems, forming peroxynitrite anion ($ONOO^-$) (Figure 11) (Beckman et al., 1990). The affinity of $O_2\cdot^-$ is higher for NO than for superoxide dismutase (SOD) (Huie and Padmaja, 1993;Cudd and Fridovich, 1982). The amount of NO and its diffusion coefficient are the limiting factors in the reaction (Saran et al., 1990) due to NOS short half-life of 3–5 s (Ignarro, 1989).

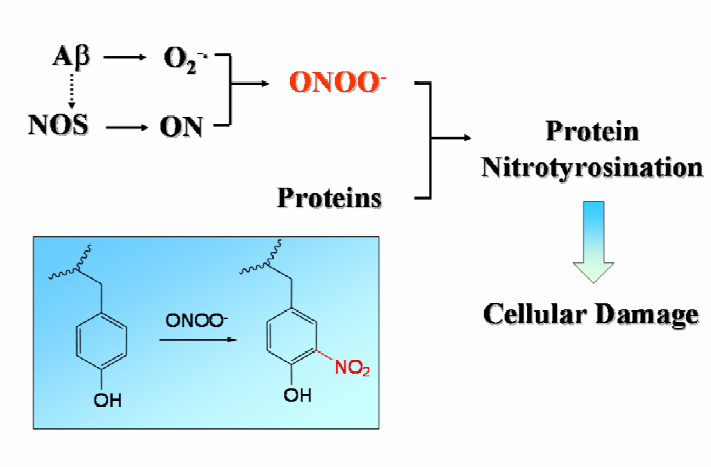

Figure 11. **Protein nitrotyrosination.** Peroxynitrite ($ONOO^-$) formation is due to the reaction of superoxide anion ($O_2^{-\bullet}$) with nitric oxide (NO). Aß fibrils are producing reactive oxygen species (ROS) and at the same time Aß can activate to the different NOSs by increasing intracellular calcium. Nitrotyrosination is produced in biological systems through the binding to protons rendering the reactive nitro group $^{\bullet}NO_2$. The nitro group reacts with tyrosine residues producing nitrotyrosine.

Under physiological conditions $ONOO^-$ has a half-life of 1–2 s and an action radius of 100 μm, being degraded into multiple toxic products (Beckman et al., 1990) or scavenged by the reaction with bicarbonate to produce nitrosoperoxycarbonate

($ONOOCO_2^-$) (Whiteman et al., 2002). $ONOO^-$ reacts with proteins in a non-enzymatic reaction called nitrotyrosination. It consists of the addition of a nitro group (NO_2) to proteins, mainly into tyrosine residues (Tyr) to give 3-nitrotyrosine. The local environment of the Tyr is important in order to be nitrated, since the proximity of negatively charged residues increases the susceptibility to nitration (Souza et al., 1999), but it is not a massive process since the nitration under inflammatory conditions affects 1–5 of every 10,000 Tyr (Brennan et al., 2002). $ONOO^-$ is the main molecules to nitrate proteins (Kanai et al., 2001;Ischiropoulos et al., 1992). The $ONOO^-$-mediated nitration depends on its secondary products ($\cdot NO_2$) when is protonated to the acidic ONOOH (Eqs 1 and 2) (Beckman and Koppenol, 1996).

$$NO + O_2\cdot^- \longrightarrow ONOO^- \longrightarrow ONOOH \longrightarrow \left[\begin{matrix}\cdot NO_2 \\ \cdot OH\end{matrix}\right] \longrightarrow NO^-_3 + H^+ \quad (1)$$

$$ONOO^- + H^+ \rightarrow ONOOH + NO \rightarrow \cdot NO_2 + NO_2 \quad (2)$$

The resulting protein nitration could be due to the action of leukocyte peroxidases, such as myeloperoxidase (MPO) (Pfeiffer et al., 2001;Sampson et al., 1998). Leukocyte peroxidases have been reported to nitrate proteins in the presence of nitrite and H_2O_2 after stimulation of immune cells (van, V et al., 1997;Eiserich et al., 1998). These enzymatic systems nitrate proteins without spatial or temporal restrictions due to the progressive generation and accumulation of nitrites, but the existence of protein nitration in leukocyte peroxidase knockout mice suggests that $ONOO^-$ may also play a key role in protein nitration (Brennan et al., 2002). It also points up the contribution of other nitration processes such as proteins with heme group plus transition metals such as iron and copper (Thomas et al., 2002).

Nitration has been proposed as a selective post-translational modification with important biological functions (Ischiropoulos, 2003). Nitrotyrosination alters the normal activity of proteins by inducing conformational changes (Cassina et al., 2000;Amici et al., 2003) or preventing their phosphorylation (Newman et al., 2002), leading to a loss of function. Examples of such post-translational modification occur with mitochondrial MnSOD (Ischiropoulos et al., 1992;Millan-Crow et al., 1996), actin (Aslan et al., 2003), glutamine synthase (GS) (Berlett et al., 1996), heme oxygenases (Kinobe et al., 2004), iron regulatory protein-1 (IRP-1) (Gonzalez et al., 2004), histone deacetylase 2 (Ito et al., 2004), mammal aldolase A (Koeck et al., 2004), p53 (Cobbs et al., 2003) and prostacyclin synthase (Hink et al., 2003). In some cases, nitrotyrosination induces a gain-function, e.g., in the case of PKC (Hink et al., 2003), cytochrome c (Cassina et al., 2000), fibrinogen (Vadseth et al., 2004), glutathione *S*-transferase (Ji and Bennett, 2003;Go et al., 1999) and poly-ADP-ribose synthetase (Zhang et al., 1994).

3.3.3. Aβ and NO

It has been proposed that NO is playing a key role in AD pathology (Guix et al., 2005). Evidence for the involvement of nNOS in AD were provided by Thorns et al. (1998), who found an increased expression of nNOS in those neurons with neurofibrillary tangles in the entorhinal cortex and hippocampus of AD patients (Thorns et al., 1998). Positive neurons for nNOS are spread all around the AD brain and NO diffusion can even reach NOS negative neurons (Hyman et al., 1992). Moreover, Aβ has recently been reported to increase the activity of nNOS in rat brain (Stepanichev et al., 2008). At the same time, several studies have shown an association between a Glu298Asp polymorphism of the eNOS gene and AD in different populations (Wang et al., 2008;Akomolafe et al., 2006;Ntais and Polycarpou, 2005;Dahiyat et al., 1999). In

fact, both eNOS and iNOS are overexpressed in the brain of AD patients as well as in APP23 transgenic mice which show a large number of Aβ senile plaques (Luth et al., 2001). More interestingly, Quinn J et al. (2001) found a strong association between NO producing neurons and Aβ-induced neuritic dysthophy in an AD transgenic mice model.

Glial cells could be contributing to the nitrative damage in AD since increased expression of iNOS and eNOS in astrocytes is associated with senile plaques (Luth et al., 2000 and 2001; Wallace et al., 1997; De la Monte et al., 2000). Moreover, nNOS-positive reactive astrocytes were found in AD patients surrounding senile plaques in CA1 and subiculum where neuron loss was massive (Simic et al., 2000). A key role for microglia in NO production after Aβ stimulation has also been reported (Weldon et al., 1998).

On the other hand, oxidative stress enhances the interaction between nNOS and the chaperone Hsp90. It results in an increased NO production (Song et al., 2001). Oxidative stress can also enhance the transcription of the iNOS gene via NF-κβ activation (Han et al., 2007; Lee et al., 2004).

Finally, there is one study reporting that some FAD–associated PS1 and PS2 mutants reduce the threshold for the activation of the inositol 1,4,5-trisphosphate receptor (InsP3R) Ca^{2+} releasing channel, enhancing the response to certain stimuli with a high calcium release from the ER (Cheung et al., 2008). This study provides a mechanistic link between PS1 function and the Ca^{2+} homeostasis and accounts, in part, for the unbalanced Ca^{2+} homeostasis seen in AD. Aβ plaques-induced oxidative stress can also mediate the opening of the cationic channels TRPM2 and TRPM7, facilitating the influx of Ca^{2+} into the neuron (McNulty and Fonfria, 2005). Both processes result in a high intraneuronal concentration of Ca^{2+} which can activate the constitutive NOS enzymes.

On the other hand, it has been demonstrated that specific cerebral regions of patients with AD have higher protein nitrotyrosination levels than controls, especially in the hippocampus and the cerebral cortex (Smith et al., 1997;Hensley et al., 1998), as well as in cerebrospinal fluid (CSF) proteins (Tohgi et al., 1999). This is sensible due to the fact that those areas around the plaques are under pro-oxidant conditions. However, some studies show no difference in 3-nitrotyrosine levels in the CSF of AD and ALS patients (Ryberg et al., 2004). Since one of the main targets for nitrotyrosination is synaptophysin (Tran et al., 2003), it has been suggested that the damage in synaptophysin is related to Aβ-induced impairment of ACh release. Other proteins nitrotyrosinated in AD are related to glucose metabolism (γ-enolase/α-enolase, lactate deshydrogenase and triosephosphate isomerase (TPI)) or cellular cytoskeleton (α-actin) (Castegna et al., 2003). We have found that Aβ induces on endothelial cells the nitrotyrosination of proteins involved in glucose metabolism (TPI), cytoskeletal integrity (vinculin), antioxidant defense (non-selenium glutathione peroxidase) and protein turnover (TCP1, eukaryotic translation elongation factor 2, 26S proteasome and mtHSP75) (Coma et al., 2005). It is possible that the depletion of acetyl-CoA by the impairment of glucose metabolism, which is used by choline acetyltransferase to acetylate choline, could result in ACh deficit (Meier-Ruge and Bertoni-Freddari, 1996). Moreover, the damage in the neuron cytoskeleton contributes to the loss of neuronal network communication (Radtke-Schuller, 2001).

4. THE TRIOSEPHOSPHATE ISOMERASE IN AD

4.1. Glucose metabolism impairment

In AD, glucose metabolism appears to be strongly affected (Harwood et al., 2005;Liang et al., 2008;Mosconi et al., 2007;Mosconi et al., 2005). It has been shown

that the impairment of brain metabolism causes mental changes that mimics the disabilities found in AD (Blass et al., 2002). Moreover, the degree of clinical disability is proportional to the degree of metabolic impairment (Blass et al., 2002). Although the causes of such glucose metabolism impairment are not yet established, oxidative stress seems to be somehow behind this observation (Gibson, 2002).

4.2. Physiological role of TPI

The glycolytic pathway converts a molecule of glucose into two molecules of pyruvate, generating 2 ATPs in 10 steps. One can split glycolysis into two phases: energy investment phase and energy generation phase. In the 5 steps energy investment phase, known also as the preparatory phase, 2 molecules of ATP are consumed in order to prepare the initial hexose (glucose) to split up into two trioses phosphate: glyceraldheyde 3-phosphate (GAP) and dihydroxiacetone phosphate (DHAP). The following 5 steps of the energy generation phase, also known as the "payoff phase", the two trioses phosphate generated are converted into high energy compounds that transfer their phosphate to ADP, giving as a result 4 molecules of ATP. Because 2 ATPs were consumed in the energy investment phase, the net balance consists of 2 molecules of ATP, plus 2 NADH reducing agents (Figure 12). Glycolysis is just the first step for the complete combustion of glucose into CO_2 and H_2O. The resulting pyruvate is then oxidized to Acetylcoenzyme A (AcCoA), whose carbons can be oxidized at the time by the mitochondrial citric acid cycle, resulting in more ATP formation.

GAP and DHAP are the last products of the energy investment phase of glycolysis, but only GAP can be used as a substrate for the following energy generation phase. For this reason, DHAP must be interconverted into its aldheyde isomer, GAP, before it can be reincorporated into the glycolytic pathway. Triosephosphate isomerase

(TPI) is the enzyme responsible for the isomerization of DHAP into GAP. Of course, due to the fact that it is an isomerase, the reaction could happen backwards. However, due to the rapidly and continuously consuming of GAP by the energy generation phase of glycolysis, the reaction is thermodynamically favoured from DHAP to GAP *in vivo*. Thus, TPI has a central role in the glycolytic pathway, ensuring the substrate for the next glycolytic phase, and also for the citric acid cycle (Mathews C.K. and Van Hole

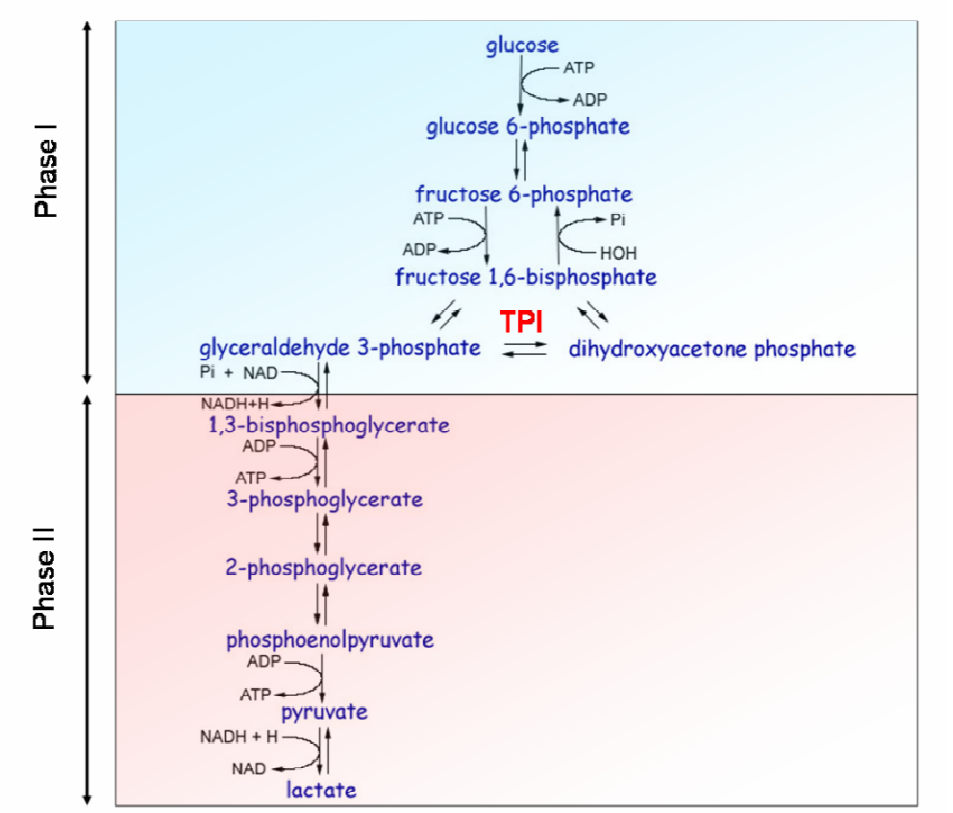

K.E., 1999).

Figure 12. **TPI role in glycolysis.** The glycolytic pathway converts a molecule of glucose into two molecules of pyruvate, generating 2 ATPs in 10 steps. Glycolysis can be splited into two phases: energy investment (phase I) and energy generation (phase II). GAP and DHAP are the last products of the phase I, but only GAP can be used as a substrate for the phase II. TPI has a central role in the glycolytic pathway, ensuring the substrate for the phase II, and consequently for the citric acid cycle.

4.3. Production of methylglioxal

In all species, TPI is composed of two identical subunits, each consisting of roughly 250 amino acid residues. The two subunits (~ 27 kDa each) interact closely and only the dimer (~ 53 kDa) is catalytically active (Figure 13B). The primary structure of the active site has been highly preserved through evolution. The active site residues of the human TPI responsible for the catalytic activity are respectively a lysine residue at position 13, a histidine at position 95 and a glutamic acid residue at position 165 (Cansu and Doruker, 2008).

TPI belongs to the class of the α/β-barrel enzymes (Cansu and Doruker, 2008). These enzymes share a common motive composed of eight alternating α-helices and β-strands. The structural α/β-elements are coiled into a barrel which inside contains an eight-stranded parallel β-sheet surrounded by eight parallel α-helices (Cansu and Doruker, 2008) (Figure 13A). The active site is found at the C-terminal end of the β-barrel. A subunit of TPI not only consists of α-helices and β-strands, but there are also two random coiled loops that play a vital role in the functioning of the enzyme. The first loop (loop 3) connects α-helix 3 with β-strand 3 and consists of residues 70-80. This loop maintains the dimeric-structure of the enzyme and forms most of the inter-subunit contacts (Borchert et al., 1994). The other loop (loop 6) is very flexible and plays an important role in the reaction of the enzyme. As the substrate binds, this loop folds over the active site, rendering it more hydrophobic. In this way the enzyme prevents the elimination of the phosphate group from the enediol intermediate during the reaction which is an important side reaction of the isomerisation and yields inorganic phosphate and the AGE-inducing agent MG (Figure 8) (Cansu and Doruker, 2008;Pompliano et al., 1990). The enzyme has evolved to avoid the releasing of MG to the solvent though a

little leak occurs. Triose phosphates in presence of TPI are considered an important source for MG.

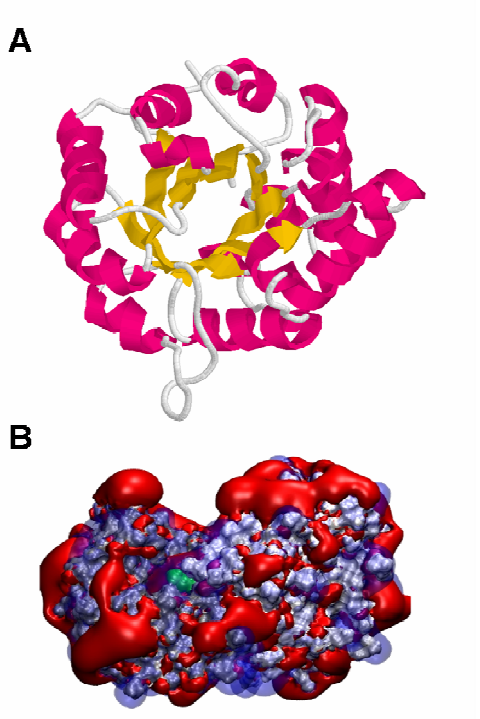

Figure 13. (**A**) TPI is a barrel protein containing eight-stranded parallel β-sheet surrounded by eight parallel α-helices. (**B**) The TPI homodimer consists of a compact globular structure.

4.4. TPI mutations and neurodegeneration

TPI deficiency is the unique glycolytic enzymopathy coupled with a progressive neurodegenerative (Poll-The BT et al., 1985;Ovadi et al., 2004;Olah et al., 2005;Olah et al., 2002) condition that remains poorly understood. The disease is caused exclusively by specific missense mutations affecting the TPI protein and clinically features hemolytic anemia, adult-onset neurological impairment, degeneration, and reduced longevity. Oláh J. et al. (Olah et al., 2005) studied two Hungarian compound

heterozygote brothers who inherited the same TPI mutations (F240L from mother and E145Stop from father), and had increased levels of DHAP. Their energetic balance was unaffected despite the lower activity of the mutant variant because of compensatory mechanisms. The neurological findings are not well explained, but the increase of DHAP could account for them, since DHAP can glycate proteins and lead to the formation of AGEs. Interestingly, it has been reported increased levels of MG and proteins glycation, as well as nitrotyrosination in TPI deficiency (Ahmed et al., 2003). Another observation supporting the role of TPI in neurodegeneration comes from an independent group, which found out that β-carbolines, endogenous neurotoxins formed from the reaction between tryptophan and MG, strongly inhibited TPI in a more potent way than any known inhibitor of the enzyme (Bonnet et al., 2004).

Moreover a low glucose turnover can highly accelerate progress of neurodegeneration, which finally leads to serious dementia of the brain. For example, the decreased glucose turnover provoked by TPI deficiency may result in cholinergic deficit. Tucek S et al. (1990) have clearly shown that in the brain the key substrate, AcCoA for the synthesis of acetylcholine is exclusively synthesised in the glycolytic pathway. At low glucose turnover by decreasing the synthetic rate of AcCoA a cholinergic deficit occurs due to the reduced acetylation of choline to acetylcholine. It is interesting to emphasize that in AD there is characteristic cholinergic deficit (Christensen et al., 2008;Weinshenker, 2008).

On the other hand, Oláh J. et al. (2002) also found that the mutated TPI from the Hungarian brothers behaved in an aberrant way, since it tended to bind to the membrane of erythrocytes and brain microtubules (Orosz et al., 2000). They concluded that the mutations caused somehow the stickiness of the enzyme and consequently, protein aggregation phenomena. Recently, it has been found out that the recessive *waste away*

mutation in *Drosophila* affects the gene that encodes for TPI (Gnerer et al., 2006). Mutants exhibit paralysis, shortened lifespan and neurodegeneration (Gnerer et al., 2006). They do not find decreased levels in ATP, but on the contrary the phenotype seems to be caused by the misfolding of the enzyme and aberrant protein-protein association, as well as increased MG levels (Gnerer et al., 2006). In this sense, TPI is very interesting since a part of the enzyme has been used to model the Aβ peptide because of their similarities regarding the secondary structure of this α/β fragment (Contreras et al., 1999).

4.5. TPI in AD

There are not mutations associated to AD in the gene that encodes for TPI. Nonetheless TPI seems to be one of the main targets for the nitrotyrosinative damage. TPI has been found to be one of the strongest nitrotyrosinated proteins in brains of patients with AD compared to brains of non-AD individuals (Castegna et al., 2003;Reed et al., 2008). We also detected nitrotyrosination of TPI in a model of Cerebral Amyloid Angiopathy (CAA) after exposing endothelial cells to Aβ peptide (Coma et al., 2005). Some studies also revealed that TPI suffers age-dependent nitrotyrosination in skeletal muscle from rats (Fugere et al., 2006;Kanski et al., 2003). Since the nitrotyrosinative damage of proteins seems to be one of the downstream effects of Aβ peptide and due to the association between TPI and neurodegeneration, TPI could play a key role in the pathophysiology of AD.

II. AIMS

We aim to demonstrate the key role of nitrative damage in AD. We set out to address this issue at two different levels. Firstly, the role of peroxynitrite in the etiophatogeny of AD will be determined. For this, we will analyze the effect of peroxynitrite by focusing on the following points:

I. Study of the Aβ production

II. Study of the Aβ species produced

III. Changes of the BACE1 expression

IV. Changes of the γ-secretase components expression and assembly

V. Study of the Aβ aggregation process

Secondly, we will direct our study to the involvement of peroxynitrite in the progression of the disease. Due to the fact that TPI is a preferred target for nitrotyrosination, we will focus on the consequences of this harmful modification. TPI has already been associated to neurodegeneration and aggregation, making it an interesting candidate of neuronal dysfunction. Because the link between plaques and NFT remains unknown, we aim to address this issue setting TPI in a central place. Specifically we will address the effect of TPI nitrotyrosination in AD as follows:

I. Study of the presence of nitro-TPI in the hippocampal region and the frontal cortex of brains from patients with AD.

II. Analysis of nitro-TPI isomerase activity and MG production

III. Study of structural changes and aggregate formation

IV. Study of its role in the formation of *tau* PHF

III. RESULTS & METHODS

CHAPTER 1

"Peroxynitrite switches the $A\beta_{42}/A\beta_{40}$ ratio and enhances $A\beta_{42}$ oligomerformation"

Francesc X. Guix, Gerard Ill-Raga, Eva Ramos, Bart De Strooper,

Miguel A. Valverde, Francisco J. Muñoz

Peroxynitrite switches the $A\beta_{42}/A\beta_{40}$ ratio and enhances $A\beta_{42}$ oligomer formation

Francesc X. Guix [a] Gerard Ill-Raga [a], Eva Ramos [a], Bart De Strooper [b,c],

Miguel A. Valverde [a], Francisco J. Muñoz [a,*]

[a] Laboratory of Molecular Physiology and Channelopathies, Department of Experimental and Health Sciences, Universitat Pompeu Fabra, Barcelona, Spain.

[b] Department for developmental and molecular Genetics – VIB, Leuven, Belgium and

[c]Center for Human Genetics, Kuleuven, Leuven; Gasthuisberg O&N, Leuven.

Running title: *Peroxynitrite increases Aß$_{42}$ production & aggregation*

[*]To whom correspondence should be addressed:

Dr. Francisco J. Muñoz
Grup de Fisiologia Molecular i Canalopaties
Departament de Ciències Experimentals i de la Salut
Universitat Pompeu Fabra
C/ Dr. Aiguader, 88, Barcelona 08003, Spain
Fax: +34 93 316 09 01; Phone: +34 93 316 08 52
e-mail: paco.munoz@upf.edu

Abstract

Alzheimer's disease (AD) is characterized by senile plaques composed of amyloid-beta peptide (Aβ). Aβ is produced by β-secretase and γ-secretase activities. The γ-secretase complex determines the length of the released Aβ. The major Aβ peptide produced by the γ-secretase contains 40 amino-acids ($A\beta_{40}$), and just a 10% of its catalytic activity yields a form with 42 amino-acids ($A\beta_{42}$). It is the most prone to aggregate and constitutes the core of senile plaques. However AD patients have elevated $A\beta_{42}$ production, the pathological mechanism for this switch remains unknown. Here we demonstrate that peroxynitrite, produced by the reaction of superoxide anion with nitric oxide, provokes some changes in the subunits that constitute γ-secretase activity and increases the $A\beta_{42}$ production. In addition, peroxynitrite enhances the aggregation of $A\beta_{42}$ producing oligomeric structures, which were more neurotoxic than non-nitrated $A\beta_{42}$ oligomers.

Keywords: Alzheimer's disease; amyloid ß-peptide; peroxynitrite; presenilin; oligomers.

Nonstandard abbreviations: Ab, antibody; Aß, amyloid ß-peptide; AD, Alzheimer's disease; ADAMs, A disintegrin and metalloproteases; Aph1, anterior pharynx-defective phenotype 1; APP, amyloid ß-protein precursor; BACE1, ß-site APP cleaving enzyme type 1; CAA, cerebral amyloid angiopathy; CTF,C-terminal fragment; FBS, fetal bovine serum; 3-morpholinosydnonimine (SIN-1); MTT, 3-(4,5-dimethylthiazol-2-yl)-2,5-diphenyltetrazolium bromide; NO, nitric oxide; NTF, N-terminal fragment; Pen-2, PS enhancer 2; PS, presenilin; SNP, sodium nitroprusside; swAPP, APP bearing the swedish mutation.

1. Introduction

Alzheimer's disease (AD) is a neurodegenerative disease characterized by senile plaques formed by the deposition of extraneuronal amyloid-beta peptide (Aβ) (Koppal et al., 1998; Opazo et al., 2002) and intraneuronal fibrillary tangles formation (Lewis et al., 2001; Gotz et al., 2001). Aβ is a small peptide produced through the consecutive processing of a type I transmembrane protein named Amyloid Precursor Protein (APP) by the cleavage of the β-secretase and the γ-secretase enzymatic activities. As a result of the γ-activity a 40 aminoacid long peptide ($A\beta_{40}$) is released. $A\beta_{40}$ is the more frequently found form of Aβ. However, sometimes the γ-secretase complex cuts two aminoacids more at the carboxyl terminus of APP yielding a larger and more toxic form called $A\beta_{42}$. The higher toxicity of this form resides on its major tendency to fibrillate. Although it is the less frequent form of Aβ, its production is increased in AD. This species is highly fibrillogenic and acts like a "seed" for $A\beta_{40}$. In fact $A\beta_{42}$ is the initial component of senile plaques followed by the subsequent $A\beta_{42}$ and $A\beta_{40}$ deposition around it, allowing the growth of the plaques (Dolev and Michaelson, 2006).

The active γ-secretase complex is formed by the assembly in the endoplasmic reticulum (ER) of 4 different proteins: pen2, Aph1, presenilin 1 (PS1) and nicastrin (Sato et al., 2007; reviewed in De strooper 2003). The catalytic activity resides on PS1 (De Strooper et al., 1998), which undergoes an endocatalytical cleavage after the association with the rest of the components, releasing a C-terminal fragment (CTF-PS1) and an N-terminal fragment (NTF-PS1) (Hebert SS et al., 2003). Both of them must heterodimerize to confer the catalytic properties to the complex (Hebert SS et al., 2003).

The $A\beta_{42}/A\beta_{40}$ ratio is elevated in AD (Gorman et al., 2008; Kumar-Singh et al., 2006; Lewczuk et al., 2004). It is known that the different components that constitute the γ-secretase complex can modulate the function of PS1 altering the ratio in the

production of $A\beta_{42}$ and $A\beta_{40}$ (Marlow et al., 2003). However, the reason behind the switch of the $A\beta_{42}/A\beta_{40}$ ratio in favour of $A\beta_{42}$ in AD is not well understood. Moreover, during the normal aging process such effect is also observable, though in a much lower scale (Shoji et al., 2001).

An increase of oxidative stress occurs in both aging and AD. In the first case, it is due to the failure of the cellular mechanisms that keep the cellular redox state. In the second case, the increment in the number of the Reactive Oxidant Species (ROS) is a direct consequence of the Aß action. There are a large number of evidences supporting the important role that plays the Aβ-induced oxidative stress in the AD etiopathology. One of the major oxidant species is peroxynitrite ($ONOO^-$), which results from the rapid and spontaneous reaction between superoxide anion and nitric oxide (NO). The toxic properties of this compound come from its capacity of modifying relevant biomolecules such as nucleic acids, lipids and proteins. Peroxynitrite reacts with the phenol ring of the tyrosyl residues of proteins in a reaction named nitrotyrosination, altering the activity of the proteins. Protein nitrotyrosination has been extensively reported to occur in AD (Guix et al. 2005, Coma et al., 2005; Guix et al., 2008).

In the present work we have studied the role of peroxynitrite in the production of amyloid attending to the nitrotyrosination of the different g-secretase component as well as to the shift in the $A\beta_{42}/A\beta_{40}$ ratio. Moreover, we have addressed the study of the effect of $A\beta_{42}$ nitration in the aggregation of the amyloid to form oligomers and fibrils. Finally, we have studied the neurotoxicity of the nitrated $A\beta_{42}$ fibrils regarding those non treated $A\beta_{42}$ fibrils.

2. Materials and Methods

2.1. Cell cultures

HEK cells expressing the Swedish mutation in APP (HEK-swAPP) were grown in DMEM medium supplemented with 10% fetal bovine serum (FBS) (Gibco BRL), 1% penicillin and 1% streptomycin. For the MTT assay SH-SY5Y cells were grown on a 96-wells plate in DMEM medium supplemented with 15% FCS (Gibco BRL), 1% penicillin and 1% streptomycin. Experiments were performed with phenol red-free media and 0.2% FBS.

2.2. Human brain samples

Human brain tissue sections and samples were supplied by the Unitat d'Anatomia Patològica (Hospital del Mar) and the Unitat de Nauropatología y Banco de Cerebros (Fundación Hospital Alcorcón). The procedure was approved by the ethics committee of the Institut Municipal d'Investigacions Mèdiques-Universitat Pompeu Fabra. Samples used in the biochemical studies were from 4 control individuals and 4 AD patients. 500 mg of frontal cortex was homogenized at 4ºC with 500 µL of a cocktail containing 480 µL NP40 lysis buffer (150 mM NaCl, 5 mM EDTA, 1% Nonidet P-40, 1 mM sodium orthovanadate, 1 mM phenylmethylsulphonyl fluoride, 0.05% aprotinin, 1mM dithioltreitol) and 120 µL of protease inhibitors (Complete mini-EDTA free) from Roche Diagnostics GmbH. Lysates were shaked at 4ºC for 30 min and centrifuged at 13,000 rpm for 15 min. Proteins in the supernatant were quantified with the Bradford assay.

2.3. Treatments

Determination of the toxicity of SIN-1 (Sigma) at different concentrations was obtained running dose-response (0–100 µM) cell viability assays using the 3-(4,5-dimethylthiazol-2-yl)-2,5-diphenyltetrazolium bromide (MTT) reduction method. HEK-

swAPP cells were grown in red phenol free medium containing 0.2 % fetal bovine serum (FBS) and challenged with different SIN-1 or peroxynitrite concentrations for 3, 6, 12 or 24h.

2.4. Co-immunoprecipitation

Cells were lysed on ice with a solution containing 1% Triton X-100 or 0.5% CHAPS, 50 mM Hepes, pH 7.6; 150 mM NaCl; 1 mM EDTA; and complete protease inhibitors (Roche). 500 μg of total protein from brains or HEK APP Swedish lysates were incubated with 1.25 μg of anti-NTF-PS1 or anti-CTF-PS1 monoclonal antibodies overnight at 4 ºC. Following the addition of protein G immobilized on sepharose (Sigma), samples were shaken for 2 h at room temperature. Aggregates were pulled down by centrifugation at 10,000 rpm for 10 min and washed thrice. Protein G and antibody were removed from the immunoprecipitated proteins by boiling the samples for 6 min at 100 ºC.

2.5. Identification of proteins by western-blot

Protein samples were analyzed by using 12% Tris-glycine gels and blotted onto nitrocellulose membrane (Millipore, Bedford, MA) for secretase components detection or 4–16% Tris-Tricine gels and blotted onto nylon membrane (Immobilon-P, Millipore) for Aβ-peptide detection. Membranes were incubated for 2 h at room temperature with different primary rabbit Abs: anti-BACE1 (1:500; Chemicon, Temecula, CA), anti-PS1-NTF, anti-PS1-CTF, anti-nicastrin, anti-Pen-2, anti-Aph1 and anti-Aβ-peptide WO2. Mouse anti-⁎-tubulin Ab (1:5000; Sigma) was incubated for 1 h at room temperature as a loading and transfer control. The peroxidase-conjugate anti-mouse and anti-rabbit Abs were used as secondary Abs (Amersham Bioscience, Barcelona, Spain). Bands were visualized using the enhanced chemiluminescence substrate Super Signal (Pierce,

Rockford, IL) or Supersignal West femto trial kit (Pierce) and Amersham Bioscience Hyperfilm ECL kit.

2.6. Membrane protein extraction and Blue Native Gels

Cells from 6 T75 flasks per condition were collected and homogenised with 3 ml homogenising buffer containing 140 mM NaCl, 20 mM Tris pH 7.4, 5 mM EDTA and protease inhibitors (Complete mini-EDTA free) from Roche Diagnostics GmbH. Homogenizes were centrifuged at 4,000 rpm for 10 min and 4ºC and the supernatant transferred to ultracentrifuge tubes. Ultracentrifugation was carried out at 100.000g for 45 min at 4ºC with a SW45Ti rotor. The supernatant was discarded and the pelled lysed with lysis buffer containing 25 mM HEPES pH 7.4, 150 mM NaCl, 0.5% CHAPS and protease inhibitors (Complete mini-EDTA free) from Roche Diagnostics GmbH. N-dodecyl-β-D-maltoside (DDM, Invitrogen) was added to the samples up to a final concentration of 1%.

For the electrophoresis, 50 μg of total protein were prepared with NativePAGE^{TM} sample buffer (4X) and NativePAGE^{TM} 0.125 % G-250 sample additive from Invitrogen. Samples were run in a 2-13% NativePAGE^{TM} Bis-tris Tris gel system (Invitrogen). The cathode buffer contained Coomassie G-250.

2.7. Aß quantification

After 24 h of treatments, media were collected and the levels of $Aß_{1–40}$ and $Aß_{1–42}$ were measured using commercial enzyme-linked immunosorbent assay kits (IBL, Gumna, Japan). Absorbances were measured by a microplate reader Bio-Rad 680 and evaluated by microplate manager software (Bio-Rad). For intracellular Aß detection, values were normalized to total cell protein concentration by Bio-Rad DC Protein Assay (Bio-Rad).

2.8. Turbidometric assay

The Aß42 (sigma) stock solution was prepared by dissolving the peptide in DMSO to a final concentration of 5 µg/µl. The turbidometric assay was carried out at room temperature, within a dark chamber in a 96-wells plate under continuous shaking (300 rpm). Each well contained 50 ng/µl Aß42 dissolved in 100 µl PBS pH 5.5 and 25 or 50 mM SIN-1. Absorbance at 405 nm was followed over the time.

2.9. Transmission electron microscopy

Mesh nickel grids were charged with UV light for 5 min and set on a drop of sample for 1 min. Then 3 consecutive washes with milliQ water were carried out (1 min in total). Finally the grid was set on a drop of 2% uranil acetate solution for 1 min and dried. Samples were observed with a Jeol 1010 electron microscope.

2.10. Statistical analysis

Data are expressed as the mean ± SEM of the values from the number of experiments as indicated in the corresponding figures. Data were evaluated statistically by using the Student's *t*-test or the one way ANOVA test followed by Bonferroni's post-hoc analysis. The level of significance was $p < 0.05$.

3. Results

3.1. Increased nitration and interaction between the CTF-PS1 and the NTF-PS1 fragments by a peroxynitrite donor (SIN-1)

After exposing HEK-swAPP cells to increasing concentrations of SIN-1, the NTF-PS1 was inmunoprecipitated and probed with an anti-CTF-PS1 antibody (figure 1A). Surprisingly, more CTF-PS1 was co-inmunoprecipitated from HEK-swAPP treated with SIN-1 in a concentration-dependent manner. CTF-PS1 appeared faintly nitrotyrosinated under these conditions. The same result was obtained when a stronger detergent was

used to disrupt the interaction between CTF-PS1 and NTF-PS1. While there is no presence of the CTF-PS1 in inmunoprecipitates of NTF-PS1 obtained from non-treated cells, a band for CTF-PS1 appears in those lanes corresponding to inmunoprecipitates of NTF-PS1 obtained from HEK-swAPP challenged with increasing concentrations of SIN-1 (figure 1B). NTF-PS1 is also faintly nitrotyrosinated. Quantification of the amount of CTF-PS1 pulled down with NTF-PS1 after exposure to 5 μM SIN-1 shows a stronger interaction between these two fragments (figure 1C). This effect can be reproduced as early as at 12h (figure 1D), but not when cells are treated with the NO donor SNP, suggesting that this is a peroxynitrite specific effect (figure 1E). Interestingly, PS1 inmunoprecipitated from AD cerebral cortex is highly nitrotyrosinated in compare to non-AD (figure 1F, supplementary 1C).

3.2. Differential expression between the different γ-secretase components after treatment with SIN-1

Peroxynitrite is known to trigger crosslinking between tyrosines forming dityrosine bridges (Fontana et al., 2006; Giulivi C et al., 2003). This could explain the stronger interaction of the PS fragments when cells are challenged with SIN-1. However the enhanced interaction between the NFT-PS1 and the CTF-PS1 is not of covalent nature since bands can be seen separately in a western blot. Crosslinking effects on PS-1 could only be detected when a very high concentration of SIN-1 was used to treat the cells (supplementary 1B). Another explanation may be the increased expression of some of the components that constitute the γ-secretase complex. It is known that some of these components are necessary for the properly assembly of the γ-secretase complex (Dries DR and Yu G, 2008). Thus peroxynitrite may be enhancing the association

between NFT-PS1 and CTF-PS1 by favouring the expression of some units of the γ-secretase.

HEK-swAPP cells challenged with 5 μM SIN-1 showed a higher expression of the PS1 holoprotein (PS1), nicastrin and Pen-2 in comparison to non-treated cells (figure 2). However less amount of NTF-PS1 was produced under this condition, pointing out to a minor endoproteolytic cleavage of PS1. Aph-1 presented no changes in the cellular levels, whereas BACE-1 seemed to decrease.

Although the endoproteolytical processing of holoPS1 seems to be diminished by SIN-1, the formation of the catalytically active mature form of the γ-secretase complex is enhanced by SIN-1 in a concentration-dependent manner (figure 2). These could be due to the major expression of nicastrin and Pen-2.

The decrease of the NTF-PS1 fragment formation in favour of the full length PS1 would suggest the formation of a less active γ-secretase complex, and as a consequence, the $A\beta_{42}$ production would be compromised. However, this result would be in agreement with a large number of evidences suggesting that a slower less-efficient form of the protease can result in a greater proportion of 42-residue Aβ (reviewed in Wolfe et al., 2007).

3.3. SIN-1 increases total Aβ by incrementing $A\beta_{42}$ but not $A\beta_{40}$

Due to the fact that our major assembly of γ-secretase complex after SIN-1 exposure would contain a less cleaved PS1, we hypothesized that this could mimic the effect of those mutations impairing activity of PS1 but incrementing at the time the $A\beta_{42}$ production. We measured the production of total Aβ, $A\beta_{42}$ and $A\beta_{40}$ in the medium of HEK-swAPP cells challenged with increasing concentrations of SIN-1 for 24h. Interestingly, only $A\beta_{42}$ was observed to increase after the treatment in a concentration-

dependent manner (figure 3A), incrementing the ration $A\beta_{42}/A\beta_{40}$ (figure 3B). The increase is clearly detected at SIN-1 concentrations ranging from 1 to 10 μM. From 10 μM on, the effect is less pronounced due probably to the toxicity of SIN-1 (supplementary 1A). A kinetic study was carried out to follow the $A\beta_{42}$ release over the time (figure 3C). The effects on $A\beta_{42}$ production can be already detected at 12h with a concentration of 5 μM SIN-1 (figure 3C). The same results were reproduced using pure peroxynitrite instead of SIN-1 (supplementary 2).

3.4. Peroxynitrite enhances the formation of toxic $A\beta_{42}$ oligomers in vitro

After having determined the effect of peroxynitrite on $A\beta_{42}$ production, we move to analyse how this anion influences the aggregative process of the peptide. Using a turbidometric assay, we followed up the aggregation of synthetic $A\beta_{42}$ over the time. The analysis of our results showed a major tendency to aggregate when this was left in presence of SIN-1 (figure 4A). The kinetics of $A\beta_{42}$ aggregation was slower when this was incubated alone. The toxicity of the aggregates obtained was analysed on SH-SY5Y cells for 24h and with an MTT assay. The sample corresponding to $A\beta_{42}$ aggregated in presence of SIN-1 was much more toxic (figure 4B). The study by ME about the nature of these $A\beta_{42}$ aggregates revealed their oligomeric structure (figure 4C), resembling those obtained without SIN-1 (figure 4D) but in a major number.

4. Discussion

During the aging process, and especially in AD, there is a switch of the Aβ production in favour of the most toxic species $A\beta_{42}$ (Shoji M et al., 2001). It is believed to be an initial step in the formation of the plaques since $A\beta_{42}$ constitutes the core for the posterior growing of these fibrillar structures. Oxidative stress also appears very early in

the first stages of AD (Resende R et al., 2008). There are several reasons to believe that oxidative stress is an etiopathogenic factor for AD. On the one hand aging, being the first risk factor for AD, courses with an unbalanced redox state due to the failure of the antioxidant mechanisms (Hensley K et al., 1994). Secondly, oxidative stress has already been described to enhance APP processing by increasing the expression of BACE1 and affecting in this way the production of both Aβ42 and Aβ40 (Coma M et al., 2008).

In the present work we demonstrate that peroxynitrite increments the total Aβ production by the release of more $A\beta_{42}$ peptide. Other oxidants have been demonstrated to increase the total Aβ production (Shen C et al., 2008; Tamagno E et al., 2008). However up to the moment any satisfactory mechanism has been provided to explain the switch of the $A\beta_{42}/A\beta_{40}$ ratio that occurs during aging and AD pathology. The fact that peroxynitrite alters the production of $A\beta_{42}$ but not $A\beta_{40}$ points to an involvement of the γ-secretase complex since it is the activity that determines the Aβ specie released. We have found that the peroxynitrite donor SIN-1 is able to nitrotyrosinate PS1, the catalytic subunit of the γ-secretase complex, which is also nitrated in cerebral cortex of AD patients. It has been previously reported that some mutations in two tyrosines near the catalytic center of PS1 lead to an increase of the $A\beta_{42}/A\beta_{40}$ ratio by affecting the orientation of the two catalytic aspartyls Asp257 and Asp385 (Wrigley et al., 2004). Thus the alteration of these tyrosines by nitrotyrosination might give a similar result providing a mechanistic explanation. In AD the non-cleaved PS1, but not its fragments, seems to be nitrated though the full length protein is believed to be catalytically inactive. At the first glance, it seems to contradict an incremented release of $A\beta_{42}$ by the mechanism previously exposed because nitration of the holoPS1 should not have any effect on the activity of the complex. Nonetheless, it has been reported that most PS1 mutants associated to FAD have reduced proteolytic efficiency but increased $A\beta_{42}$

production (Wolfe et al, 2007). On the other hand the major part of PS1 is normally found as a holoprotein whereas just a little part undergoes endoproteolysis (Thinakaran et al., 1997). Nitrotyrosination of PS1 could also stabilize the holoprotein and prevent its degradation, since uncleaved PS holoprotein is rapidly degraded, whereas PS-NTF and PS-CTF exist as a stable 1:1 heterodimer in the high molecular weight γ-secretase complex (Dries DR and Yu G, 2008). Non-cleaved PS1 has been reported to be able to assembly with the other components (Wang et al, 2004). Thus, a slower γ-secretase activity could give as a result a major $A\beta_{42}$ production.

Furthermore we have observed a direct effect of SIN-1 on the γ-secretase assembly. More mature complex (~250 kDa) is formed after exposure of HEK-swAPP to SIN-1. The amount of mature complex is known to be directly related to the amount of APP cleaved. The increase in some of the components that constitutes the γ-secretase activity is a mechanism to form more complex. For this reason we evaluated their levels. Nicastrin and Pen-2 were specially enhanced by SIN-1, contributing probably to the establishment of the complex. Nicastrin acts as the substrate receptor (Dries DR and Yu G, 2008), whereas Pen-2 is the last one to join the components. The complex needs Pen-2 to go from the ER to the Golgi (Dries DR and Yu G, 2008). Interestingly the levels of holoPS1 seem to be enhanced by SIN-1, whereas its endoproteolysis is impaired. Thus, peroxynitrite stabilizes the holoPS1, probably inducing a less γ-secretase activity, what could account for the switch to $A\beta_{42}$ production by the mechanism explained previously.

In summary, our data supports the role of peroxynitrite as an etiopathogenic factor to develop AD. Firstly, nitrotyrosination of the holoPS1 occurs under the presence of peroxynitrite, which seems to be stabilized against its endoproteolitic cleavage. Secondly, two components of γ-secretase, nicastrin and Pen-2, are more

expressed and specially the last one can contribute to give stability. Thirdly, the interaction between CTF-PS1 and NTF-PS1 is strengthened. Finally peroxynitrite induces the formation of more mature complex. On the other hand we have demonstrated that peroxynitrite enhances the toxicity of the $A\beta_{42}$ peptide by inducing its aggregation yielding oligomers.

Disclosure statement

All the authors of the present manuscript disclose any actual or potential conflicts of interest including any financial, personal or other relationships with other people or organizations within 3 years of beginning the work submitted that could inappropriately influence (bias) their work.

Ethical statement

All the procedures of the present work using human samples have been previously approved by the Ethical Commite of the Institute Municipal de Investigació Mèdica and Universitat Pompeu Fabra (IMIM-UPF).

Aknowledgements

Work supported by Spanish Ministerio de Sanidad (FIS: PRO1208; Red HERACLES RD06/0009/002), Educación y Ciencia (BIO2005-01591; SAF2006-4973; CSD2006-00012), Generalitat de Catalunya (GSR2005-266; 2005-SGR00037 and VPH NOE (ICT-223920). Work in the lab of BDS is supported by a Methusalem grant of the Flemish government, and by funds of VIB and KUL.

FIGURE 1

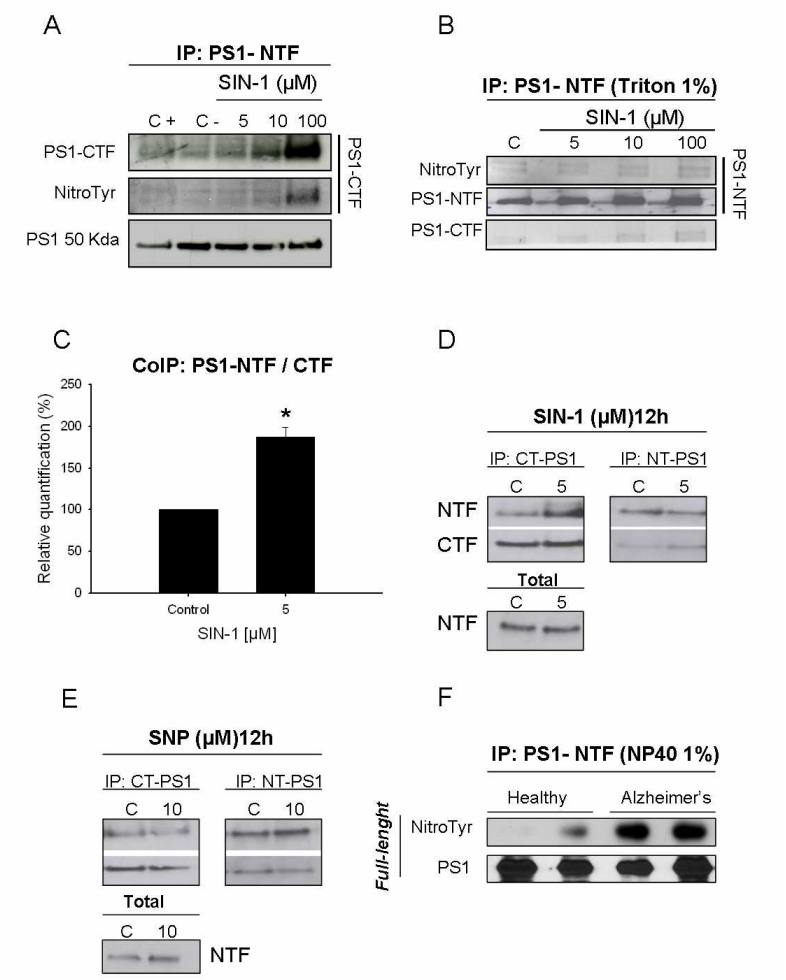

Fig. 1. Peroxynitrite induces PS1 nitrotyrosination. (A**)** CTF-PS1 co-inmunoprecipitates with NTF-PS1 when HEK-swAPP cells are exposed to increasing concentrations of SIN-1 for 24h. CTF-PS1 appears nitrotyrosinated after SIN-1 exposure. The total PS1 levels do not change. (B) Interaction between CTF-PS1 and NTF-PS1 is resistant to detergent treatment when HEK-swAPP cells are exposed to increasing concentrations of SIN-1. NTF-PS1 appears faintly nitrated after SIN-1 exposure. (C**)** Quantification of the CTF-PS1 co-inmunoprecipitated with NTF-PS1 in presence of 5 μM SIN-1 for 24h. Data are the mean ± SEM of 3 independent experiments. * $p < 0,05$ by Student's t test analysis. (D**)** The same results were obtained after just 12h of exposure to 5 μM SIN-1 but not with a SNP, a NO donor (E). (F**)** Nitrotyrosination of PS1 in the cerebral cortex of AD patients.

FIGURE 2

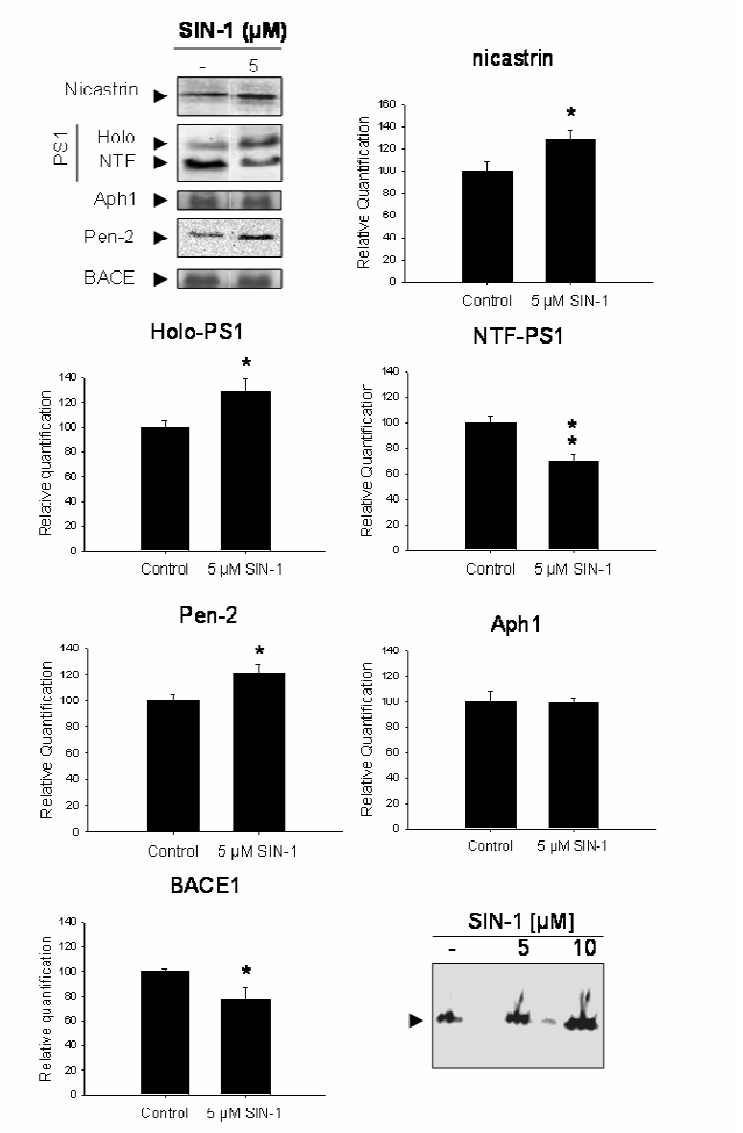

Fig. 2. Peroxynitrite is modulating the expression of the different components of γ- and β- secretases. (A) HEK-swAPP cells to 5 μM SIN-1 for 24h and γ- and ß-secretase were studied by western-blots and (B-G). Data are the mean ± SEM of 3 independent experiments. * p <0,05; ** p <0,005 by Student's t test analysis. (H) SIN-1 favours the assembly of the mature γ-secretase complex in a concentration-dependent pattern.

FIGURE 3

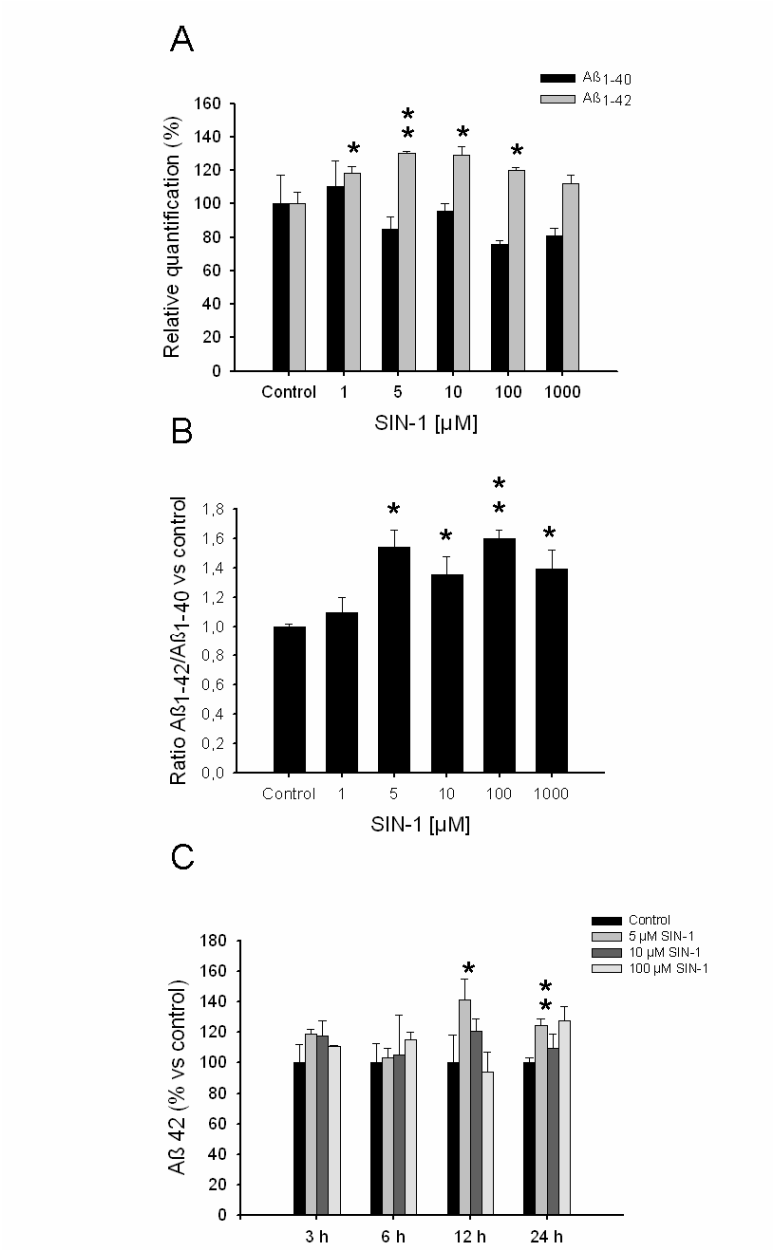

Fig. 3. Peroxynitrite is increasing the $A\beta_{42}/A\beta_{40}$ ratio. (A,B) $A\beta_{42}$ and $A\beta_{40}$ in the media of HEK-swAPP cells exposed to increasing concentrations of SIN-1. (C) Time course of $A\beta_{42}$ production. Data are the mean ± SEM of 3 independent experiments. * p <0,05; ** p <0,005 by Student's t test analysis.

FIGURE 4

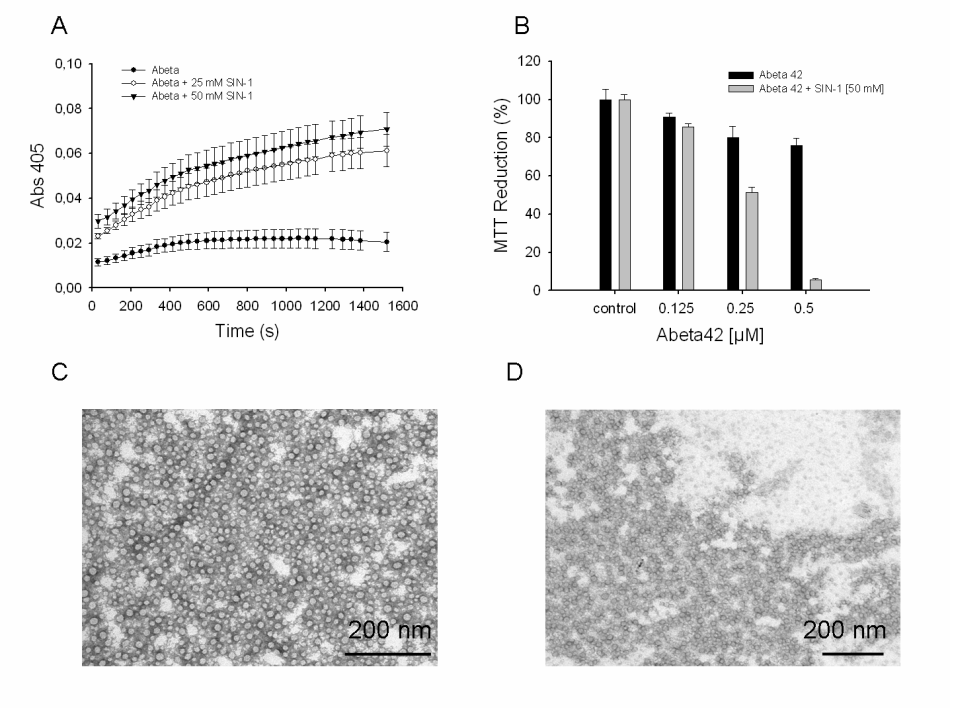

Fig. 4. Peroxynitrite is increasing Aß$_{42}$ oligomer formation and neurotoxicity. (A) Turbidomentric analysisy of Aβ_{42} aggregation in the presence of 25 and 50 mM SIN-1. (B) Nitrated Aβ_{42} oligomer-induced neurotoxicity on neuroblastoma cells. Data are the mean ± SEM of 3 independent experiments. * p <0,05; ** p <0,005 by Student's t test analysis. (C) Electron microscopy picture of Aβ_{42} oligomers obtained in presence of 50 mM SIN-1 and (D) without peroxynitrite.

5. References

Castegna, A., Thongboonkerd, V., Klein, J.B., Lynn, B., Markesbery, W.R., Butterfield, D.A., 2003. Proteomic identification of nitrated proteins in Alzheimer's disease brain. J Neurochem. 85, 1394-401.

Coma, M., Guix, F.X., Ill-Raga, G., Uribesalgo, I., Alameda, F., Valverde, M.A., Muñoz, F.J., 2008. Oxidative stress triggers the amyloidogenic pathway in human vascular smooth muscle cells. Neurobiol Aging. 29, 969-80.

De Strooper, B., 2003. Aph-1, Pen-2, and Nicastrin with Presenilin generate an active gamma-Secretase complex. Neuron. 38, 9-12.

De Strooper, B., Saftig, P., Craessaerts, K., Vanderstichele, H., Guhde, G., Annaert, W., Von Figura, K., Van Leuven, F., 1998. Deficiency of presenilin-1 inhibits the normal cleavage of amyloid precursor protein. Nature. 391, 387-90.

DeKosky, S.T., Abrahamson, E.E., Ciallella, J.R., Paljug, W.R., Wisniewski, S.R., Clark, R.S., Ikonomovic, M.D., 2007. Association of increased cortical soluble abeta42 levels with diffuse plaques after severe brain injury in humans.Arch Neurol. 64, 541-4.

Deng-Bryant, Y., Singh, I.N., Carrico, K.M., Hall, E.D., 2008. Neuroprotective effects of tempol, a catalytic scavenger of peroxynitrite-derived free radicals, in a mouse traumatic brain injury model. J Cereb Blood Flow Metab. 28, 1114-26.

Dolev, I., Michaelson, D.M., 2006. The nucleation growth and reversibility of Amyloid-beta deposition in vivo. J Alzheimers Dis. 10, 291-301

Dries, D.R., Yu, G., 2008. Assembly, maturation, and trafficking of the gamma-secretase complex in Alzheimer's disease. Curr Alzheimer Res.5, 132-46.

Fontana, M., Pecci, L., Schininá, M.E., Montefoschi, G., Rosei, M.A., 2006. Oxidative and nitrative modifications of enkephalins by reactive nitrogen species. Free Radic Res. 40, 697-706.

Giulivi, C., Traaseth, N.J., Davies, K.J., 2003. Tyrosine oxidation products: analysis and biological relevance. Amino Acids. 25, 227-32.

Gorman, P.M., Kim, S., Guo, M., Melnyk, R.A., McLaurin, J., Fraser, P.E., Bowie, J.U., 2008. Chakrabartty A. Dimerization of the transmembrane domain of amyloid precursor proteins and familial Alzheimer's disease mutants. BMC Neurosci. 9, 17.

Götz, J., Chen, F., van Dorpe, J., Nitsch, R.M., 2001. Formation of neurofibrillary tangles in P301l tau transgenic mice induced by Abeta 42 fibrils. Science 293, 1491-1495.

Guix, F.X., Coma, M., Ill-Raga, G., Muñoz, F.J. Protein nitrotyrosination in Alzheimer's disease. In: Neurodegenerative diseases: from molecular concepts to

therapeutic targets. Chapter 11. Editors: R. von Bernhardt et al, © 2008 Nova Science Publishers, Inc. pp. 133-143.

Guix, F.X., Uribesalgo, I., Coma, M., Munoz, F.J., 2005. The physiology and pathophysiology of nitric oxide in the brain. Prog Neurobiol 76,126-152.

Hébert , S.S., Godin, C., Lévesque, G., 2003. Oligomerization of human presenilin-1 fragments. FEBS Lett. 550, 30-4.

Hensley, K., Carney, J.M., Mattson, M.P., Aksenova, M., Harris, M., Wu, J.F., Floyd, R.A., Butterfield, D.A., 1994. A model for beta-amyloid aggregation and neurotoxicity based on free radical generation by the peptide: relevance to Alzheimer disease. Proc Natl Acad Sci U S A. 91, 3270-4.

Koppal, T., Subramaniam, R., Drake, J., Prasad, M.R., Dhillon, H., Butterfield, D.A., 1998. Vitamin E protects against Alzheimer's amyloid peptide (25-35)-induced changes in neocortical synaptosomal membrane lipid structure and composition. Brain Res. 786, 270-273.

Kumar-Singh, S., Theuns, J., Van Broeck, B., Pirici, D., Vennekens, K., Corsmit, E., Cruts, M., Dermaut, B., Wang, R., Van Broeckhoven, C., 2006. Mean age-of-onset of familial alzheimer disease caused by presenilin mutations correlates with both increased Abeta42 and decreased Abeta40.Hum Mutat. 27, 686-95.

Lewczuk, P., Esselmann, H., Otto, M., Maler, J.M., Henkel, A.W., Henkel, M.K., Eikenberg, O., Antz, C., Krause, W.R., Reulbach, U., Kornhuber, J., Wiltfang, J., Neurochemical diagnosis of Alzheimer's dementia by CSF Abeta42, Abeta42/Abeta40 ratio and total tau. Neurobiol Aging. 25, 273-81

Lewis, J., Dickson, D.W., Lin, W.L., Chisholm, L., Corral, A., Jones, G., Yen, S.H., Sahara, N., Skipper, L., Yager, D., Eckman, C., Hardy, J., Hutton, M., McGowan, E., 2001. Enhanced neurofibrillary degeneration in transgenic mice expressing mutant tau and APP. Science 293, 1487-1491.

Marlow, L., Canet, R.M., Haugabook, S.J., Hardy, J.A., Lahiri, D.K., Sambamurti, K., 2003. APH1, PEN2, and Nicastrin increase Abeta levels and gamma-secretase activity. Biochem Biophys Res Commun.307, 756.

Opazo, C., Huang, X., Cherny, R.A., Moir, R.D., Roher, A.E., White, A.R., Cappai, R., Masters, C.L., Tanzi, R.E., Inestrosa, N.C., Bush, A.I., 2002. Metalloenzyme-like activity of Alzheimer's disease beta-amyloid. Cu-dependent catalytic conversion of dopamine, cholesterol, and biological reducing agents to neurotoxic H(2)O(2). J. Biol. Chem. 277, 40302-40308.

Resende, R., Moreira, P.I., Proença, T., Deshpande, A., Busciglio, J., Pereira, C., Oliveira, C.R., 2008. Brain oxidative stress in a triple-transgenic mouse model of Alzheimer disease. Free Radic Biol Med. 44, 2051-7.

Sato, T., Diehl, T.S., Narayanan, S., Funamoto, S., Ihara, Y., De Strooper, B., Steiner, H., Haass, C., Wolfe, M.S., 2007. Active gamma-secretase complexes contain only one of each component. J Biol Chem. 282, 33985-93.

Shen, C., Chen, Y., Liu, H., Zhang, K., Zhang, T., Lin, A., Jing, N., 2008. Hydrogen peroxide promotes Abeta production through JNK-dependent activation of gamma-secretase. J Biol Chem. 283, 17721-30.

Shoji, M., Kanai, M., Matsubara, E., Tomidokoro, Y., Shizuka, M., Ikeda, Y., Ikeda, M., Harigaya, Y., Okamoto, K., Hirai, S., 2001. The levels of cerebrospinal fluid Abeta40 and Abeta42(43) are regulated age-dependently. Neurobiol Aging. 22, 209-15.

Singh, I.N., Sullivan, P.G., Hall, E.D., 2007. Peroxynitrite-mediated oxidative damage to brain mitochondria: Protective effects of peroxynitrite scavengers. J Neurosci Res. 85, 2216-23.

Tamagno, E., Parola, M., Bardini, P., Piccini, A., Borghi, R., Guglielmotto, M., 2005. Santoro G, Davit A, Danni O, Smith MA, Perry G, Tabaton M. Beta-site APP cleaving enzyme up-regulation induced by 4-hydroxynonenal is mediated by stress-activated protein kinases pathways. J Neurochem. 92, 628-36.

Thinakaran, G., Harris, C.L., Ratovitski, T., Davenport, F., Slunt, H.H., Price, D.L., Borchelt, D.R., Sisodia, S.S., 1997. Evidence that levels of presenilins (PS1 and PS2) are coordinately regulated by competition for limiting cellular factors. J Biol Chem. 272, 28415–22.

Wang, J., Brunkan, A.L., Hecimovic, S., Walker, E., Goate, A., 2004. Conserved "PAL" sequence in presenilins is essential for gamma-secretase activity, but not required for formation or stabilization of gamma-secretase complexes. Neurobiol Dis. 15, 654–66.

Wolfe, M.S., 2007. When loss is gain: reduced presenilin proteolytic function leads to increased Abeta42/Abeta40. Talking Point on the role of presenilin mutations in Alzheimer disease.EMBO Rep. 8, 136-40.

Wrigley, J.D., Nunn, E.J., Nyabi, O., Clarke, E.E., Hunt, P., Nadin, A., De Strooper, B., Shearman, M.S., Beher, D., 2004 Conserved residues within the putative active site of gamma-secretase differentially influence enzyme activity and inhibitor binding. J Neurochem. 90, 1312-20.

6. Supplementary material

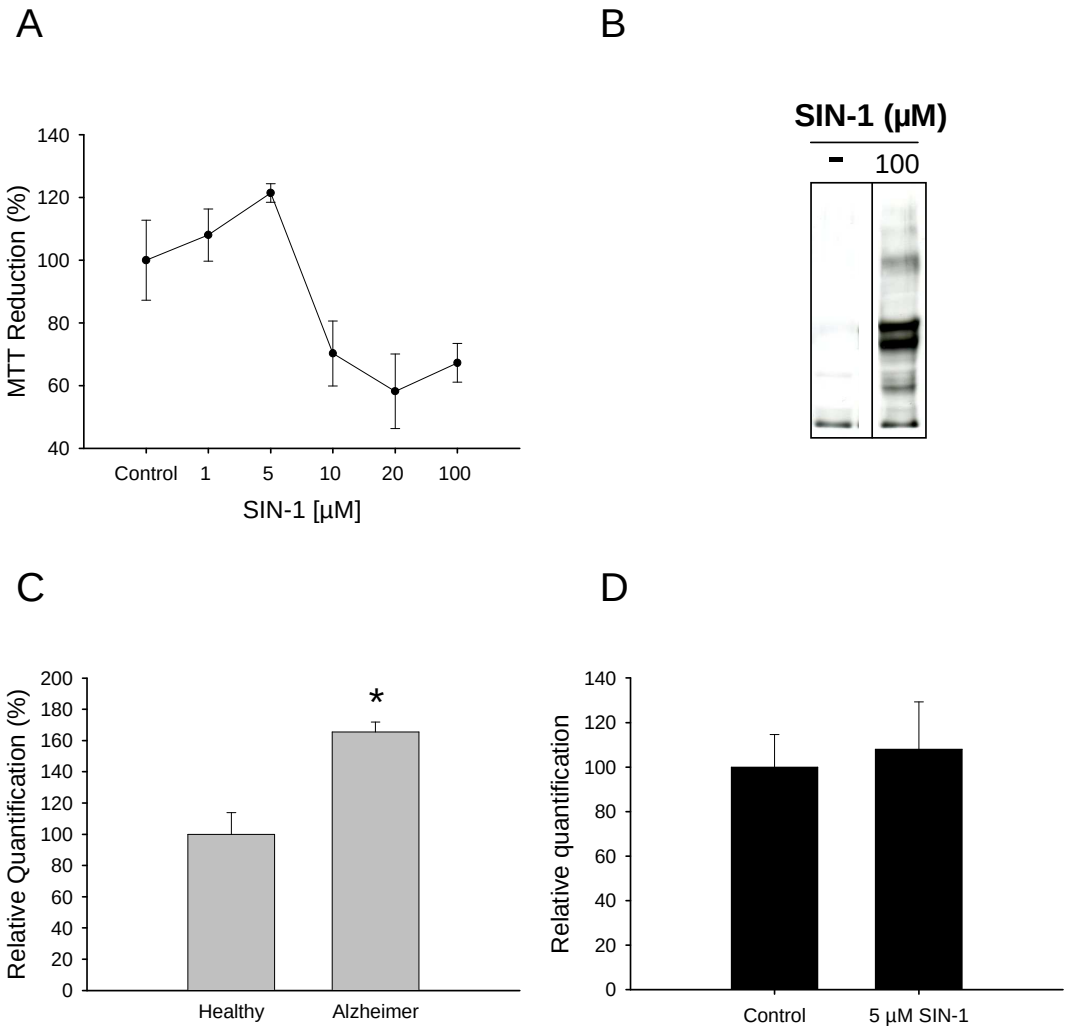

Fig. 1S. (A) Cell viability of HEK APPsw cells exposed to increasing SIN-1 concentration. Data are the mean ± SEM of 3 independent experiments. * p<0,01 by Student's t analysis. (B) PS1 western blot of SH-SY5Y cell lysates showing high molecular bands after treatment with a 100 µM SIN-1. (C) PS1 nitrotyrosination in healthy and AD cerebral cortex. Data are the mean ± SEM of 4 samples from different individuals. * p<0,01 by Student's t analysis. (D) Tubulin quantification as a control for the total protein charge, corresponding to the experiment in figure 2.

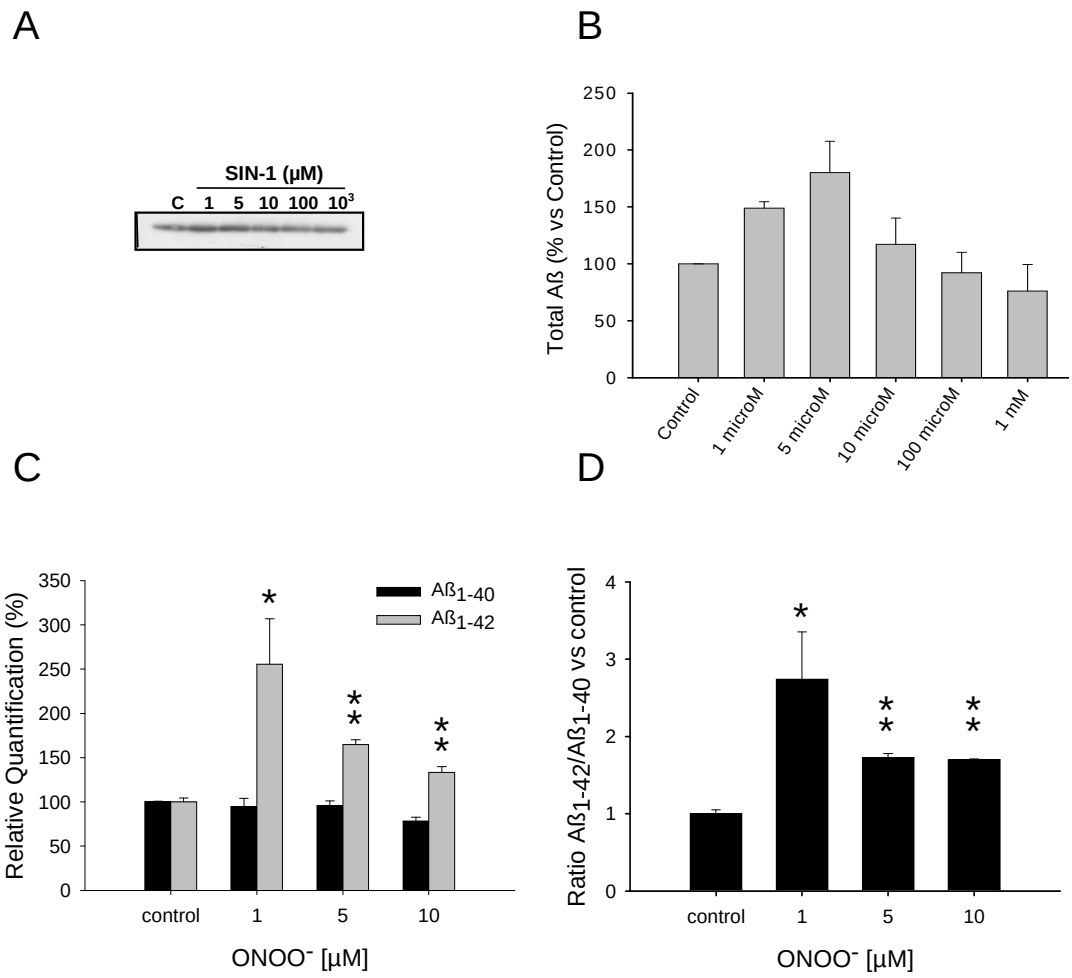

Fig. 2S. (A) Secreted Aß western blot from media of HEK APPsw cells exposure to increasing concentrations of SIN-1. (B) Quantification of secreted Aß western blots normalized by secreted αAPP. Data are the mean ± SEM of 3 independent experiments. * p<0,01 by Student's t analysis. (C,D) Secreted Aβ by HEK APPsw cells after exposure to peroxynitrite. The pattern resembles that of figure 3 where SIN-1 was used instead of peroxynitrite. Data are the mean ± SEM of 3 independent experiments. * p<0,05; ** p<0,01 by Student's t analysis.

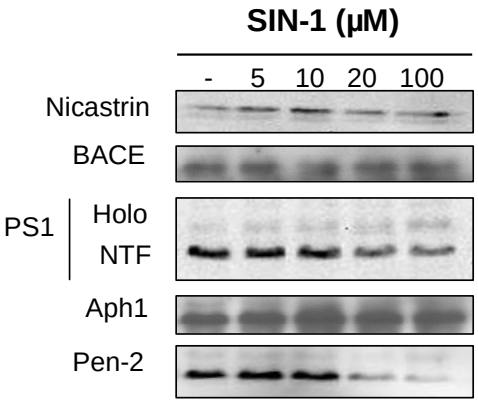
SIN-1 (μM)
- 5 10 20 100
Nicastrin
BACE
PS1
Holo
NTF
Aph1
Pen-2

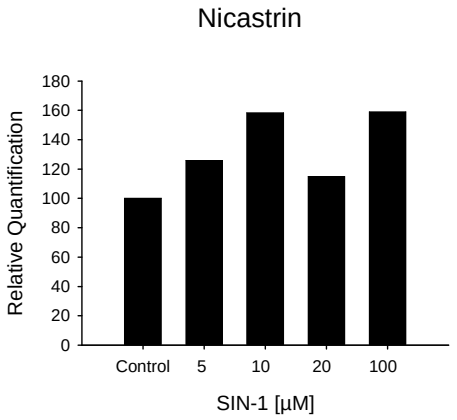
Nicastrin
Relative Quantification
0 20 40 60 80 100 120 140 160 180
Control 5 10 20 100
SIN-1 [μM]

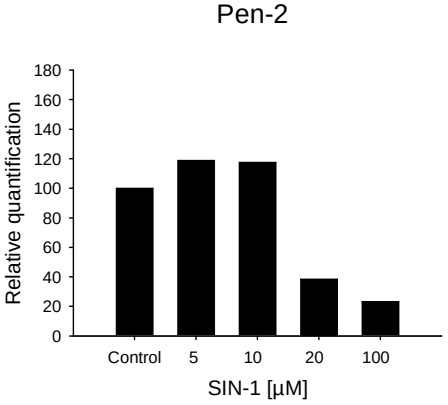
Pen-2
Relative quantification
0 20 40 60 80 100 120 140 160 180
Control 5 10 20 100
SIN-1 [μM]

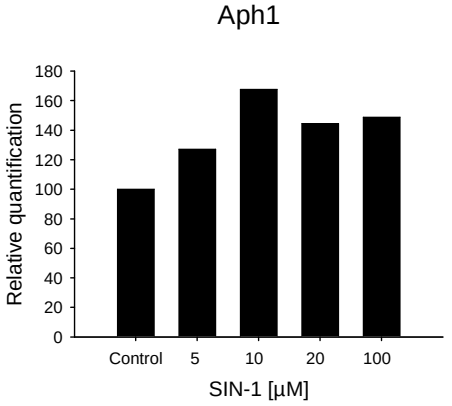
Aph1
Relative quantification
0 20 40 60 80 100 120 140 160 180
Control 5 10 20 100
SIN-1 [μM]

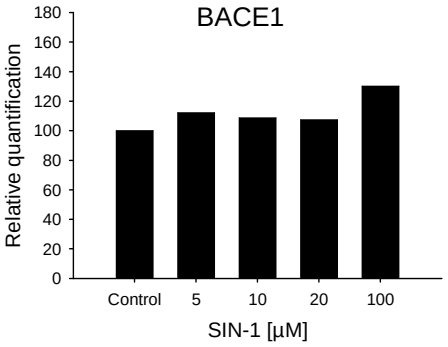
BACE1
Relative quantification
0 20 40 60 80 100 120 140 160 180
Control 5 10 20 100
SIN-1 [μM]

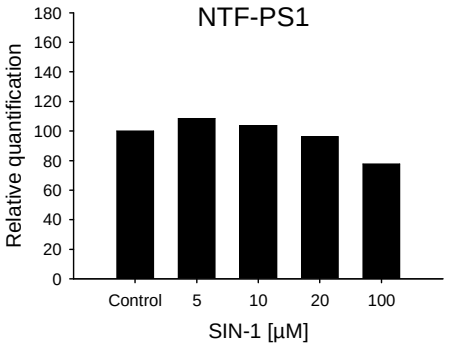
NTF-PS1
Relative quantification
0 20 40 60 80 100 120 140 160 180
Control 5 10 20 100
SIN-1 [μM]

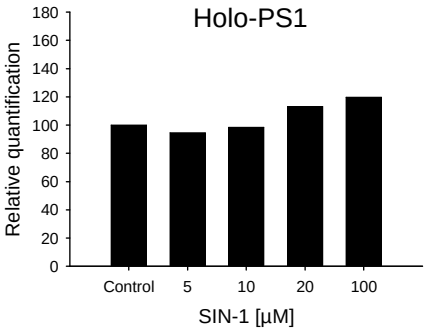
Holo-PS1
Relative quantification
0 20 40 60 80 100 120 140 160 180
Control 5 10 20 100
SIN-1 [μM]

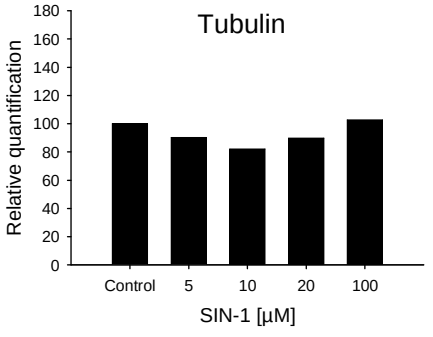
Tubulin
Relative quantification
0 20 40 60 80 100 120 140 160 180
Control 5 10 20 100
SIN-1 [μM]

Fig. 3S. Expression of the components of the γ-secretase complex in HEK APPsw cells, after exposure to increasing concentrations of SIN-1. At non-toxic concentrations, Pen-2, Aph1 and nicastrin tends to be increased, accordingly to the experiment shown in figure 2.

CHAPTER 2

"Amyloid-dependent triosephosphate isomerase nitrotyrosination induces glycation and tau fibrillation"

Francesc X. Guix, Gerard Ill-Raga, Ramona Bravo, Tadashi Nakaya, Gianni de Fabritiis, Mireia Coma, Gian Pietro Miscione, Jordi Villà-Freixa, Toshiharu Suzuki, Xavier Fernàndez-Busquets, Miguel A. Valverde, Bart de Strooper, and Francisco J. Muñoz.

Amyloid-dependent triosephosphate isomerase nitrotyrosination induces glycation and tau fibrillation

Francesc X. Guix[1,5], Gerard Ill-Raga[1], Ramona Bravo[2], Tadashi Nakaya[3], Gianni de Fabritiis[4], Mireia Coma[1], Gian Pietro Miscione[4], Jordi Villà-Freixa[4], Toshiharu Suzuki[3], Xavier Fernàndez-Busquets[2], Miguel A. Valverde[1], Bart de Strooper[5,6], and Francisco J. Muñoz[1 *]

[1] Laboratory of Molecular Physiology and Channelopathies, Department of Experimental and Health Sciences, Universitat Pompeu Fabra (UPF), Spain; [2] Biomolecular Interactions Team, Nanobioengineering Group, Institute for Bioengineering of Catalonia, and Nanoscience and Nanotechnology Institute, University of Barcelona, Barcelona Science Park; [3]Laboratory of Neuroscience, Graduate School of Pharmaceutical Sciences, Hokkaido University, Sapporo, Japan; [4] Unitat de Recerca en Informàtica Biomèdica, UPF-Institut Municipal d'Investigació Mèdica; [5] Department for developmental and molecular Genetics – VIB, Leuven, Belgium and [6]Center for Human Genetics, Kuleuven, Leuven; Gasthuisberg O&N, Leuven

Running title: NitroTPI glycates and aggregates tau

Total characters including spaces in the Title: 100

Total words in Summary: 149 words

Total words in the Text (figure legends and references not included): 5,205

[*]To whom correspondence should be addressed:

Dr. Francisco J. Muñoz
Grup de Fisiologia Molecular i Canalopaties
Departament de Ciències Experimentals i de la Salut
Universitat Pompeu Fabra
C/ Dr. Aiguader, 88, Barcelona 08003, Spain
Fax: +34 93 316 09 01; Phone: +34 93 316 08 52
e-mail: paco.munoz@upf.edu

Summary

Alzheimer's disease (AD) neuropathology is characterized by neuronal death, amyloid ß-peptide (Aß) deposits and neurofibrillary tangles (NFT) composed of paired helical filaments (PHF) of tau protein. Although crucial for our understanding of the pathogenesis of AD, the molecular mechanisms linking Aß and PHF still remain unknown. Here we show that Aß-induced nitro-oxidative damage promotes the nitrotyrosination of the glycolytic enzyme triosephosphate isomerase (TPI). It results in a decrease in the isomerase activity which yields a slowing in the glycolytic flow. Moreover, nitro-TPI triggers the production of the highly neurotoxic methylglyoxal. This finding correlates with the widespread glycation found in the cortex from AD patients and the hippocampus from double transgenic mice overexpressing the amyloid precursor protein and presenilin-1. Furthermore, nitro-TPI aggregates in beta-sheet structures and binds tau monomers inducing formation of PHF. Thus we demonstrate here a mechanism for Aß toxicity which could induce NFT formation in AD brains.

Key words: Alzheimer's disease; amyloid ß-peptide; tau protein; triosephosphate isomerase; peroxynitrite.

Nonstandard abbreviations used: Alzheimer's disease (AD); Atomic Force Microscopy (AFM); dihydroxyacetone phosphate (DHAP); D-glyceraldehyde 3-phosphate (GAP); methylglyoxal (MG); neurofibrillary tangles (NFT); paired helical filaments (PHF); peroxynitrite donor (SIN-1); presenilin 1 (PS1); Transmission electron microscopy (TEM); triosephosphate isomerase (TPI).

Introduction

Since the characterization of amyloid ß-peptide (Aß) deposition (Masters and Beyreuther, 2006) and the subsequent formation of neurofibrillary tangles (NFT) (Brion et al., 1985; Iqbal et al., 1984) as the two defining pathological hallmarks of Alzheimer's disease (AD), a fair amount of research on AD has been directed towards the identification of the molecular mechanism linking Aß and NFT. Interestingly, aggregation of Aß (either in oligomeric or insoluble mature fibrils) is mainly extracellular while NFT (composed of paired helical filaments (PHF) of tau protein) appear intracellularly (Gotz et al., 2001; Alonso et al., 2008). In addition to this spatial segregation, Aß accumulation and NFT also show temporal separation in AD brains, i.e., Aß accumulation appears before NFT (Gotz et al., 2001; Del Toro et al., 2005). Altogether, the existing data suggest a hierarchical relationship between Aß and tau, although the underlying mechanisms are unknown. The activation of phosphorylation pathways (Liou et al., 2003; Bhat et al., 2004; Otth et al., 2002) is the current hypothesis associating Aß and PHF, but the fact that PHF formation can occur in the absence of tau phosphorylation (Chang et al., 2008; Mudher and Lovestone, 2002) suggests that phosphorylation rather than a trigger is an enhancer of tau fibrillization (Kuret et al., 2005). Thus, the crucial questions of what unleashes PHF formation and which are the mechanisms linking Aß and PHF remain unanswered at the molecular level.

AD, as other amyloidoses, presents insoluble accumulations of ß-sheet containing proteins, which otherwise should be soluble in biological fluids. A widely accepted view is that the process is entirely pathological, requiring triggers that relieve the conformational barrier to spontaneous protein aggregation. These can be of genetic origin, e.g., disease-causing mutations in the proteins themselves or in regulators of their metabolism. In the case of the tau protein, mutations in its encoding gene do not

generate AD, but are responsible for another neurodegenerative disorder known as frontotemporal dementia with Parkinsonism (reviewed in Wszolek et al., 2006). Alternatively, increased expression of tau protein, but also other changes in the cellular environment like the presence of agents that act as seeds for heterogeneous nucleation and aggregation, such as anionic surfactants and polyanions (Sibille et al., 2006; Chirita et al., 2003) can induce tangle formation. However, none of these mechanisms have provided insight into the molecular link between Aß and NFT.

TPI is a key enzyme in cell metabolism that controls the glycolytic flow and energy production through the interconversion of dihydroxyacetone phosphate (DHAP) and D-glyceraldehyde 3-phosphate (G3P) (Richard, 1993). Notably, TPI is the only glycolytic enzyme whose functional deficiency is associated to neurodegeneration (Eber et al., 1991; Ovadi et al., 2004). In particular, inefficient glycolysis (Hoyer et al., 1988) and ATP depletion (Keil et al., 2004) are characteristic in AD brains. Nitrotyrosination of TPI occurs in AD (Coma et al., 2005) as the result of Aß-dependent oxidative stress due to the formation of the powerful nitrating agent peroxynitrite by the reaction of nitric oxide and superoxide anion (Coma et al., 2005; Guix et al., 2005).

Here, we have discovered a mechanism that can account for the spatial and temporal progression from Aß toxicity to NFT in AD brain. Aβ-induced oxidative and nitrative stress, induces nitrotyrosination of TPI, a key enzyme of the glycolysis pathway. This causes the generation of toxic intermediates and abnormal glycation of proteins, and also a conformational change in TPI itself, making it prone to aggregate. More interestingly, the nitrotyronisated TPI is able to induce a conformational change in tau and precipitates PHF formation.

Materials and methods

Materials

Synthetic Aß peptide corresponding to the human $Aß_{1-40}$ Dutch variant containing the glutamic acid to glutamine substitution ($Aß_{E22Q}$) was purchased from Oncogene. $Aß_{E22Q}$ produces more stable fibrils than wild-type Aß, but there are no differences in the amyloidogenic properties of both species. Rabbit TPI, SIN-1 and Protein G immobilized on sepharose were purchased from Sigma-Aldrich.

Human brain samples

Human brain tissue sections and samples were supplied by the Banc de Teixits Neurològics (Serveis Científico-Tècnics, Hospital Clínic, Universitat de Barcelona), the Unitat d'Anatomia Patològica (Hospital del Mar) and the Unitat de Nauropatología y Banco de Cerebros (Fundación Hospital Alcorcón). The procedure was approved by the ethics committee of the Institut Municipal d'Investigacions Mèdiques-Universitat Pompeu Fabra. Brain sections (5 µm) were obtained from the frontal cortex of 4 healthy aged individuals and 5 AD patients at stage VI. Brain samples from the frontal cortex of 2 individuals with Parkinson's disease and 2 with frontotemporal dementia were also used in the study. Samples used in the biochemical studies were from 9 control individuals and 13 AD patients. 500 mg of either frontal cortex or hippocampus were homogenized at 4ºC with 500 µL of a cocktail containing 480 µL NP40 lysis buffer (150 mM NaCl, 5 mM EDTA, 1% Nonidet P-40, 1 mM sodium orthovanadate, 1 mM phenylmethylsulphonyl fluoride, 0.05% aprotinin, 1mM dithioltreitol) and 120 µL of protease inhibitors (Complete mini-EDTA free) from Roche Diagnostics GmbH.

Lysates were shaked at 4ºC for 30 min and centrifuged at 13,000 rpm for 15 min. Proteins in the supernatant were quantified with the Bradford assay.

Mice brain samples

Cerebral paraffined slides from wild type black mice or APPswe/PS1 L166P mice were deparaffined with Clear Rite 3 and subsequent washes with decreasing ethanol dilutions. The Tyramide Signal Amplification kit (PerkinElmer) was used for the inmunofluorescence, following the instructions given by the company. Briefly, slides were incubated 7 min with a 70 % formic acid solution in order to expose the epitopes. After 1h of quenching endogenous peroxidase activity with a 30 % H_2O_2 solution, slides were blocked 1h at RT with 2% normal serum in TNB blocking buffer. The same solution was used to dilute 1:100 the following primary antibodies: anti-TPI (ProteinTech Group, Chicago), 6E10 anti-Aβ, anti-MG (CosmoBio) and anti-nitrotyrosine (Abcam). The primary antibodies were incubated overnight at 4 ºC. The secondary antibodies were diluted 1:500 in TNB blocking solution without serum with the exception of the anti-MG, which was diluted 1:200. Slides were developed by 6 min incubation with the Tyr-FITC reagent at darkness (1:50 in 1x Reagent Diluent). All the washes were performed with TNT 1x buffer. For the TPI-amyloid colocalization study a HRP-bound antibody against rabbit was used. For the MG-amyloid colocalization study a HRP-bound antibody against mouse was used together with a co-staining with thioflavine T to detect amyloid deposits.

Western blot

Gels were transferred to nitrocellulose membranes and incubated for 2 h at room temperature with a rabbit anti-nitrotyrosine polyclonal antibody (1:1000, Invitrogen), a

sheep anti-TPI polyclonal antibody (1:200, Nordic), a mouse anti-tau monoclonal antibody (1:1000, Santa Cruz) or a mouse anti-argpyrimidine antibody (1:1000, CosmoBio). Donkey anti-rabbit and donkey anti-sheep peroxidase-conjugated secondary antibodies (1:5,000, Amersham Bioscience) were incubated for 1 h at room temperature. Bands were visualized using the enhanced chemiluminescence substrate (Super Signal; Pierce) and the Hyperfilm ECL kit from Amersham Bioscience.

Immunoprecipitation

500 μg of total protein from brains or SH-SY5Y cells (human neuroblastoma cells) lysates were incubated with 1.25 μg of anti-TPI polyclonal antibody overnight at 4 ºC. Following the addition of protein G immobilized on sepharose (Sigma), samples were shaken for 2 h at room temperature. Aggregates were pulled down by centrifugation at 10,000 rpm for 10 min and washed thrice. Protein G and antibody were removed from the immunoprecipitated proteins by boiling the samples for 6 min at 100 ºC.

Quantification of nitrotyrosinated TPI in brains

TPI was inmunoprecipitated from either cerebral cortex or hippocampus of control and AD patients. Samples were resuspended in 100 μL of basic PBS (pH 12) and boiled before the removal of protein G by centrifugation. Nextly, absorbance was measured at 420 nm to determine the amount of nitrotyrosines in the samples. Free nitrotyrosine (Sigma) was used to make a standard curve.

Immunohistochemistry and immunofluorescence

Frontal cortex sections were pretreated with 50% formic acid for 1 min to expose TPI epitopes. Sections were treated with 4% H_2O_2 and incubated with rabbit anti-

nitrotyrosine polyclonal antibody (1:500) for 2 h at room temperature followed by the incubation with donkey anti-rabbit peroxidase-conjugated antibody (1:500) for 1 h at room temperature. Contiguous sections were incubated with sheep anti-TPI polyclonal antibody (1:100) and donkey anti-sheep peroxidase-conjugated antibody (1:500) for 1 h at room temperature. Slides were treated with Peroxidase Substrate Kit DAB (Vector). Samples were counterstained with hematoxylin, dehydrated and fixed with Eukitt (O.Kindler GmbH &CO). Representative digital images were taken with a Leica DMR microscope and analyzed with Leica IM50 software. To demonstrate the presence of MG in the human samples from AD brains the slides were analyzed by inmunofluorescence following the protocol previously mentioned. The content of MG was determined with an anti-MG monoclonal antibody. The inmunofluorescence experiment on tissue slides was performed as explained previously for the mice brain samples.

For the immunofluorescence experiment on TPI aggregates two different secondary antibodies were used: an Alexa568-bound rabbit antibody for TPI and an Alexa488 –bound mouse antibody for tau. As a negative control a primary antibody against human syntaxin 1A was used.

Overexpression of TPI in HEK cells

TPI was amplified by PCR from purified human chromosomal DNA and cloned into a construct containing a 5'upstream Flag sequence. A TPI carrying double tyrosine mutation (Y164F/Y208F) was generated and cloned into the same construct. HEK cells were seeded in 6-well plates at a density of 500,000 cells per well and grown for 12h with Dulbecco's modified Eagle's medium (DMEM) supplemented with 10% FBS. Afterwards, 2 μg per well of each contruct was transfected using 2 μL Lipofectamine

2000 (Invitrogen). After 24h, the medium was substituted by DMEM without FBS and cells were treated with 0.5 μM pre-aggregated Aβ or left without treatment (mock). After 24h, cells were lysed and TPI was inmunoprecipitated with an anti-Flag antibody (Sigma). A western blot was run and an anti-nitrotyrosine antibody used to visualize the bands.

TPI nitration *in vitro*

Rabbit TPI (1.25 μg/μL unless otherwise indicated) was dissolved in 50 mM tetraethylammoniun (pH 7.4-7.6) and exposed to SIN-1 at the concentrations specified in each assay. Nitration process was carried out under shaking at 300 rpm for 3 hours and at room temperature. SIN-1 was eliminated from the samples with a PD-10 desalting column (Amersham). The elution profile is shown in the supplementary material.

Kinetic studies and MG measurement

The isomerase activity of TPI was measured spectrophotometrically using glyceraldehyde 3-phosphate (G3P) or dihydroxyacetone phosphate (DHAP) as substrates and coupling the products obtained to α-glycerophosphate dehydrogenase or G3P dehydrogenase respectively. The final volume was 500 μL in both cases. The assay mixture for the G3P to DHAP direction contained 50 mM triethanolamine/HCl (pH 7.6), 0.2 mM NADH, 0.1 mM EDTA, D,L-G3P (1, 0.5, 0.33, 0.2 and 0.05 mM), 3 ng of TPI and 0.9 units of α-glycerophosphate dehydrogenase**.** The assay mixture for the DHAP to G3P direction contained 50 mM triethanolamine/HCl (pH 7.4), 0.72 mM NAD^+, 0.47 mM Na_3AsO_4, DHAP (0.3, 0.6, 1.2, 2.4, 4.8 and 9,5 mM), 10 ng of TPI and 3.24 units of α-glycerophosphate dehydrogenase**.** MG generated during the isomerization reaction

was quantified in both reactions enzymatically through conversion to S-lactoyl glutathione by glyoxalase I, and the reaction was followed spectrophotometrically at 240 nm. Initial velocity mean for each substrate concentration was transformed to be plotted on a Eadie-Hofstee graph (to calculate Km) or on a Woolf-Hanes graph (to calculate Vmax). Values of $p<0.05$ were obtained for all the parameters of the linear regression models after student's t test statistical analysis.

Computational modeling of TPI

The crystal structure was downloaded from the PDB data bank (PDB:8TIM). Using the package VMD [VMD], we have selected chain A for the molecular dynamics simulations. The protein was solvated in TIP3P water and ion to neutralize the charge for a total system size of around 50 thousand atoms. Using the molecular dynamics package NAMD2.6 [NAMD], the protein restrained with a harmonic potential of 25 Kcal/mol the entire system was energy minimized for 1000 steps and thermalized reinitializing atom velocities twice. The constrained was then removed and the system equilibrated for further 10 ps. Finally a Langevin piston barostat at 1 atm was applied for 3 ns. The production run consists of 4 ns of simulation in the same condition. The most important simulation parameters setting are: time step of 2 fs, a cut of 12 A and update of the pairlist every 20 iterations, long range forces are computed every 4 fs and long range electrostatic was resolved with the PME method with at least one grid point each Angstrom. Four tyrosines are present for each monomer of TPI. The first two Y47 and Y67 stays at the interface of the dimer in opposite orientations, such that tyrosines from different monomers do not face each other, while the remaining two Y164 and Y208 are interacting directly and sit very close to the catalytic site E165 and a large loop overshading the catalytic site formed by at least K13, H95 and E165. Y208 is hydrogen

bonded with A176 in this loop effectively shortening the length of the loop with a short pinch. The deprotonated tyrosines were modeled by removing the hydrogen atom of the hydrophilic end of the tyrosines Y164 and Y208 and by assigning a total -1 charge to each. The other two tyrosines far away from the catalytic site are left in the native state. From the equilibrated structure a 10 ns simulation with the deprotonated tyrosines was run.

Turbidometric analysis

Turbidometric experiments were carried out at room temperature, within a dark chamber in a 96-wells plate under continuous shaking (300 rpm). The protein concentration of the wells containing rabbit TPI or bovine RNase was 2.5 μg/μL. Final volume for all the wells was 100 μL. Specific conditions for each well are indicated in the legend of the Fig 3.

Thioflavin staining

Control and nitrotyrosinated TPI were shaked at 300 rpm and at room temperature for 1 day or 5 days. Before microscope observation, Thioflavin T (1 mM) was added to each sample at 1:1 (v/v) and incubated in the darkness for 15 min. Samples were put on coverslips and examined under blue light with a Leica DMR microscope coupled to a DFC300 FX camera. Representative images were taken with the Leica IM50 software.

Transmission electron microscopy

Mesh nickel grids were charged with UV light for 5 min and set on a drop of sample for 1 min. Then 3 consecutive washes with milliQ water were carried out (1 min in total).

Finally the grid was set on a drop of 2% uranil acetate solution for 1 min and dried. Samples were observed with a Jeol 1010 electron microscope.

Atomic force microscopy

Imaging was performed with a commercial MultiMode atomic force microscope controlled by a Nanoscope IV electronics (Digital Instruments) equipped with either a 12-μm scanner (E-scanner) or a 120-μm scanner (J-scanner). Except where otherwise indicated, all images were taken in liquid using a tapping-mode liquid cell without the O-ring seal. Oxide-sharpened pyramidal Si_3N_4 tips mounted on triangular 100-μm long cantilevers (k = 0.08 N/m) were purchased from Olympus. The liquid cell and the tip were cleaned with ethanol and thoroughly rinsed with deionized water before use. For high-resolution imaging the microscope head was placed on a vibration-isolated stone plate. After the indicated incubation times and immediately before imaging, 10 μL of the sample were allowed to adsorb for about 5-10 min at room temperature on freshly cleaved muscovita mica (Asheville-Schoonmaker Mica Co.) or highly ordered pyrolytic graphite (Nt-MDT Co.), and finally overlaid with ~100 μL of incubation buffer.

Confocal microscopy

TPI immunoprecipitated from healthy or Alzheimer cortex was immobilized on microscope coverslides coated with gelatin (5% in deionized water). Samples were fixed with a solution of 4% formaldehyde for 30 min and incubated for 2 h at room temperature with a mouse anti-phospho-tau monoclonal antibody (1:1,000 Innogenetics) followed by incubation with Alexa fluor 488 goat anti-mouse polyclonal antibody (1:500) for 1 h at room temperature. Digital images were taken with a Leica TCS SP confocal microscope and analyzed with Leica confocal software.

Results

Aβ promotes TPI nitrotyrosination *in vitro* and in AD

Aß induced nitro-oxidative stress on human neuroblastoma cells results in nitrotyrosination of TPI (Fig. 1A). Double transgenic mice overexpressing APP and presenilin 1 (PS1), showed TPI aggregates (Fig. 1B) and nitrotyrosination (Fig. 1C) in identical hippocampal areas. Similarly, colocalization of TPI (Fig. 1D) and anti-nitrotyrosine staining (Fig. 1E) was found in the parenchyma of human AD brains. Moreover, higher levels of nitro-TPI were also detected in extracts from hippocampus (Fig. 1F) and frontal cortex (Fig. 1G) obtained from AD brains, compared to healthy subjects.

Aß-induced TPI nitrotyrosination causes a loss of enzymatic specificity

TPI has four Tyr residues. Tyr164 and Tyr208 are more prone to modification by nitric oxid because they are in the proximity of negative charged amino acids and also more exposed to external agent (Fig. S1). We modelled the functional consequences of TPI nitrotyrosination using full-atom molecular dynamics. The loop 6 (Fig. S1) is very flexible and plays an important role in the reactivity of the enzyme (Alber et al., 1981). Nitration of Tyr164 and Tyr208 would destabilize the close state of loop 6 because the interaction between Tyr208 and Ala176 through an H-bond gets compromised (Fig. 2A-B; Fig. S2). Indeed, purified TPI after nitrotyrosination with a peroxynitrite donor (SIN-1) displayed a significant decrease in isomerase activity in both directions of the catalysis, i.e. using DHAP (Fig. 2C) or GAP (Fig. 2D) as substrate. The specific enzymatic activity constants (K_{cat}/K_m) were 0.13±0.007 mM^{-1} min^{-1} for control TPI and 0.06±0.02 mM^{-1} min^{-1} for nitro TPI using DHAP as substrate, and 3.49±2.30 mM^{-1} min^{-}

^{1} for control TPI and 0.87±0.41 mM^{-1} min^{-1} for nitro TPI using GAP as substrate (see Fig. S3 and table in supplementary materials). Decreased isomerase activity should slow the glycolytic flow and reduce ATP formation. The isomerisation of DHAP and GAP proceeds through an enediol phosphate. This intermediate is very unstable and can suffer ω-elimination of the phosphate group to yield inorganic phosphate and methylglyoxal (MG) (Ovadi et al., 2004; Richard, 1993). MG is a toxic compound involved in advanced glycation end-products formation (Kuhla et al., 2005; Richard, 1993). In accordance with the decreased efficiency of nitro-TPI we found a significant increase in MG production ($p<0.05$), independent of whether DHAP or GAP was used as substrate (Fig. 2E). Thus, nitrotyrosination of TPI results in reduced catalytic activity and increased occupancy of the enzyme by the substrate, and consequently, a higher production of the toxic MG. This hypothesis was confirmed using HEK cells overexpressing wild-type and mutant TPI (Tyr164Phe and Tyr208Phe mutations that mimic the effect of nitrotyrosination on loop stability). Mutant TPI showed increased MG production, detected by western blots using anti-argpyrimidin which recognizes products of aminoacid glycation (Fig. 2F).

Interestingly, brains of double transgenic mice showed overlapping Aß deposits (Fig. 3A and 3C) with TPI (Fig. 3B) and MG positive areas (Fig. 3D) in the hippocampus. Moreover TPI (Fig. 3E) co-localized with MG (Fig. 3F) in mice. MG levels were significantly higher in human AD brains (Fig. 3H) than in healthy controls (Fig. 3G), corroborating the pathological significance of our biochemical findings.

TPI nitrotyrosination induces its aggregation

TPI belongs to the class of the α/β barrel enzymes (Dabrowska et al., 1978; Pompliano et al., 1990). TPI contains ß strands (Dabrowska et al., 1978) and a TPI fragment 186–

218 from the N-terminal of region III is able to form amyloid-like fibrils *in vitro* (Contreras et al., 1999). Turbidometric analysis of TPI in solution demonstrated rapid induction of TPI aggregation upon nitrotyrosination with SIN-1 (Fig. 4A), resulting in the appearance of multimeric TPI bands of higher electrophoretic mobility (Fig. 4B). RNAse (also a dimeric protein with several Tyr) did not aggregate upon SIN-1 treatment, suggesting that this effect was rather specific for TPI (Fig. S4). Transmission electron microscopy (TEM) analysis identified large aggregates of nitro-TPI (Fig. 4D), which were not appearing in the control TPI reaction (Fig. 4C). TPI also aggregates *in vivo*. When TPI was immunoprecipitated from human cortex (Fig. 4E-F; S5) and hippocampus (Fig. S5), large protein aggregates were obtained from AD brains and not from healthy controls. Nitro-TPI aggregates generated *in vitro* exhibited positive thioflavin staining at day five (insets Fig. 4C-D), further confirming that TPI aggregates displayed ß-sheet structure (Grabowski et al., 2001). These nitro-TPI aggregates continue to produce toxic MG. We reasoned that these TPI aggregates, due to their amyloid-like structure, might also act as nucleation centers for fibrillation of other intracellular proteins in the cell (inset Fig. 4F). TPI aggregation could also affect substrate access to and occupancy of the catalytic center, thereby, contributing to the increased MG production.

Nitrotyrosinated TPI interacts with tau protein to form PHFs

Mutations in TPI make it more prone to associate with and influence assembly of brain microtubules (Orosz et al., 2000). Therefore, we addressed the possibility that nitrotyrosinated TPI might provide a nucleation center for tau aggregation and subsequent PHF formation. Human neuroblastoma cells were treated with increasing concentrations of Aß and proteins were immunoprecipitated with anti-TPI antibody.

Tau-positive material was present in the immunoprecipitates indicating that tau becomes associated to nitroTPI in an Aß dose-dependent pattern (Fig. 5A). This interaction was critically dependent on the nitrotyrosination of TPI, as treatment with 2-phenyl-4,4,5,5,-tetramethylimidazoline-1-oxyl 3-oxide (PTIO; a NO scavenger) or the free radical scavenger (trolox) markedly reduced the binding of tau to TPI in the presence of Aß (Fig. 5B). The unspecific TPI binding to protein G sepharose was excluded (Fig. 5C, E, F and G). In triple transgenic mice that overexpressed APP, PS1 and tau (Oddo et al., 2003) we found a massive presence of tau (50 Kda isoform) in the TPI immunoprecipitated material (Fig. 5E, 6 and S6). Similarly, tau immunoreactivity associated with immunoprecipitated TPI was detected in samples obtained from human AD cortex but not from healthy subjects (Fig. 5F, 6 and S6). Tau binding to TPI seems rather specific for AD brain as cortex samples from Parkinson's disease and frontotemporal dementia patients turned out to be negative for tau in the TPI immunoprecipitates (Fig. G). TPI immunoprecipitates tau in both AD brains and transgenic mice but no another protein highly expressed in brain such as syntaxin 1A (Fig. 6).

We further investigated how nitro-TPI affected tau aggregation *in vitro*. TPI and nitro-TPI were incubated with tau protein and samples were analysed by Atomic Force Microscopy (AFM) (Fig. 7A-D) and TEM (Fig. 7F and 7G). Abundant PHF-like structures were found in samples containing nitro-TPI plus tau (Fig. 7C and 7D) with the characteristic twisted fibrils structure that is also seen in twisted PHF in AD brains (Fig. 7D) (Herzig et al., 2006). Samples containing tau plus unmodified TPI showed only few fibrillar aggregates, not displaying PHF structure (Fig. 7A and 7B). In control experiments using another nitrosylated cytoplasmic? Protein, nitro-human RNAse 3, no PHF formation was observed, indicating specificity of our observations (Fig. S7). In

agreement with the AFM data, western blot analysis of the samples revealed that, unlike control TPI, nitro-TPI induced stable PHFs that did not enter into the SDS gel (Fig. 7E). Nitro-TPI promoted PHFs at very low tau concentrations (65 nM) which are well below the concentrations (1-10 μM) used in previous studies to trigger PHF formation with exogenous triggers such as heparin, anionic surfactants and calcium (Grabowski et al., 2001).

Discussion

In the present work we have studied the possible pathophysiological relevance of TPI nitrotyrosination in AD. First, we have demonstrated that Aß induces TPI nitrotyrosination in neuronal cells. Accordingly, TPI nitrotyrosination was also observed in the brain of AD patients and mice overexpressing both APP and PS1, but not in control brains. Second, the Aß-induced nitrosylation of TPI affects its function and could result in inefficient glycolysis in AD. In fact, ATP depletion has been reported in AD patients (Hoyer et al., 1988). TPI nitrotyrosination decreased both isomerase activities, which slows the glycolytic flow and the ATP formation and, will likely, result in decreased production of acetyl-coenzyme A (Acetyl-CoA) as well. A reduction in the bioavailability of acetyl-CoA, a precursor of acetylcholine synthesis, could be contributing to the characteristic cholinergic deficit in AD. Moreover, TPI is the only glycolytic enzyme that has been implicated before in neurodegeneration (Eber et al., 1991; Ovadi et al., 2004; Valentin et al., 2000). In all these studies high levels of DHAP are found as a result of decreased TPI isomerase activity, and DHAP is the main source for toxic MG production. MG is a very unstable intermediate and toxic triose involved in AGEs formation and implicated before in AD pathogenesis (Ahmed et al., 2003). TPI prevents MG production by folding its loop 6 over the catalytic centre when the

substrate binds. Nitration of Y164 keeps loop 6 open via a hydrogen bond with T168, allowing the entry of water into the active siten resulting in the hydrolysis of the phosphate of the enediol intermediate to yield MG.

On the other hand, mutated TPI becomes misfolded forming several ß strands (Rice et al., 1990) and such misfolded protein could also promote neurodegenerative disease (Olah et al., 2002). Some mutations in TPI make it more prone to associate to brain microtubules, which influences their polymerization (Orosz et al., 2000). Interestingly, a fragment of TPI is structurally homologous to the Aß peptide and is able to form amyloid *in vitro* (Contreras et al., 1999). We have demonstrated that nitrotyrosination induces indeed the aggregation of TPI. This nitrotyrosinated TPI forms large structures with ß-sheet folds, that are induced in neurons cultured in vitro in the presence of Aß and, importantly, are observed in cortex from AD brain. The large size of nitrotyrosinated TPI aggregates make them resistant to degradation by the proteosome. Then they can grow and act as intracellular “seeds” for the fibrillation of other proteins due to its amyloid-like structure.

NFT formation due to tau aggregation is considered a key event in AD neurodegeneration. Neurons bearing NFTs, are not necessarily dead but unable to communicate with other neurons due to the disruption of the cytoskeleton. NFTs are downstream of Aß action since mutations in human amyloid precursor protein (APP) produce an early onset of AD with NFTs present in the brains of these patients (Cras et al., 1998; Sturchler-Pierrat and Sommer, 1999). On the other hand, mutations in human tau producing frontal dementia do not show any alteration of Aß (Yancopoulou et al., 2003). Despite all these evidences relating Aß to NFT formation, there is no experimental explanation for the link between these two major events in AD. The participation of cyclin-dependent kinases (Maccioni et al., 2001) or glycogen synthase

kinase-3ß (Bhat et al., 2004) signalling are among the few hypothesis attempting to explain this link at a molecular level, although it remains unexplained how Aß would then trigger the generation of PHFs. Hyperphosphorylation of PHFs has been proposed to mediate PHF formation, but a phosphorylation-independent mechanism is also involved in the PHF formation (Goedert et al., 1996). We demonstrate here a direct association between PHF and nitrotyrosinated TPI in AD brains. This association appears rather specific as a limited survey of material obtained from Parkinson's disease and fronto temporal dementia did not reveal association of TPI and tau in co-immunoprecipitation experiments. Therefore, and based on our cellular experiments, we speculate that the nitrative stress induced by Aβ in AD is critical for nitro-TPI induced tau aggregation. Moreover, nitrotyrosinated TPI aggregates induce the fibrillation of tau to form PHFs in the absence of tau phosphorylation. It is conceivable that hyperphosphorylation of tau is an event posterior to PHF formation. The conformational changes of tau aggregated into PHFs could indeed expose the phosphorylation sites to kinases.

In summary, our data show that nitrotyrosinated TPI might affect multiple mechanisms relevant to the pathophysiology of AD. It compromises cellular metabolism by reducing the glycolytic flow and ATP generation and by increasing the production of methylglioxal. More interestingly, nitro-TPI adopts a ß-sheet structure with the capability to trigger PHF formation in the absence of tau phosphorylation. Finally, our results provide also a mechanistic explanation linking oxidative stress, which is at the core of the etiopathogenic loop described in sporadic AD (Frederikse et al., 1996; Miranda et al., 2000; Opazo et al., 2002), via the production of peroxynitrite and nitrotyrosination of TPI, to Aß-induced toxicity and tau pathology.

Funding

Work supported by Spanish Ministerio de Sanidad (FIS: PRO1208; Red HERACLES RD06/0009/002), Educación y Ciencia (BIO2005-01591; SAF2006-4973; CSD2006-00012), Generalitat de Catalunya (GSR2005-266; 2005-SGR00037); and the EC funded STREP project QosCosGrid (IST-033883) and VPH NOE (ICT-223920). Work in the lab of BDS is supported by a Methusalem grant of the Flemish government, and by funds of VIB and KUL.

Acknowledgements

We acknowledge to the Banc de Teixit Neurologic del Hospital Clinic de Barcelona and to Unidad de Neuropatología y Banco de Cerebros of Fundación Hospital Alcorcón for providing the brain samples. We acknowledge David Andreu for technical support and Dr. Frank LaFerla for providing us mice material. Finally, we acknowledge the computer resources, technical expertise and assistance provided by the Barcelona Supercomputing Center**.**

Supplementary online material

Figure S1: TPI conformational changes upon substrate binding

Figure S2: Zoom in the region controlling the L6 conformation

Figure S3: Kinetic study of normal and nitrotyrosinated TPI.

Figure S4: Nitrotyrosination is inducing TPI aggregation but not for RNAse.

Figure S5: Electron microscopy images from TPI aggregates.

Figure S6: Inmunofluorescence analysis of TPI aggregates from human cerebral cortex of healthy and AD patients, and hippocampus of AD patients.

Figure S7: PHFs were not obtained when tau was incubated with nitro-RNAse.

Table 1: Kinetic parameters of normal and nitro-TPI.

FIGURE 1

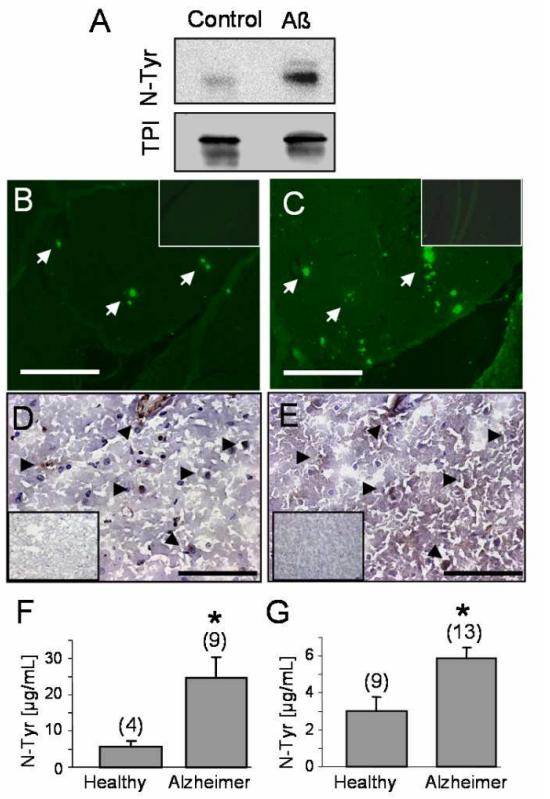

Fig. 1 TPI nitrotyrosination is dependent on the Aβ presence. (**A**) SH-SY5Y cells were treated with 1 µM $Aß_{1-42}$ and TPI was immunoprecipitated. Blots were performed with either anti-nitrotyrosine or anti-TPI antibodies. (**B, C**) Hippocampus from double transgenic mice overexpressing APP and PS1, and (**D, E**) frontal cortex sections obtained from AD brain patients were immunostained with antibodies against (**B, D)** TPI or (**C**, **E**) against nitrotyrosine. No staining is shown in wild-type mice for (inset **B**) TPI and (inset **C**) nitrotyrosine, and in healthy human controls for (inset **D**) TPI and (inset **E**) nitrotyrosine. Bars are 250 µm (**B**, **C**) and 98 µm (**D**, **E**). TPI was immunoprecipitated from healthy and AD (**F**) hippocampus or (**G**) cortex and nitrotyrosine was measured. The number of independent samples is indicated between brackets; * $p < 0.05$ by student's t analysis.

FIGURE 2

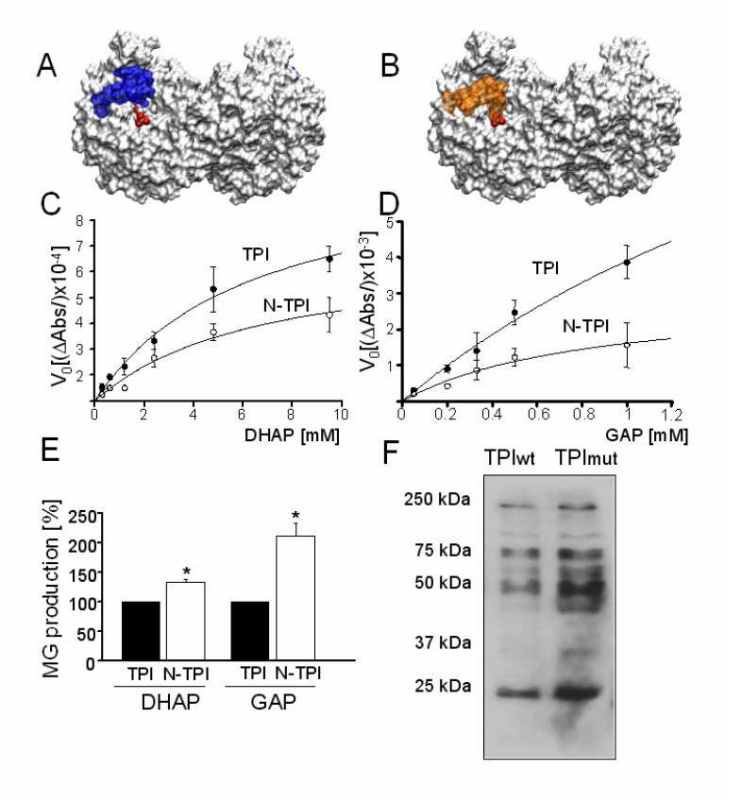

Fig. 2 TPI nitrotyrosination induces a decrease in its isomerase activity but an increase in MG production. (**A**) The solvent surface accessible area (SASA) of the TPI enzyme (PDB:1NEY) in its dimmer conformation is computed over the average conformation of a multi nanosecond trajectory of a molecular dynamics run (white surface) bound with the DHAP substrate in the catalytic site. (**B**) The same loop is plotted in orange in a similar simulation but introducing nitrated tyrosines at 164 and 208. In average the loop assumes a more closed conformation. Nitrotyrosination decreases the catalytic efficiency of TPI. The activity of control and nitrotyrosinated TPI was measured in both directions (**C**) from DHAP to GAP and (**D**) from GAP to DHAP. The respective Michaelis-Menten curves show that the nitrotyrosination of TPI produces a significant decrease in the TPI isomerase activity of the enzyme. n=3-5 experiments for each point. (**E**) MG production by TPI or nitro-TPI using DHAP or GAP as initial substrates. n=4 independent experiments; * $p<0.05$ by student's t analysis. (**F**) Western blot analysis of MG production using anti-argpyrimidin, which recognizes glication products. 100 µg protein extract from HEK cells overexpressing wild type (first lane) or double mutant (Tyr164 and 208 by Phe164 and 208) TPI were applied.

FIGURE 3

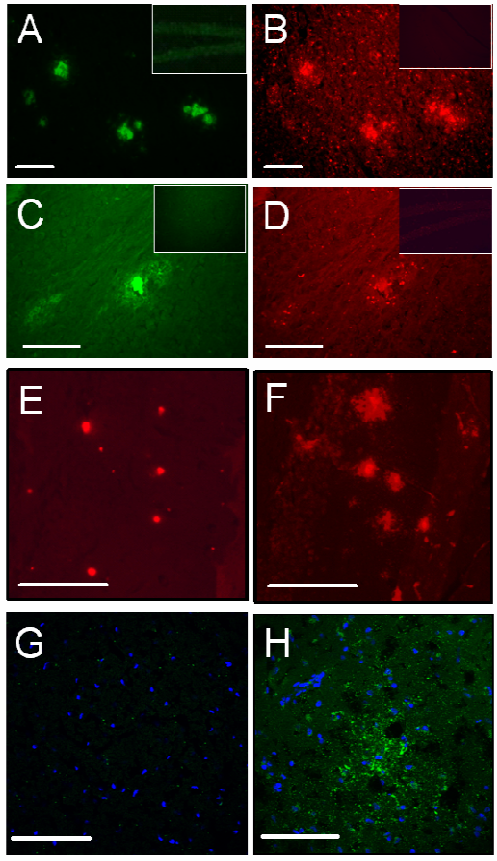

Fig. 3 MG production is increased in APP-PS1 double transgenic mice and AD patients. Consecutive serial hippocampal sections from double transgenic mice were immunostained to demonstrate the presence of (**A**) Aβ and (**B**) TPI; (**C**) Aβ identified by thioflavine T staining and (**D**) MG; and, (**E**) TPI and (**F**) MG. Controls with wild type mice were performed for (insets **A** and **C**) Aβ, (inset **B**) TPI and (inset **D**) MG. Cortex samples from (**G**) healthy and (**H**) AD patients were immunostained with anti-MG antibody producing green fluorescence. Nuclei were stained in blue. Bars are 75 µm (**A**-**D**), 125 µm (**E**, **F**) and 250 µm (**G**, **H**).

FIGURE 4

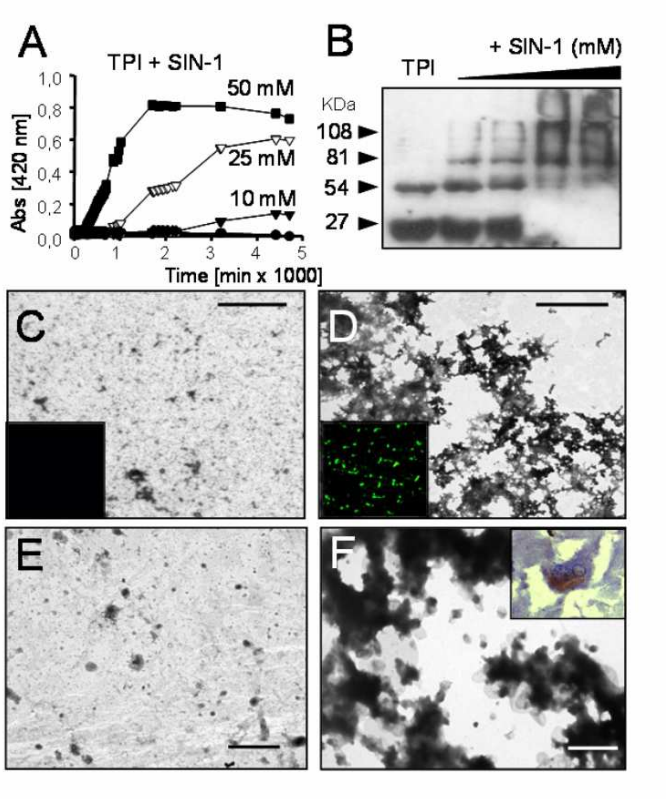

Fig. 4 The nitrotyrosination of TPI is inducing its aggregation. (**A**) The *in vitro* aggregation was followed by a turbidometric assay of TPI (●) and TPI+SIN-1 (10 mM (▼), 25 mM (▽), 50 mM (■)) followed by measuring A_{402}. (**B**) Western blot detection with an anti-TPI antibody of TPI nitrotyrosinated with SIN-1 (48 h) demonstrated the presence of TPI oligomers proportional to increasing concentrations of SIN-1 (0, 10, 25 and 50 mM). Transmission electron microscopy images of immunoprecipitates were obtained using anti-TPI antibody in samples from (**C**) control TPI and (**D**) TPI nitrotyrosinated *in vitro*; and, human cortex from (**E**) healthy and (**F**) AD patiens. Immunoprecipitates of (inset **C**) normal TPI were negative for thioflavine T staining but they were positive for (inset **D**) nitro-TPI indicating the folding in β-sheet structure. (inset **F**) The intracellular aggregation of TPI was demonstrated in cells from sections of AD patient cortex. Bars are 1 µm (**C**, **D**) and 2 µm (**E**, **F**).

FIGURE 5

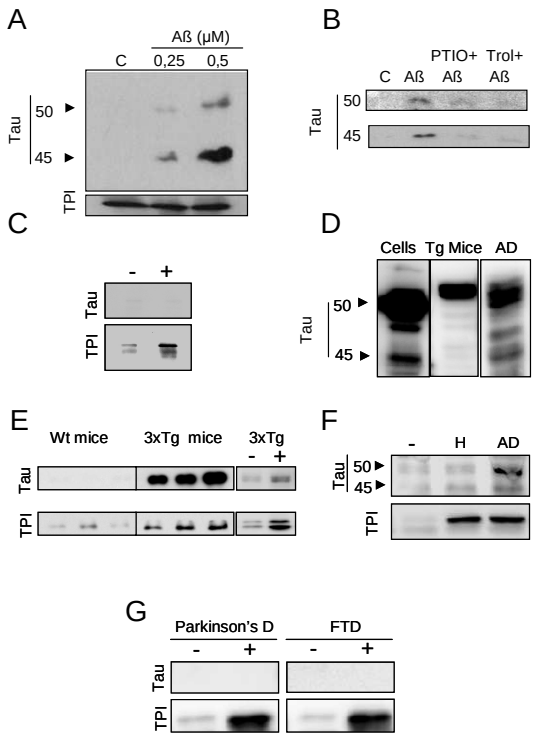

Fig. 5 Tau protein coimmunoprecipitates with nitro-TPI. All the cell lysates and tissue samples were immunoprecipitated with an anti-TPI antibody. (**A**) SH-SY5Y cells were treated with two sub-lethal concentrations of Aß fibrils. Western blots were performed with antibodies anti-tau and anti-TPI. (**B**) SH-SY5Y cells were pretreated with PTIO (a NO scavenger) or Trolox (a free radical scavenger) before adding the Aß fibrils. A western blot was performed with an anti-tau antibody. (**C**) Controls were performed to assay the unspecific TPI binding to protein G sepharose (lane -) compared to the normal anti-TPI immunoprecipitation (lane +). (**D**) Total lysates from SH-SY5Y cells, 3xTg mice and AD cortex were applied to western blot to identify the most abundant tau isoforms. (**E**) Co-immunoprecipitation of tau (50 KDa) with TPI was also assessed in three different mice overexpressing APP, PS1 and human tau. The respective controls for the immunoprecipitation without anti-TPI (lane -) and with anti-TPI (lane +) are also shown in the panel. (**F**) The presence of tau in the TPI immunoprecipitates obtained from healthy and AD cortex was analysed by immunoblotting with antibodies anti-tau and anti-TPI. The control for the unspecific binding to protein G-sepharose is shown in the panel (lane -). (**G**) TPI immunoprecipitates obtained from frontal cortex of Parkinson's disease and frontotemporal dementia patiens are shown with the respective controls for the unspecific binding to protein G-sepharose.

FIGURE 6

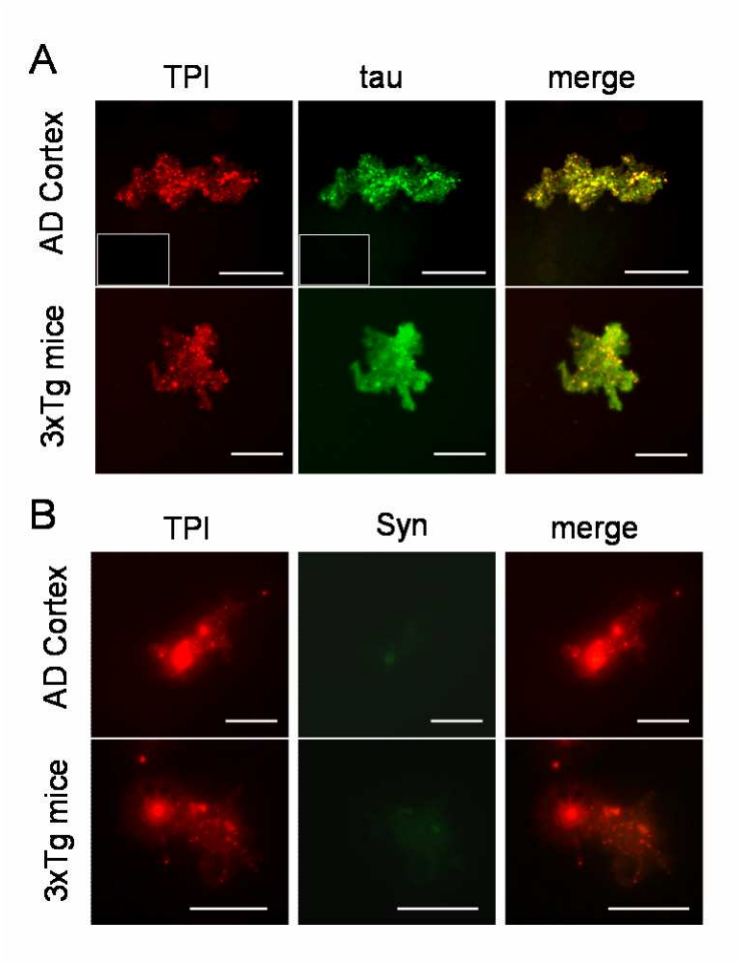

Fig. 6 Co-localization of TPI and tau protein in brain samples. (**A**) TPI immunoprecipitates obtained from AD and triple transgenic mice overexpressing APP, PS1 and tau were immunolabeled with anti-TPI and tau. (**B**) TPI immunoprecipitates obtained from AD and triple transgenic mice were immunolabeled with anti-TPI and anti-syntaxin 1A as a control of the specificity of the tau binding to TPI. (Insets **A**) Controls with secondary antibody were performed for both TPI and tau .Bars are 100 µm (AD cortex; **A**), 50 µm (3xTg mice; **A**) and 37,5 µm (**B**).

FIGURE 7

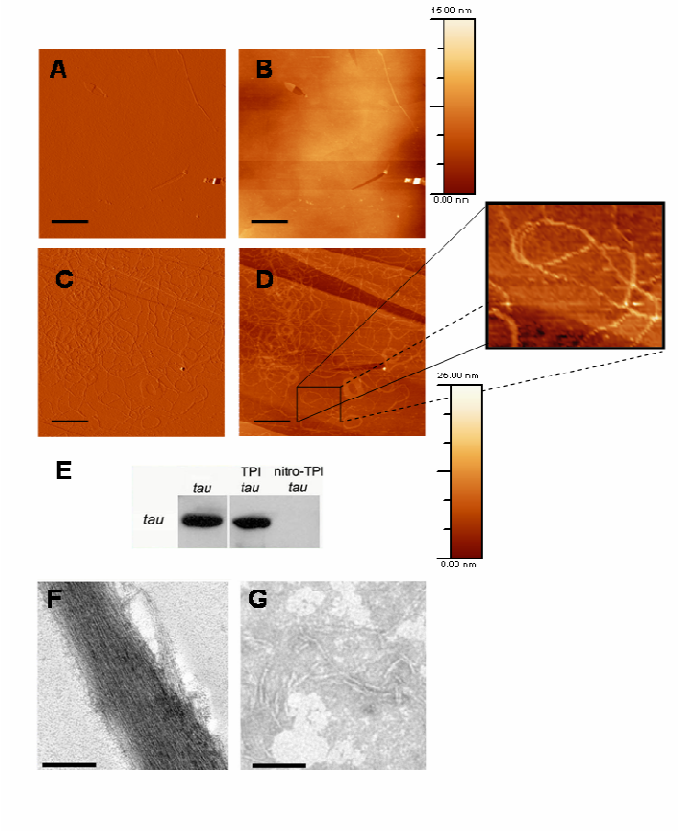

Fig. 7 Fibrillation of tau into PHFs demonstrated by AFM and TEM. Tau was incubated for 4 days in the presence of (**A, B**) TPI or (**C, D**) nitro-TPI at a 1:1 (w/w) ratio and seeded on graphite surfaces for AFM visualization. (**A, B)** Tau-control TPI samples show few fibrils without defined structure. (**C, D)** Tau-nitro-TPI samples exhibit abundant fibrils that are similar in morphology to PHFs when their topography is visualized. (**E)** Western blot detection of tau in the samples used for AFM studies: control of tau alone, TPI+tau and nitro-TPI+tau. (**F, G)** TEM images of the fibrils found in tau-nitro-TPI samples.

References

Ahmed N, Battah S, Karachalias N, Babaei-Jadidi R, Horanyi M, Baroti,K, et al. Increased formation of methylglyoxal and protein glycation, oxidation and nitrosation in triosephosphate isomerase deficiency. Biochim Biophys Acta 2003; 1639: 121–32.

Alonso AC, Li B, Grundke-Iqbal I, Iqbal K. Mechanism of tau-induced neurodegeneration in Alzheimer disease and related tauopathies. Curr Alzheimer Res. 2008; 5:375-84.

Bhat RV, Budd Haeberlein SL, Avila J. Glycogen synthase kinase 3: a drug target for CNS therapies. J. Neurochem. 2004; 89: 1313-1317.

Brion JP, Couck AM, Passareiro E, Flament-Durand J. Neurofibrillary tangles of Alzheimer's disease: an immunohistochemical study. J Submicrosc Cytol. 1985; 17:89-96.

Chang E, Kim S, Yin H, Nagaraja HN, Kuret J. Pathogenic missense MAPT mutations differentially modulate tau aggregation propensity at nucleation and extension steps. J Neurochem. 2008; 107:1113-23.

Chirita CN, Necula M, Kuret J. Anionic micelles and vesicles induce tau fibrillization in vitro. J Biol Chem. 2003; 278: 25644-50.

Coma M, Guix FX, Uribesalgo I, Espuna G, Sole M, Andreu D, et al. Lack of oestrogen protection in amyloid-mediated endothelial damage due to protein nitrotyrosination. Brain 2005; 128: 1613-1621.

Contreras CF, Canales MA, Alvarez A, De Ferrari GV, Inestrosa NC. Molecular modeling of the amyloid-beta-peptide using the homology to a fragment of triosephosphate isomerase that forms amyloid in vitro. Protein Eng 1999; 12: 959-966.

Cras P, van Harskamp F, Hendriks L, Ceuterick C, van Duijn CM, Stefanko SZ, et al.. Presenile Alzheimer dementia characterized by amyloid angiopathy and large amyloid core type senile plaques in the APP 692Ala-->Gly mutation. Acta Neuropathol. (Berl) 1998; 96: 253-260.

Dabrowska A, Kamrowska I, Baranowski T. Purification, crystallization and properties of triosephosphate isomerase from human skeletal muscle. Acta Biochim. Pol. 1978; 25: 247-256.

Del Toro D, Coma M, Uribesalgo I, Guix FX, Muñoz FJ. The Amyloid beta-Protein Precursor and Alzheimer's Disease- Therapeutic Approaches. Curr. Med. Chem. 2005; 5: 271-283.

Eber SW, Pekrun A, Bardosi A, Gahr M, Krietsch WK, Kruger J, et al. Triosephosphate isomerase deficiency: haemolytic anaemia, myopathy with altered mitochondria and mental retardation due to a new variant with accelerated enzyme catabolism and diminished specific activity. Eur. J. Pediatr. 1991; 150: 761-766.

Frederikse PH, Garland D, Zigler JS, Piatigorsky J. Oxidative stress increases production of beta-amyloid precursor protein and beta-amyloid (Abeta) in mammalian lenses, and Abeta has toxic effects on lens epithelial cells. J. Biol. Chem. 1996; 271: 10169-10174.

Goedert M, Jakes R, Spillantini MG, Hasegawa M, Smith MJ, Crowther RA. Assembly of microtubule-associated protein tau into Alzheimer-like filaments induced by sulphated glycosaminoglycans. Nature 1996; 383: 550-553.

Gotz J, Chen F, van Dorpe J, Nitsch RM. Formation of neurofibrillary tangles in P301l tau transgenic mice induced by Abeta 42 fibrils. Science 2001; 293: 1491-1495.

Grabowski TJ, Cho HS, Vonsattel JP, Rebeck GW, Greenberg SM. Novel amyloid precursor protein mutation in an Iowa family with dementia and severe cerebral amyloid angiopathy. Ann. Neurol. 2001; 49: 697-705.

Guix FX, Uribesalgo I, Coma M, Munoz FJ. The physiology and pathophysiology of nitric oxide in the brain. Prog. Neurobiol. 2005; 76: 126-152.

Herzig MC, Van Nostrand WE, Jucker M. Mechanism of cerebral beta-amyloid angiopathy: murine and cellular models. Brain Pathol. 2006; 16: 40-54.

Hoyer S, Oesterreich K, Wagner O. Glucose metabolism as the site of the primary abnormality in early-onset dementia of Alzheimer type? J. Neurol. 1988; 235: 143-148.

Iqbal K, Zaidi T, Thompson CH, Merz PA, Wisniewski HM. Alzheimer paired helical filaments: bulk isolation, solubility, and protein composition. Acta Neuropathol. 1984; 62:167-77.

Keil U, Bonert A, Marques CA, Scherping I, Weyermann J, Strosznajder JB, et al. Amyloid beta-induced changes in nitric oxide production and mitochondrial activity lead to apoptosis. J. Biol. Chem. 2004; 279: 50310-50320.

Kuhla B, Luth HJ, Haferburg D, Boeck K, Arendt T, Munch G. Methylglyoxal, glyoxal, and their detoxification in Alzheimer's disease. Ann. N. Y. Acad. Sci. 2005; 1043: 211-216.

Kuret J, Congdon EE, Li G, Yin H, Yu X, Zhong Q. Evaluating triggers and enhancers of tau fibrillization. Microsc.Res.Tech. 2005; 67: 141-155.

Lewis J, Dickson DW, Lin WL, Chisholm L, Corral A, Jones G, et al. Enhanced neurofibrillary degeneration in transgenic mice expressing mutant tau and APP. Science 2001; 293: 1487-1491.

Liou YC, Sun A, Ryo A, Zhou XZ, Yu ZX, Huang HK, et al. Role of the prolyl isomerase Pin1 in protecting against age-dependent neurodegeneration. Nature 2003; 424: 556-61.

Maccioni RB, Munoz JP, Barbeito L. The molecular bases of Alzheimer's disease and other neurodegenerative disorders. Arch. Med. Res. 2001; 32: 367-381.

Masters CL, Beyreuther K. Alzheimer's centennial legacy: prospects for rational therapeutic intervention targeting the Abeta amyloid pathway. Brain. 2006; 129:2823-39.

Miranda S, Opazo C, Larrondo LF, Munoz FJ, Ruiz F, Leighton F, et al. The role of oxidative stress in the toxicity induced by amyloid beta-peptide in Alzheimer's disease. Prog. Neurobiol. 2000; 62: 633-648.

Mudher A, Lovestone S. Alzheimer's disease-do tauists and baptists finally shake hands? Trends Neurosci. 2002; 25: 22-6.

Oddo S, Caccamo A, Shepherd JD, Murphy MP, Golde TE, Kayed R, et al. Triple-transgenic model of Alzheimer's disease with plaques and tangles: intracellular Abeta and synaptic dysfunction. Neuron. 2003; 39: 409-21.

Olah J, Orosz F, Keseru GM, Kovari Z, Kovacs J, Hollan S, et al. Triosephosphate isomerase deficiency: a neurodegenerative misfolding disease. Biochem. Soc. Trans. 2002; 30: 30-38.

Opazo,C., Huang,X., Cherny,R.A., Moir,R.D., Roher,A.E., White,A.R., Cappai,R., Masters,C.L., Tanzi,R.E., Inestrosa,N.C. et al 2002. Metalloenzyme-like activity of Alzheimer's disease beta-amyloid. Cu-dependent catalytic conversion of dopamine, cholesterol, and biological reducing agents to neurotoxic H_2O_2. *J. Biol. Chem.* **277**:40302-40308.

Orosz F, Wagner G, Liliom K, Kovacs J, Baroti K, Horanyi M, et al. Enhanced association of mutant triosephosphate isomerase to red cell membranes and to brain microtubules. Proc. Natl. Acad. Sci. U. S. A. 2000; 97: 1026-1031.

Otth C, Concha II, Arendt T, Stieler J, Schliebs R, Gonzalez-Billault C, et al. AbetaPP induces cdk5-dependent tau hyperphosphorylation in transgenic mice Tg2576. J. Alzheimers. Dis. 2002; 4: 417-430.

Ovadi J, Orosz F, Hollan S. Functional aspects of cellular microcompartmentation in the development of neurodegeneration: mutation induced aberrant protein-protein associations. Mol. Cell Biochem. 2004; 256-257: 83-93.

Pompliano DL, Peyman A, Knowles JR. Stabilization of a reaction intermediate as a catalytic device: definition of the functional role of the flexible loop in triosephosphate isomerase. Biochemistry 1990; 29: 3186-3194.

Rice PA, Goldman A, Steitz TA. A helix-turn-strand structural motif common in alpha-beta proteins. Proteins 1990; 8: 334-340.

Richard JP. Mechanism for the formation of methylglyoxal from triosephosphates. Biochem. Soc. Trans. 1993; 21: 549-553.

Sturchler-Pierrat C, Sommer B. Transgenic animals in Alzheimer's disease research. Rev. Neurosci. 1999; 10: 15-24.

Valentin C, Cohen-Solal M, Maquat L, Horanyi M, Inselt-Kovacs M, Hollan S. Identical germ-line mutations in the triosephosphate isomerase alleles of two brothers are associated with distinct clinical phenotypes. C. R. Acad. Sci. III 2000; 323: 245-250.

Wszolek ZK, Tsuboi Y, Ghetti B, Pickering-Brown S, Baba Y, Cheshire WP. Frontotemporal dementia and parkinsonism linked to chromosome 17 (FTDP-17). Orphanet J Rare Dis 2006; 9: 1-30.

Yancopoulou D, Crowther RA, Chakrabarti L, Gydesen S, Brown JM, Spillantini MG. Tau protein in frontotemporal dementia linked to chromosome 3 (FTD-3). J. Neuropathol. Exp. Neurol. 2003; 62: 878-882.

SUPPLEMENTARY MATERIAL

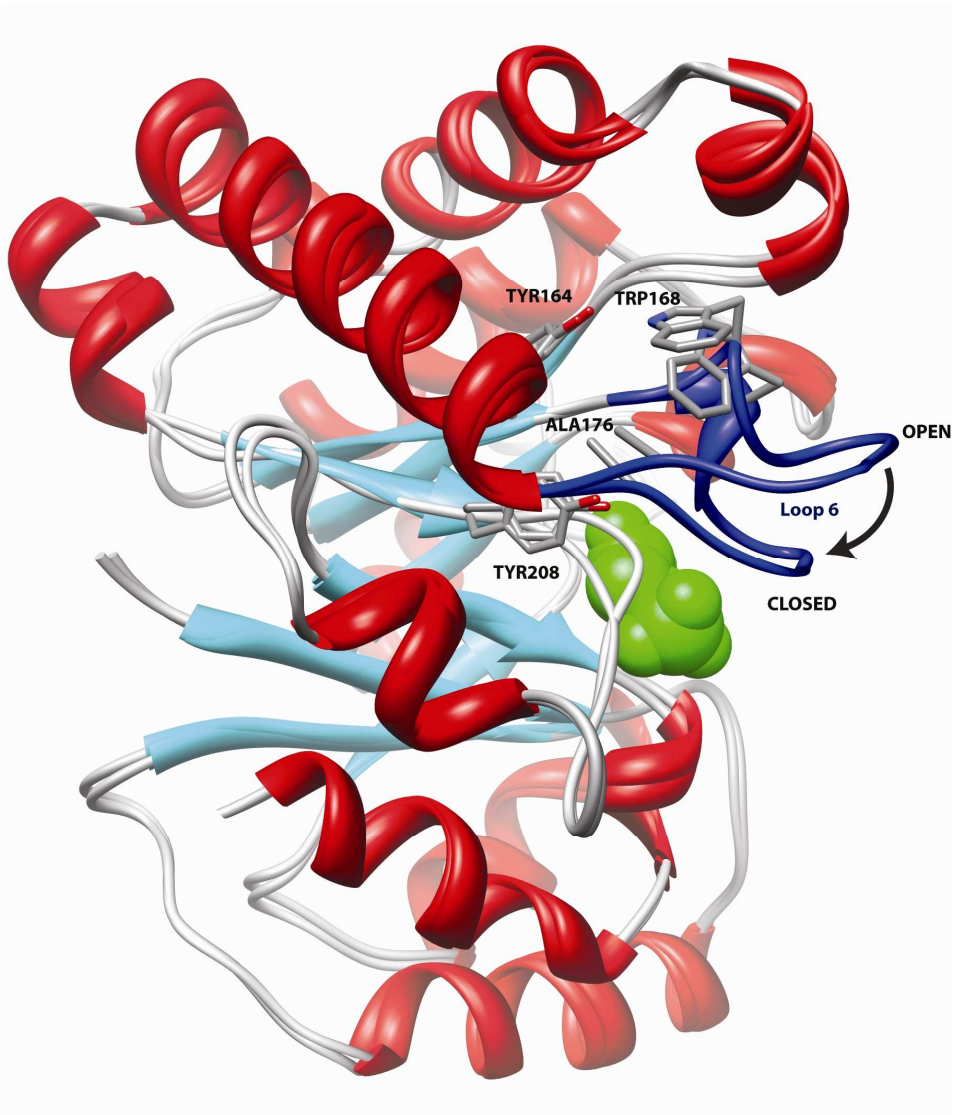

Fig. S1 TPI conformational changes upon substrate binding. Superposition of open (PDB code: 1LZO) and closed (PDB code: 1LYX) conformations of TPI. The only relevant structural difference involves Loop 6 (L6), depicted in dark blue. The substrate is represented in green.

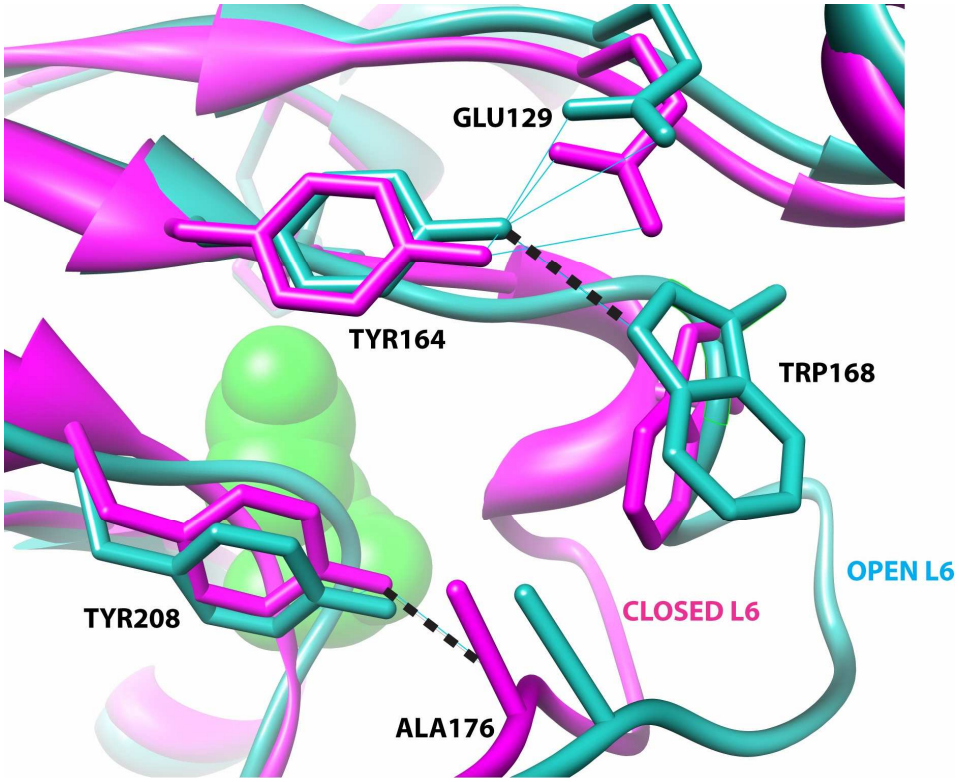

Fig. S2 Zoom in the region controlling the L6 conformation. Tyr164 forms a hydrogen bond network with Glu129 and Trp168 in the open state, but only with Glu129 in the closed state. On the contrary, Tyr208 forms a hydrogen bond with the backbone of Ala176 only in the closed conformation. The substrate is represented in green.

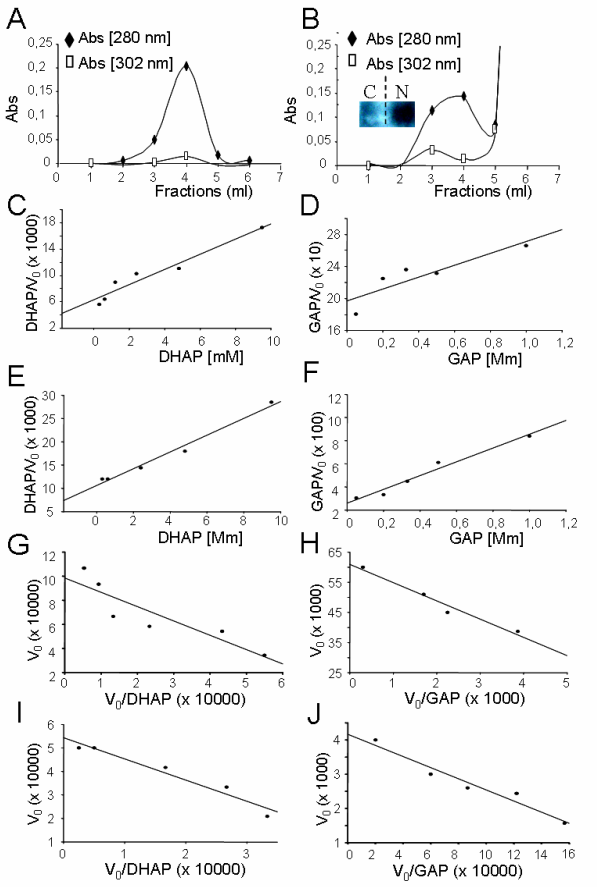

Figure S3. Kinetic study of normal and nitrotyrosinated TPI. Panel **A** and **B** show the elution pattern of protein and salt, measured at 280 nm and 302 nm respectively, of TPI after passing through a desalting column in order to eliminate the salt SIN-1, the nitrating agent used to nitrotyrosinate TPI *in vitro*. Panel **A** corresponds to the elution of non-nitrated TPI and panel **B** to TPI treated with SIN-1. We chose fraction 4 to perform the enzymatic study because TPI concentration is maximal in this fraction (abs 280 nm) while SIN-1 has been successfully eliminated (abs 302 nm). As a nitrotyrosination control, a western blot was carried out with the TPI from fraction 4. Panels **C**-**J** show the linearization models plotted from Michaelis-Menten graphs in order to calculate the kinetic parameters. Panels **C**-**F** show the Woolf-Hanes representation of (**C**, **D**) control TPI and (**E**, **F**) nitrotyrosinated TPI. Panels **G**-**J** show the Eadie-Hofstee representation for (**G**, **H**) control TPI and (**I**, **J**) nitrotyrosinated TPI.

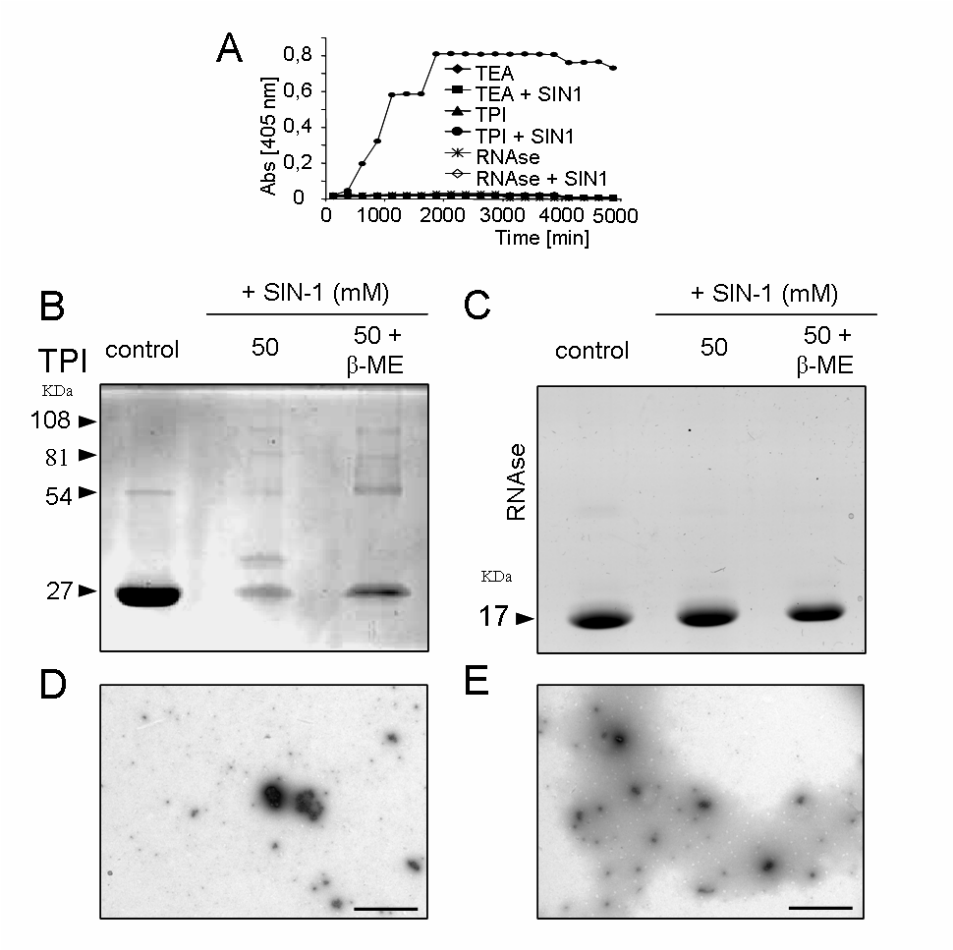

Figure S4. Nitrotyrosination is inducing TPI aggregation but not for RNAse. (**A**) Turbidometric study of TPI aggregation. Bovine RNAse was used as a control of nitrotyrosination-induced aggregation since it has a similar size (aprox. 17 KDa) to TPI and similar number of Tyr residues (6 Tyr) than TPI (4 Tyr). TPI and RNAse were previously treated or not with SIN-1 and resuspended in TEA medium. They were left under shaking at room temperature, and absorbance values at 405 nm were taken during the experiment. Only TPI that had been treated with SIN-1 showed increasing aggregation on the course of the experiment. (**B**) TPI nitrated with 50 mM SIN-1 appears as a ladder of bands on an acrylamide gel stained with coomassie after 48h of SIN-1 treatment. The weight of the bands corresponds to the monomer, dimmer, trimmer, and so on. These aggregates are resistant to β-mercaptoethanol. (**C**) The same experiment than in **B** but with RNAse instead of TPI. In this case no oligomeric structures are formed after SIN-1 exposure. Electron microscopy of RNAse (**D**) non-treated and (**E**) treated with 50 mM SIN-1 were shaking for 2 days and any aggregates were observed. Bars are 1 µm.

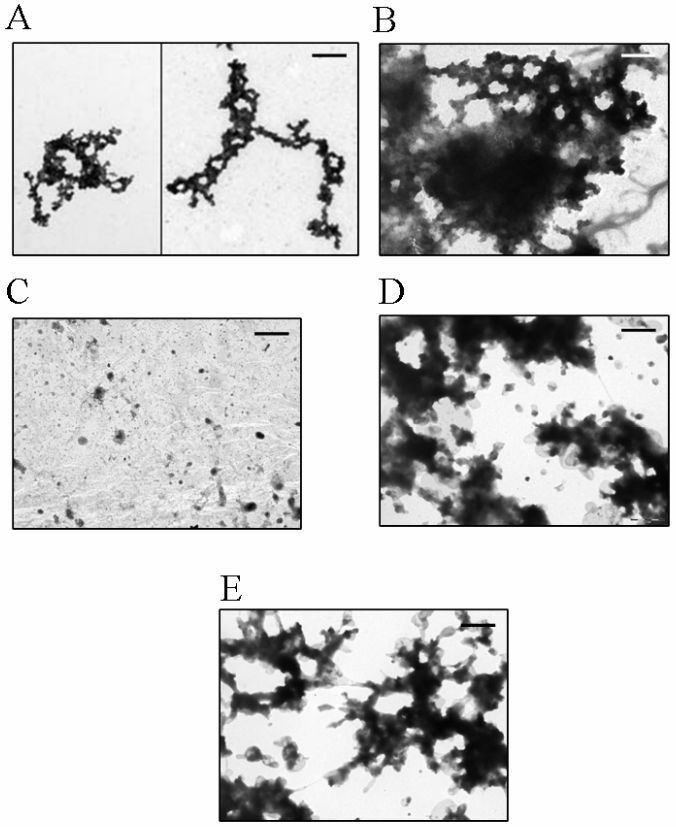

Figure S5. Electron microscopy images from TPI aggregates. (**A**, **B**) Electron microscopy of purified TPI exposed to 50 mM SIN-1 and shaked for 4 days. Large necklace-like aggregates appear all over the sample. TPI inmunoprecipitated from (**C**) healthy human cortex, (**D**) AD patient cortex and (**E**) AD patient hippocampus. In the healthy cortex there are not aggregates but in the AD cortex and hippocampus there is a large number of big aggregates that resembles those formed *in vitro*. Bars are 2 µm (**A-E**).

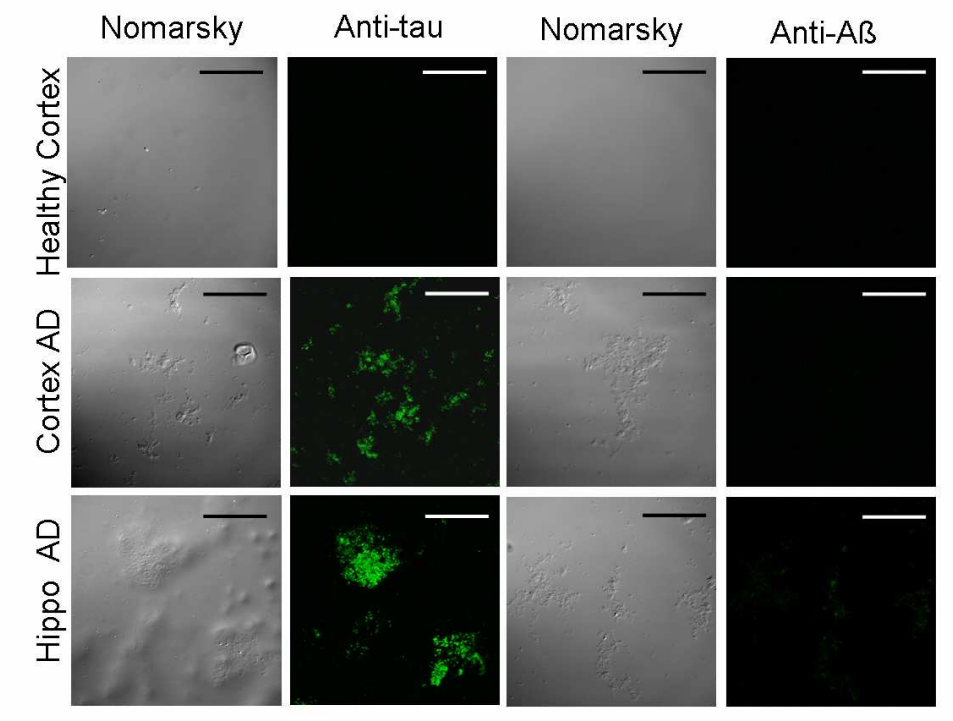

Figure S6. Inmunofluorescence analysis of TPI aggregates from human cerebral cortex of healthy and AD patients, and hippocampus of AD patients. Sample brains were immunoprecipitated by using an anti-TPI antibody and then immunolabelled with anti-tau and anti-Aβ. There was not any TPI aggregate in the healthy cerebral cortex (as observed in Nomarsky images), thus negative staining for tau was obtained. In AD cortex and hippocampus we have obtained TPI aggregates (Nomarsky images) that were positive for tau immunostaining, indicating that they were co-immunoprecipitated. These TPI aggregates were negative for Aß immunostaining as it was expected since Aß is released to the extracelular brain parenchyma. Bars are 37 µm.

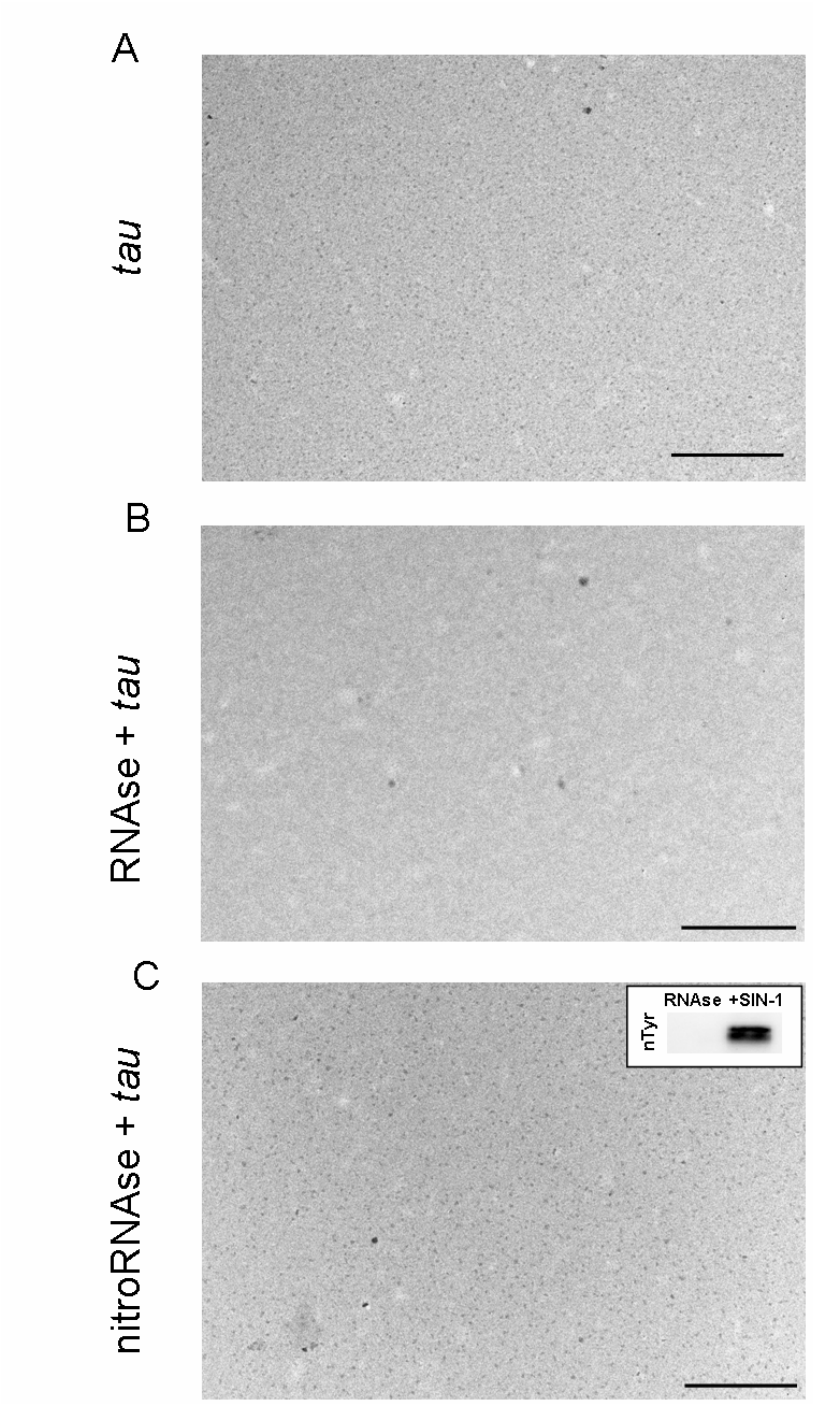
A
tau
B
RNAse + tau
C
nitroRNAse + tau
RNAse +SIN-1
nTyr

Figure S7. PHFs were not obtained when tau was incubated with nitro-RNAse. Human RNAse 3 was used as a control to demonstrate the specificity of TPI nitrotyrosination to induce tau fibrillation. Human RNAse 3 is a protein with a similar size (aprox. 19 KDa) to that of TPI (26 KDa) and both proteins share the same number of Tyr residues (4 Tyr). Tau protein was incubated (A) alone, (B) with non treated RNAse 3 and (C) with RNAse treated with 50 mM SIN-1. (Inset C) RNAse 3 was confirmed to be nitrotyrosinated after exposure to 50 mM SIN-1. Results were analysed by electron microscopy. Bars are 500 µm (A-C).

Supplementary materials and methods

Human RNAse 3 nitration *in vitro*. Human RNAse 3 (1.25 µg/µL unless otherwise indicated) was dissolved in 50 mM tetraethylammoniun (pH 7.4-7.6) and exposed to SIN-1 at the concentrations specified in each assay. Nitration process was carried out under shaking at 300 rpm for 3 hours and at room temperature. SIN-1 was eliminated from the samples with a PD-10 desalting column (Amersham).

RNAse 3-Tau co-aggregation study. RNAse 3 and nitroRNAse3 (4 µg/ml) were co-incubated with tau protein to 1:1 (w/w) at 25ºC for 4 days and analysed under electron microscopy.

TABLE 1

Substrate [a]	**GAP**		**DHAP**	
	Control TPI	**Nitrotyr. TPI**	**Control TPI**	**Nitrotyr. TPI**
Km (mM)	1.65 ± 0.41	0.62 ± 0.16	0.84 ± 0.42	1.11 ± 0.15
Vmax x 10^{-3} ($mM \cdot s^{-1}$)	2.16 ± 1.32	0.2 ± 0.04	0.14 ± 0.04	0.09 ± 0.01
Kcat x 10^{5} (min^{-1})	5.75 ± 3,51	0.53 ± 0.21	0.11 ± 0.28	0.07 ± 0.01
Kcat/Km x 10^{5} ($mM^{-1}min^{-1}$)	3.49 ± 2.30	0.87 ± 0.41	0.13 ± 0.07	0.06 ± 0.02
MG formation (% respect to control) [b]	100	211.18 ± 21.16	100	132.68 ± 5.66

a *Total TPI for enzymatic assay was 3 ng for GAP and 10 ng for DHAP.*

b *MG measurement was made with 0.5 mM GAP or 2.4 mM DHAP after 10 min of adding substrate.*

The number of experiments was 3-6.

IV. DISCUSSION

Peroxynitrite as an etiopathogenic factor to develop AD

Nitro-oxidative stress seems to be the underlying cause of AD etiopatogeny (Resende et al., 2008). ROS are being produced physiologically as a consequence of a wide number of chemical reactions from cell metabolism. There are different mechanisms responsible for the elimination of these harmful compounds. However, during aging these mechanisms are also attacked by the same compounds that they must detoxify, and ROS start to accumulate, affecting other cellular machinery. There are several reasons to propose that ROS are key etiopathogenic factors for AD. Firstly, aging is the most important risk factor to develop the disorder (Hensley et al., 1994). Secondly, BACE1, the key enzyme to initiate the production of Aβ from APP, is enhanced at the transcriptional level by oxidative stress through the action of the JNK and p38 MAPK intracellular signaling pathways (Coma et al., 2008). Moreover, Aβ fibrils are also an important source of ROS (Behl et al., 1994). In this way, oxidative stress is producing a lethal loop in AD involved in both the etiology as well as the progression of the disease. Microglia and astrocytes are also producing an increased oxidative stress surrounding the amyloid deposits where they turn reactive cells by the respiratory burst with the activation of NOX (Wilkinson and Landreth, 2006).

One of the most reactive species produced by nitro-oxidative stress is peroxynitrite, which comes from the reaction between superoxide anion and NO. Peroxynitrite reacts with a large number of biomolecules, from DNA and lipids to proteins. In particular its reaction with proteins is directed to tyrosine residues producing the nitrotyrosination of the proteins. The importance of protein nitrotyrosination resides on the fact that, up to day, it has not been found any activity capable of repairing this damage. The proteins carrying one or more nitrotyrosines will be degraded or accumulated into the cell (Guix et al., 2005). In the present work we

have demonstrated that PSs are markedly nitrotyrosinated in AD brains compared to brains from non-AD patients. We also found out that peroxynitrite not only nitrotyrosinates the catalytic activity of the γ-secretase, but also increases the levels of some of the complex components, resulting an increase in γ-secretase complex in the plasmatic membranes of peroxynitrite treated cells. This process yields to an increased APP processing and Aβ release into the medium. Surprisingly, the Aβ species incremented under this condition is $A\beta_{42}$, the more aggregative and toxic form of the peptide. This finding is very interesting since it has been reported that old people has a higher $A\beta_{42}/A\beta_{40}$ ratio compared to young people (Shoji et al., 2001). The increase in nitrotyrosination-mediated $A\beta_{42}$ production could be due to a major retention of the complex in a certain compartmental microenvironment, since localization has been reported to play a role in the cleavage specificity and activity of the γ-secretease (Morais et al., 2008). It is the case of some PS1 mutations that augment $A\beta_{42}$ levels principally in Golgi-like vesicles (Xia et al., 1998). However it does not seem feasible because PS is only active when is forming part of the γ-secretase complex. In addition, the assembly of all the components of the complex can only be carried out when they leave the ER. Another explanation may involve the nitrotyrosination of the two conserved tyrosines (Y256 & Y389) close to the catalytic aspartyls of PS (D257 & D385). They are capable of hydrogen bonding and it seems to be important for the right position of the aspartyl residues and, as a result, for the correct function of the enzyme (Wrigley et al., 2004). Interestingly, the mutation of these tyrosines to phenylalanine increments the formation of $A\beta_{42}$ (Wolfe et al., 1999). Thus, their nitrotyrosination could also affect the establishment of hydrogen bonds and give rise to an incremented formation of $A\beta_{42}$.

In addition, peroxynitrite is not only increasing the $A\beta_{42}$ production, but also its aggregation in a time and concentration manner. When we analyzed the nature of the aggregates we found that they were round oligomeric structures. Recent studies support the idea that Aβ oligomers are the most toxic form of Aβ aggregates because they can impair the synaptic plasticity at the place they are produced (Selkoe, 2008;Shankar et al., 2008;Cerpa et al., 2008). We confirmed it by measuring their toxicity in cultured neuroblastoma cells, which resulted to be very high. The oligomers induce neuronal damage before the appearance of mature Aβ fibrils as they are in the senile plaques (Kirschner et al., 1986).

Our data gives an explanation to the strong relationship between aging and AD, and sets peroxynitrite in the spotlight of the disease's etiology. However our data does not explain why only some people suffer from sporadic AD, since incremented oxidative stress is a common event in the aging process of all individuals. One plausible hypothesis is that some people own a better battery of genes to protect the cells against oxidative stress. It involves having more efficient antioxidant enzymes such as SOD, glutathione reductase or glutathione peroxidase. Indeed, some studies have found an association between certain polymorphisms in genes codifying antioxidant enzymes and an increased risk of suffering from late-onset AD. Thus the V allele of the glutathione S-transferase gene increments the risk of suffering AD, whereas the GSTT1 polymorphism indicates protection against AD (Pinhel et al., 2008). On the other hand some polymorphisms in the SOD2 gene are also linked to a higher risk to develop AD (Wiener et al., 2007).

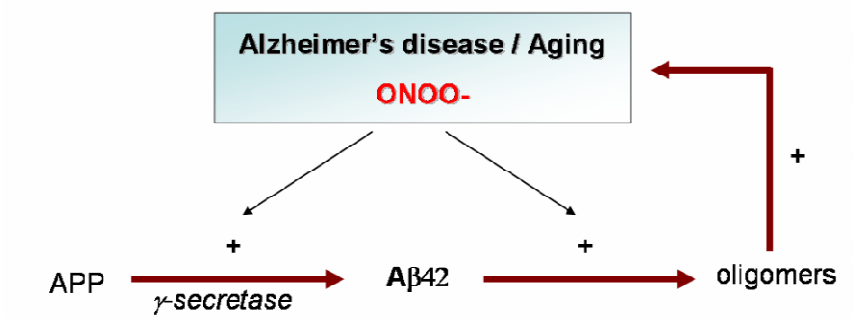

Figure 1. **Role of peroxynitrite in the etiology of AD**. Scheme showing the involvement of peroxynitrite in the $A\beta_{42}$ production and aggregation

Peroxynitrite, glycolytic metabolism and AGEs

The second part of the present thesis addresses the link between peroxynitrite and the molecular changes that occur inside the neurons of an AD patient. Memory loss is due to the breakdown of synaptic connections which at time depend on the preserved synaptic architecture. The dendrites and axons appear with an abnormal shape and direction ("dystrophic neurites") in AD, especially in those areas where there is a big density of senile plaques (Irizarry et al., 1997;Knowles et al., 1999). It is due in part to the alteration in the neuronal cytoskeleton. Instead of an ordered architecture, neurons accumulate proteins in form of aggregates that disturb the natural shape of neurites. These inclusions (NFT) composed mainly by tau protein appear always after the extraneuronal plaque formation (Gotz et al., 2001). Other diseases without amyloid pathology also show NFT as the result of tau mutations such as Frontotemporal Dementia (FD) or Progressive Supranuclear Palsy (Heutink, 2000).

We found TPI to be highly nitrotyrosinated in the hippocampus and frontal cortex of people with AD. It is in accordance with previous works showing the same results (Castegna et al., 2003;Reed et al., 2008). We went further and demonstrated that TPI nitrotyrosination affects its important function in glycolysis and turns the enzyme

into a source of MG, a powerful glycating agent. In the context of the brain, it has a high relevance since its main energetic source is glucose. In fact, depleted glucose metabolism has been found in brains from people with AD in several studies (Harwood et al., 2005;Liang et al., 2008;Mosconi et al., 2007;Mosconi et al., 2005). In addition, TPI deficiency could lead to a decrease of AcCoA availability. AcCoA is not only the initial substrate for the mitochondrial tricarboxylic cycle, but also the substrate for the synthesis of the neurotransmitter ACh. Interestingly the cholinergic system is the major neurotransmitter system affected in the very early stages of AD having a dramatic depletion of ACh (Zhang, 2004). Moreover mitochondrial failure is common in the disease, but it could also be due to the direct damage of the mitochondrial enzymes (Sompol et al., 2008).

However other studies have reported that yeasts carrying a less active form of TPI are more resistant to oxidative stress (Ralser et al., 2006). In the same work they show that yeasts can growth in a normal medium with glucose having a residual 30% TPI activity, giving relative importance to the partial loss of the glycolytic pathway (Ralser et al., 2006). In this way, a small level of TPI nitrotyrosination may work as a sensor of ROS levels. Thus a little blockage of the glycolytic pathway could be beneficial for the neurons since there would be less AcCoA available for the mitochondrial metabolism, reducing the mitochondrial activity, which is an important source of ROS, and restoring in this way the normal redox state.

The increased MG formation that occurs when TPI is nitrotyrosinated could have a more detrimental effect on the brain than the loss of partial TPI activity. Aging is associated to the accumulation of aberrant proteins that can be triggered by ROS (Lavie et al., 1982;Gracy et al., 1985) and the glycation of proteins giving rise to Advanced Glycation End-products (AGEs) (Masoro et al., 1989;Cefalu et al., 1995;Sell et al.,

1996). MG is one of these glycating agents, and proteins modified by MG can form adducts and aggregates. The formation of AGEs is very important in AD. Indeed, tau protein has been reported to be glycated in AD patients (Yan et al., 1994;Kuhla et al., 2007), which may contribute to its fibrillation and the disruption of the neurites, contributing to the impairment of memory. AGEs are also able to activate the microglia, releasing more oxidants and worsening the progression of the disease. We found a high signal for argpyrimidine, a MG-induced modification on proteins, in brains from AD patients and PS1/APPsw mice. The elevated levels of MG in AD had already been reported previously (Kuhla et al., 2005), however any mechanism was given to explain it. We give a molecular mechanism linking oxidative stress and AGEs formation. This model correlates well with the clinical observations. Aged people have elevated AGEs, but people with AD have still more AGEs than non-AD old people (Luth et al., 2005;Dei et al., 2002). It can be explained by the fact that old people have increased ROS levels, but the production of ROS in people suffering from AD is still more dramatic because of the presence of senile plaques. Thus, it is expected that in AD TPI is more nitrotyrosinated than in old people, what leads to a higher production of MG.

Peroxynitrite: a link between Aβ deposits and the formation of NFT

On the other hand we found out that nitrotyrosination of the enzyme triggers its aggregation in a time-dependent manner. We detected inclusions of TPI spread over the cerebral parenchyma of both AD patients and PS1/APPsw mice, especially on those areas containing more plaques. The exact mechanism by which nitrotyrosination induces its aggregation can not be deduced directly from our data. Nonetheless, TPI seems to have an intrinsic propensity to misfold and induce aberrant protein-protein

interaction. It is suggested by studies on the behaviour of TPI mutants obtained from patients with deficiency of its activity. TPI has 8 α-helix and 8 β-sheet in normal conditions (Cansu and Doruker, 2008). Interestling a fragment of TPI with a very high sequence homology with Aβ is able to give amyloid *in vitro* (Contreras et al., 1999). The reason by which TPI nitrotyrosination triggers its aggregation could have to do with the destabilization of the dimer. The monomer contains 4 tyrosines: two close to the catalytic centre and two in the face that interacts with the other monomer. It has been previously reported that changes in the interface between the monomers can induce conformational changes in the catalytic centre and therefore affect the activity of the enzyme (Borchert et al., 1995;Cansu and Doruker, 2008). Thus, one may consider that modifying the residues localized around the catalytic centre could also affect the dimerization and stability of TPI. Recently it was found that dimer dissociation leads to unfolding of the enzyme, what could be an initial step to aggregation (Tellez et al., 2008). It may also happen that peroxynitrite nitrates directly the tyrosines in the interface between the monomers. In this way nitrotyrosines can form adducts with other nitrotyrosines and drive the aggregation of the enzyme.

In the literature there is a large body of evidence linking nitrative/oxidative stress and protein aggregation. The role of oxidative stress in aberrant protein-protein interaction has been described in some myofibrillar myopathies (Janue et al., 2007). Moreover peroxynitrite triggers the nitration and aggregation of α-synuclein of the frontal cortex of patients suffering from Pick's disease (Dalfo et al., 2006). Even tau protein has been reported to be nitrated *in vitro* by peroxynitrite, and this compound induces not only its oligomerization, but also its disassembly from microtubules (Zhang et al., 2005). However this study was carried out using a very high concentration of tau (1 μg/μL), and at the end the nature of such fibrils was not studied. In another study, the

authors observed that peroxynitrite could also mediate the aggregation of tau protein by forming adducts between tyrosines. However, they used 75 μM arachidonic acid to induce the fibrillation of 4 μM tau, both in concentrations very far from the physiological ones (Reynolds et al., 2005).

This work demonstrates that nitro-TPI serves as a seed for the posterior fibrillation of tau protein. The interaction between tau and nitro-TPI probably is an early event that depends on the misfolding of the enzyme and interacts with free tau protein avoiding its assembly to microtubules. It is interesting because shows how a damage in a particular protein can induce indirectly the aggregation of another protein. Secondly, this model does not take into account the tau phosphorylation state. Actually we demonstrate that tau can fibrillate without being phosphorylated, and what is more important, at a very low concentration of the protein. All the *in vitro* fibrillation studies of tau carried out in the past were performed at a very high concentration of the protein (1-10 μM), sometimes adding polyanionic anions or calcium (Kuret et al., 2005). The same results were obtained with hyperphosphorylated tau, probably meaning that hyperphosphorylation is an epiphenomenon or plays another role in the disease, likely by detaching it from microtubules.

However peroxynitrite can also induce the accumulation of intracellular tau concentrations by destroying the proteasome activity. Our group demonstrated the nitrotyrosination of one subunit of the 26s proteasome in a model of Cerebral Amyloid Angiopathy (Coma et al., 2005). The effect of this nitration was not evaluated, but another study found accumulation of tau protein in the hippocampus of rats injected with SIN-1, a peroxynitrite donor (Zhang et al., 2006). The authors explained these results by an experimentally observed 36 % decrease of the 26S proteasome activity, leading to less tau degradation. Tau accumulated in those rats was nitrated and

phosphorylated by p38 MAPKs and GSK-3β, indicating that peroxynitrite can also activate some kinases. Interestingly the authors demonstrate that nitrated tau is resistant to proteasome degradation (Zhang et al., 2006). Although some studies have argued that nitration is avoiding tau aggregation (Reynolds et al., 2005), Zhang et al. demonstrated that nitrated tau is accumulated in the hippocampus of SIN-1 injected rats (Zhang et al., 2006). However they could not simultaneously nitrate and phosphorylate tau *in vitro* because both modifications seemed to be incompatible *in vitro* (Zhang et al., 2006). Thus they could not reproduce the fibrillation of tau.

Although our model provides a direct link between Aβ toxicity and NFT formation, there are some aspects that remain without an explanation. Tau is known to be cleaved by proteolitic enzymes even after forming PHFs. Caspase-3 have been shown to cleave tau at D421 in a transgenic mice model and cultured cortical neurons exposed to $A\beta_{42}$ (Ramalho et al., 2008). Caspase-6 has also been involved in the cleavage of tau (Albrecht et al., 2007). However the AD phosphorylated tau at S422 prevents its cleavage by caspase-3 (Guillozet-Bongaarts et al., 2006). Thus phosphorylation would play a protective role through the prevention of NFT formation, setting doubt on the role of hyperphosphorylation in AD pathology. However other authors have shown on a mice model of human tauopathy that tau truncation is not a necessary event for its fibrillation (Delobel et al, 2008).

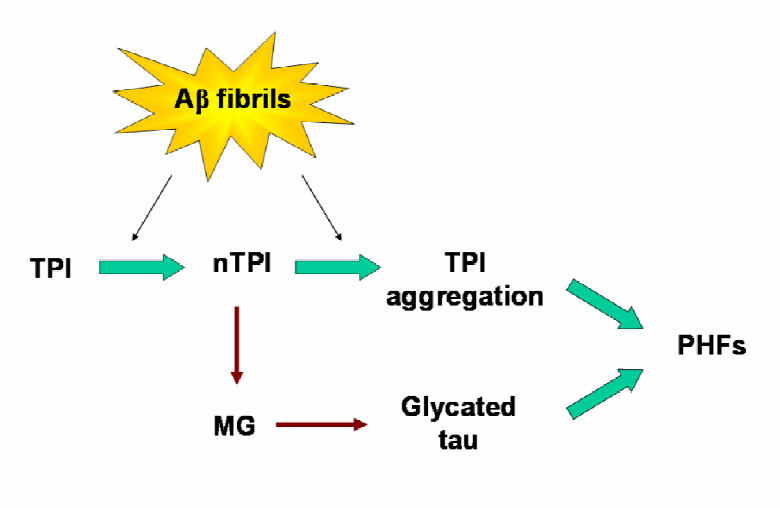

Figure 2. Amyloid-induced TPI nitrotyrosination increases MG and PHFs formation. Nitrated TPI releases more MG to the cytosol, what could also contribute to tau glycation and detaching from microtubules. If peroxynitrite formation increases in time, nitroTPI starts to aggregate and forms a seed where tau can begin to fibrillate.

Therapeutic strategies

Our data supports the role of peroxynitrite as an etiopathogenic factor for AD. The therapeutic strategies directed to reduce the peroxynitrite levels could delay the onset of the disease. At the same time, they could also reduce the symptoms by acting at the pathophysiological level, preventing the appearance of newly-formed NTF, or reducing the MG levels. One approach could consist of peroxynitrite-chelating compounds or antioxidants. Antioxidants have already demonstrated to be effective in protecting cells against Aβ-induced cytotoxicity. In fact several studies have been directed to test the efficiency of antioxidants in treating AD, normally by using vitamins or antioxidant cocktails (Gilgun-Sherki et al., 2003;Sano et al., 2008). However the trials have not shown a truly protective role of the available antioxidants against AD (Gilgun-Sherki et al., 2003;Sano et al., 2008), though other studies carried out in animal models point out to a rapid learning improvement (Head, 2008). Probably they need to

be improved at several levels such as the blood-brain barrier permeability, the right delivery of the drug or the appropriate timing of administration.

Regarding the use of a peroxynitrite chelator, this should not show cross-reactivity against NO, since this would interfere with the normal function of this gas in the CNS. In addition, NO mediates vasodilatation and allows a normal blood supply to the brain. The blocking of NO could also affect to the normal cerebral blood flux and impair the cognitive skills.

Another approach could consist of repairing the already existent damage. It is more complicated because nitrotyrosination is an irreversible modification. However some studies points to the existence of a cellular *denitrase* activity or activities (Kamisaki et al., 1998;Irie et al., 2003;Gorg et al., 2007;Smallwood et al., 2007;Kuo et al., 1999a;Kuo et al., 1999b). Although one may suggest that the called *denitrate* activity is just the proteasome-dependent degradation of nitrated proteins, there is a body of evidence supporting its existence. Firstly, the proteasome inhibitor lactacystin and general protease inhibitors do not reverse the *denitrase* activity (Irie et al., 2003). Secondly, the activity seems to be enhanced by the presence of Ca^{2+} (Kuo et al., 1999a;Kuo et al., 1999b). Thirdly, *denitrase* is destroyed by heat or trypsin treatment, demonstrating the proteic nature of the activity (Irie et al., 2003). Interestingly the *denitrase* activity has been proved to recover the activity of nitrated glutamine synthase (Gorg et al., 2007). Two different denitrase enzymes have been proposed to coexist: a type I or reductant-dependent and a type II or reductant-independent activity (Kuo et al., 1999a;Kuo et al., 1999b). These activities result in a net NO^{3-} production (Kuo et al., 1999a) as follows:

$$\text{Protein-Tyr-}NO_2 + H_2O \longrightarrow \text{Protein-Tyr-H} + H^+ + NO^{3-}$$

Glutathione-S-transferase has been proposed to be a type I *denitrase* enzyme. Interestingly the denitrase activity has been described also in crude brain extracts and glutathione-S-transferase seems to occur in the brain (Kuo et al., 1999a). Recently, it has been demonstrated that the lipoproteic fraction from the plasma is able to denitrate nitrotyrosinated albumin (Leger et al., 2008). We also detected a *denitrase* activity in lysates of SH-SY5Y cells (Figure 3). However, we could not reproduce the *denitrase* activity with the glutathione-S-transferase in our system. The finding of such a detoxifying mechanism and the study of those pathways regulating it could serve us to correct this damage and restore part of the function of the neurone.

Summarizing the specific therapeutic approaches should direct to scavenging peroxynitrite but without affecting to nitric oxide and to eliminate the nitrotyrosination of proteins by enhancing the denitrase activity.

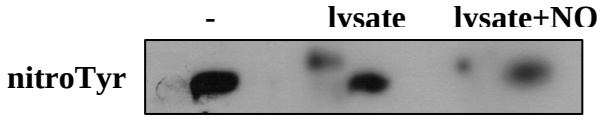

Figure 3. The denitrase activity as a therapeutic approach. NitroTPI bound to a nitrocellulose membrane was incubated with PBS or lysates of SH-SY5Y pre-treated or not with NO to stimulate a putative denitrase activity. All the incubations were performed with protease inhibitors. The nitroTPI found in the piece of membrane that had been incubated with SH-SY5Y lysates were less reactive to an antibody against nitrotyrosine.

V. CONCLUSIONS

From the present work we have obtained the following conclusions:

1. Peroxynitrite contributes to the switch of the $A\beta_{42}/A\beta_{40}$ ratio, as it happens in AD, by affecting to the γ-secretase activity.
2. Peroxynitrite induces the holoPS1 nitrotyrosination, which seems to inhibit partially its endoproteolitic cleavage.
3. Peroxynitrite increases the expression of nicastrin and Pen-2, which yields to an enhancement in the formation of mature γ-secretase complex in the membrane.
4. Peroxynitrite strengthens the interaction between CTF-PS1 and NTF-PS1, which could be related with the increased Aß formation.
5. Peroxynitrite enhances the aggretation into oligomers of $A\beta_{42}$ peptide, and these oligomers are significatively more neurotoxic that those non-nitrotyrosinated.
6. Aß-produced peroxynitrite is nitrotyrosinating TPI.
7. TPI nitrotyrosination is decreasing the catalytic isomerase activity but increasing the MG formation.
8. TPI nitrotyrosination is inducing the aggregation and misfolding in ß-sheet of TPI.
9. Nitro-TPI aggregates are inducing the tau fibrillation in PHFs.

VI. REFERENCES

Ahmed N, Battah S, Karachalias N, Babaei-Jadidi R, Horanyi M, Baroti K, Hollan S, Thornalley PJ (2003) Increased formation of methylglyoxal and protein glycation, oxidation and nitrosation in triosephosphate isomerase deficiency. Biochim Biophys Acta 1639:121-132.

Akomolafe A, Lunetta KL, Erlich PM, Cupples LA, Baldwin CT, Huyck M, Green RC, Farrer LA (2006) Genetic association between endothelial nitric oxide synthase and Alzheimer disease. Clin Genet 70:49-56.

Albrecht S, Bourdeau M, Bennett D, Mufson EJ, Bhattacharjee M, LeBlanc AC (2007) Activation of caspase-6 in aging and mild cognitive impairment. Am J Pathol 170:1200-1209.

Allinson TM, Parkin ET, Turner AJ, Hooper NM (2003) ADAMs family members as amyloid precursor protein alpha-secretases. J Neurosci Res 74:342-352.

Alzheimer A. (1906) Über einen eigenartigen schweren Erkrankungsprozeß der Hirnrinde. Neurologisches Centralblatt 23:1129-1136.

Amici M, Lupidi G, Angeletti M, Fioretti E, Eleuteri AM (2003) Peroxynitrite-induced oxidation and its effects on isolated proteasomal systems. Free Radic Biol Med 34:987-996.

Antony Bayer, Jan Reban (2004) Alzheimer's disease and relative conditions. pp 3-330. MEDEA Press.

Aslan M, Ryan TM, Townes TM, Coward L, Kirk MC, Barnes S, Alexander CB, Rosenfeld SS, Freeman BA (2003) Nitric oxide-dependent generation of reactive species in sickle cell disease. Actin tyrosine induces defective cytoskeletal polymerization. J Biol Chem 278:4194-4204.

Basha MR, Wei W, Bakheet SA, Benitez N, Siddiqi HK, Ge YW, Lahiri DK, Zawia NH (2005) The fetal basis of amyloidogenesis: exposure to lead and latent overexpression of amyloid precursor protein and beta-amyloid in the aging brain. J Neurosci 25:823-829.

Bayer TA, Cappai R, Masters CL, Beyreuther K, Multhaup G (1999) It all sticks together--the APP-related family of proteins and Alzheimer's disease. Mol Psychiatry 4:524-528.

Beckman JS, Beckman TW, Chen J, Marshall PA, Freeman BA (1990) Apparent hydroxyl radical production by peroxynitrite: implications for endothelial injury from nitric oxide and superoxide. Proc Natl Acad Sci U S A 87:1620-1624.

Beckman JS, Koppenol WH (1996) Nitric oxide, superoxide, and peroxynitrite: the good, the bad, and ugly. Am J Physiol 271:C1424-C1437.

Behl C, Davis JB, Lesley R, Schubert D (1994) Hydrogen peroxide mediates amyloid beta protein toxicity. Cell 77:817-827.

Berlett BS, Friguet B, Yim MB, Chock PB, Stadtman ER (1996) Peroxynitrite-mediated nitration of tyrosine residues in Escherichia coli glutamine synthetase mimics adenylylation: relevance to signal transduction. Proc Natl Acad Sci U S A 93:1776-1780.

Bertram L, Tanzi RE (2004) Alzheimer's disease: one disorder, too many genes? Hum Mol Genet 13 Spec No 1:R135-R141.

Bird TD (2008) Genetic aspects of Alzheimer disease. Genet Med 10:231-239.

Blass JP, Gibson GE, Hoyer S (2002) The role of the metabolic lesion in Alzheimer's disease. J Alzheimers Dis 4:225-232.

Bonnet R, Pavlovic S, Lehmann J, Rommelspacher H (2004) The strong inhibition of triosephosphate isomerase by the natural beta-carbolines may explain their neurotoxic actions. Neuroscience 127:443-453.

Borchert TV, Abagyan R, Jaenicke R, Wierenga RK (1994) Design, creation, and characterization of a stable, monomeric triosephosphate isomerase. Proc Natl Acad Sci U S A 91:1515-1518.

Borchert TV, Zeelen JP, Schliebs W, Callens M, Minke W, Jaenicke R, Wierenga RK (1995) An interface point-mutation variant of triosephosphate isomerase is compactly folded and monomeric at low protein concentrations. FEBS Lett 367:315-318.

Borghi R, Patriarca S, Traverso N, Piccini A, Storace D, Garuti A, Cirmena G, Odetti P, Tabaton M (2006) The increased activity of BACE1 correlates with oxidative stress in Alzheimer's disease. Neurobiol Aging.

Brechard S, Tschirhart EJ (2008) Regulation of superoxide production in neutrophils: role of calcium influx. J Leukoc Biol 84:1223-1237.

Bredt DS, Snyder SH (1994) Nitric oxide: a physiologic messenger molecule. Annu Rev Biochem 63:175-195.

Brennan ML, Wu W, Fu X, Shen Z, Song W, Frost H, Vadseth C, Narine L, Lenkiewicz E, Borchers MT, Lusis AJ, Lee JJ, Lee NA, bu-Soud HM, Ischiropoulos H, Hazen SL (2002) A tale of two controversies: defining both the role of peroxidases in nitrotyrosine formation in vivo using eosinophil peroxidase and myeloperoxidase-deficient mice, and the nature of peroxidase-generated reactive nitrogen species. J Biol Chem 277:17415-17427.

Buxbaum JD, Liu KN, Luo Y, Slack JL, Stocking KL, Peschon JJ, Johnson RS, Castner BJ, Cerretti DP, Black RA (1998) Evidence that tumor necrosis factor alpha converting enzyme is involved in regulated alpha-secretase cleavage of the Alzheimer amyloid protein precursor. J Biol Chem 273:27765-27767.

Cansu S, Doruker P (2008) Dimerization affects collective dynamics of triosephosphate isomerase. Biochemistry 47:1358-1368.

Capell A, Beher D, Prokop S, Steiner H, Kaether C, Shearman MS, Haass C (2005) Gamma-secretase complex assembly within the early secretory pathway. J Biol Chem 280:6471-6478.

Cassina AM, Hodara R, Souza JM, Thomson L, Castro L, Ischiropoulos H, Freeman BA, Radi R (2000) Cytochrome c nitration by peroxynitrite. J Biol Chem 275:21409-21415.

Castegna A, Thongboonkerd V, Klein JB, Lynn B, Markesbery WR, Butterfield DA (2003) Proteomic identification of nitrated proteins in Alzheimer's disease brain. J Neurochem 85:1394-1401.

Cefalu WT, Bell-Farrow AD, Wang ZQ, Sonntag WE, Fu MX, Baynes JW, Thorpe SR (1995) Caloric restriction decreases age-dependent accumulation of the glycoxidation products, N epsilon-(carboxymethyl)lysine and pentosidine, in rat skin collagen. J Gerontol A Biol Sci Med Sci 50:B337-B341.

Cerpa W, Dinamarca MC, Inestrosa NC (2008) Structure-function implications in Alzheimer's disease: effect of Abeta oligomers at central synapses. Curr Alzheimer Res 5:233-243.

Charlwood J, Dingwall C, Matico R, Hussain I, Johanson K, Moore S, Powell DJ, Skehel JM, Ratcliffe S, Clarke B, Trill J, Sweitzer S, Camilleri P (2001) Characterization of the glycosylation profiles of Alzheimer's beta -secretase protein Asp-2 expressed in a variety of cell lines. J Biol Chem 276:16739-16748.

Cheng A, Wang S, Cai J, Rao MS, Mattson MP (2003) Nitric oxide acts in a positive feedback loop with BDNF to regulate neural progenitor cell proliferation and differentiation in the mammalian brain. Dev Biol 258:319-333.

Cheung KH, Shineman D, Muller M, Cardenas C, Mei L, Yang J, Tomita T, Iwatsubo T, Lee VM, Foskett JK (2008) Mechanism of Ca2+ disruption in Alzheimer's disease by presenilin regulation of InsP3 receptor channel gating. Neuron 58:871-883.

Christensen DZ, Bayer TA, Wirths O (2008) Intracellular Abeta triggers neuron loss in the cholinergic system of the APP/PS1KI mouse model of Alzheimer's disease. Neurobiol Aging.

Cobbs CS, Whisenhunt TR, Wesemann DR, Harkins LE, Van Meir EG, Samanta M (2003) Inactivation of wild-type p53 protein function by reactive oxygen and nitrogen species in malignant glioma cells. Cancer Res 63:8670-8673.

Coma M, Guix FX, Ill-Raga G, Uribesalgo I, Alameda F, Valverde MA, Munoz FJ (2008) Oxidative stress triggers the amyloidogenic pathway in human vascular smooth muscle cells. Neurobiol Aging 29:969-980.

Coma M, Guix FX, Uribesalgo I, Espuna G, Sole M, Andreu D, Munoz FJ (2005) Lack of oestrogen protection in amyloid-mediated endothelial damage due to protein nitrotyrosination. Brain 128:1613-1621.

Connor JR, Menzies SL, St Martin SM, Mufson EJ (1992) A histochemical study of iron, transferrin, and ferritin in Alzheimer's diseased brains. J Neurosci Res 31:75-83.

Contreras CF, Canales MA, Alvarez A, De Ferrari GV, Inestrosa NC (1999) Molecular modeling of the amyloid-beta-peptide using the homology to a fragment of triosephosphate isomerase that forms amyloid in vitro. Protein Eng 12:959-966.

Coraci IS, Husemann J, Berman JW, Hulette C, Dufour JH, Campanella GK, Luster AD, Silverstein SC, El-Khoury JB (2002) CD36, a class B scavenger receptor, is expressed on microglia in Alzheimer's disease brains and can mediate production of reactive oxygen species in response to beta-amyloid fibrils. Am J Pathol 160:101-112.

Cudd A, Fridovich I (1982) Electrostatic interactions in the reaction mechanism of bovine erythrocyte superoxide dismutase. J Biol Chem 257:11443-11447.

Czech C, Tremp G, Pradier L (2000) Presenilins and Alzheimer's disease: biological functions and pathogenic mechanisms. Prog Neurobiol 60:363-384.

Dahiyat M, Cumming A, Harrington C, Wischik C, Xuereb J, Corrigan F, Breen G, Shaw D, St CD (1999) Association between Alzheimer's disease and the NOS3 gene. Ann Neurol 46:664-667.

Dalfo E, Martinez A, Muntane G, Ferrer I (2006) Abnormal alpha-synuclein solubility, aggregation and nitration in the frontal cortex in Pick's disease. Neurosci Lett 400:125-129.

Dar MS, Morselli PL, Bowman ER (1985) The enzymatic systems involved in the mammalian metabolism of methylamine. Gen Pharmacol 16:557-560.

De Strooper B, Annaert W (2000) Proteolytic processing and cell biological functions of the amyloid precursor protein. J Cell Sci 113 (Pt 11):1857-1870.

De Strooper B, Saftig P, Craessaerts K, Vanderstichele H, Guhde G, Annaert W, von FK, Van LF (1998) Deficiency of presenilin-1 inhibits the normal cleavage of amyloid precursor protein. Nature 391:387-390.

De Strooper B, Simons M, Multhaup G, Van LF, Beyreuther K, Dotti CG (1995) Production of intracellular amyloid-containing fragments in hippocampal neurons expressing human amyloid precursor protein and protection against amyloidogenesis by subtle amino acid substitutions in the rodent sequence. EMBO J 14:4932-4938.

Deane R, Sagare A, Zlokovic BV (2008) The role of the cell surface LRP and soluble LRP in blood-brain barrier Abeta clearance in Alzheimer's disease. Curr Pharm Des 14:1601-1605.

Dei R, Takeda A, Niwa H, Li M, Nakagomi Y, Watanabe M, Inagaki T, Washimi Y, Yasuda Y, Horie K, Miyata T, Sobue G (2002) Lipid peroxidation and advanced glycation end products in the brain in normal aging and in Alzheimer's disease. Acta Neuropathol 104:113-122.

DeKosky ST, Abrahamson EE, Ciallella JR, Paljug WR, Wisniewski SR, Clark RS, Ikonomovic MD (2007) Association of increased cortical soluble abeta42 levels with diffuse plaques after severe brain injury in humans. Arch Neurol 64:541-544.

Del Toro D, Coma M, Uribesalgo I, Guix FX, Muñoz FJ (2005) The amyloid beta-protein precursor and Alzheimer's disease - Therapeutic approaches. Curr Med Chem 5:271-283.

Deng-Bryant Y, Singh IN, Carrico KM, Hall ED (2008) Neuroprotective effects of tempol, a catalytic scavenger of peroxynitrite-derived free radicals, in a mouse traumatic brain injury model. J Cereb Blood Flow Metab 28:1114-1126.

Dickson DW, Farlo J, Davies P, Crystal H, Fuld P, Yen SH (1988) Alzheimer's disease. A double-labeling immunohistochemical study of senile plaques. Am J Pathol 132:86-101.

Dinerman JL, Dawson TM, Schell MJ, Snowman A, Snyder SH (1994) Endothelial nitric oxide synthase localized to hippocampal pyramidal cells: implications for synaptic plasticity. Proc Natl Acad Sci U S A 91:4214-4218.

Ding H, Johnson GV (2008) The last tangle of tau. J Alzheimers Dis 14:441-447.

Dolev I, Michaelson DM (2006) The nucleation growth and reversibility of Amyloid-beta deposition in vivo. J Alzheimers Dis 10:291-301.

Drubin DG, Kirschner MW (1986) Tau protein function in living cells. J Cell Biol 103:2739-2746.

Eanes ED, Glenner GG (1968) X-ray diffraction studies on amyloid filaments. J Histochem Cytochem 16:673-677.

Ebadi M, Sharma SK (2003) Peroxynitrite and mitochondrial dysfunction in the pathogenesis of Parkinson's disease. Antioxid Redox Signal 5:319-335.

Ehehalt R, Keller P, Haass C, Thiele C, Simons K (2003) Amyloidogenic processing of the Alzheimer beta-amyloid precursor protein depends on lipid rafts. J Cell Biol 160:113-123.

Eiserich JP, Hristova M, Cross CE, Jones AD, Freeman BA, Halliwell B, van d, V (1998) Formation of nitric oxide-derived inflammatory oxidants by myeloperoxidase in neutrophils. Nature 391:393-397.

El KJ, Hickman SE, Thomas CA, Cao L, Silverstein SC, Loike JD (1996) Scavenger receptor-mediated adhesion of microglia to beta-amyloid fibrils. Nature 382:716-719.

Eliezer D, Barre P, Kobaslija M, Chan D, Li X, Heend L (2005) Residual structure in the repeat domain of tau: echoes of microtubule binding and paired helical filament formation. Biochemistry 44:1026-1036.

Evin G, Zhu A, Holsinger RM, Masters CL, Li QX (2003) Proteolytic processing of the Alzheimer's disease amyloid precursor protein in brain and platelets. J Neurosci Res 74:386-392.

Findeis MA (2007) The role of amyloid beta peptide 42 in Alzheimer's disease. Pharmacol Ther 116:266-286.

Fugere NA, Ferrington DA, Thompson LV (2006) Protein nitration with aging in the rat semimembranosus and soleus muscles. J Gerontol A Biol Sci Med Sci 61:806-812.

Gasser A, Forbes JM (2008) Advanced glycation: implications in tissue damage and disease. Protein Pept Lett 15:385-391.

Gibson GE (2002) Interactions of oxidative stress with cellular calcium dynamics and glucose metabolism in Alzheimer's disease. Free Radic Biol Med 32:1061-1070.

Gilgun-Sherki Y, Melamed E, Offen D (2003) Antioxidant treatment in Alzheimer's disease: current state. J Mol Neurosci 21:1-11.

Gluck MA, Myers CE, Nicolle MM, Johnson S (2006) Computational models of the hippocampal region: implications for prediction of risk for Alzheimer's disease in non-demented elderly. Curr Alzheimer Res 3:247-257.

Gnerer JP, Kreber RA, Ganetzky B (2006) wasted away, a Drosophila mutation in triosephosphate isomerase, causes paralysis, neurodegeneration, and early death. Proc Natl Acad Sci U S A 103:14987-14993.

Go YM, Patel RP, Maland MC, Park H, Beckman JS, rley-Usmar VM, Jo H (1999) Evidence for peroxynitrite as a signaling molecule in flow-dependent activation of c-Jun NH(2)-terminal kinase. Am J Physiol 277:H1647-H1653.

Goedert M, Spillantini MG (2006) A century of Alzheimer's disease. Science 314:777-781.

Goedert M, Spillantini MG, Jakes R, Rutherford D, Crowther RA (1989a) Multiple isoforms of human microtubule-associated protein tau: sequences and localization in neurofibrillary tangles of Alzheimer's disease. Neuron 3:519-526.

Goedert M, Spillantini MG, Potier MC, Ulrich J, Crowther RA (1989b) Cloning and sequencing of the cDNA encoding an isoform of microtubule-associated protein tau containing four tandem repeats: differential expression of tau protein mRNAs in human brain. EMBO J 8:393-399.

Gonzalez D, Drapier JC, Bouton C (2004) Endogenous nitration of iron regulatory protein-1 (IRP-1) in nitric oxide-producing murine macrophages: further insight into the mechanism of nitration in vivo and its impact on IRP-1 functions. J Biol Chem 279:43345-43351.

Good PF, Perl DP, Bierer LM, Schmeidler J (1992) Selective accumulation of aluminum and iron in the neurofibrillary tangles of Alzheimer's disease: a laser microprobe (LAMMA) study. Ann Neurol 31:286-292.

Gorg B, Qvartskhava N, Voss P, Grune T, Haussinger D, Schliess F (2007) Reversible inhibition of mammalian glutamine synthetase by tyrosine nitration. FEBS Lett 581:84-90.

Gorman PM, Kim S, Guo M, Melnyk RA, McLaurin J, Fraser PE, Bowie JU, Chakrabartty A (2008) Dimerization of the transmembrane domain of amyloid precursor proteins and familial Alzheimer's disease mutants. BMC Neurosci 9:17.

Gotz J, Chen F, van DJ, Nitsch RM (2001) Formation of neurofibrillary tangles in P301l tau transgenic mice induced by Abeta 42 fibrils. Science 293:1491-1495.

Gracy RW, Chapman ML, Cini JK, Jahani M, Tollefsbol TO, Yuksel KU (1985) Molecular basis of the accumulation of abnormal proteins in progeria and aging fibroblasts. Basic Life Sci 35:427-442.

Grillo MA, Colombatto S (2008) Advanced glycation end-products (AGEs): involvement in aging and in neurodegenerative diseases. Amino Acids 35:29-36.

Guillozet-Bongaarts AL, Cahill ME, Cryns VL, Reynolds MR, Berry RW, Binder LI (2006) Pseudophosphorylation of tau at serine 422 inhibits caspase cleavage: in vitro evidence and implications for tangle formation in vivo. J Neurochem 97:1005-1014.

Guix FX, Uribesalgo I, Coma M, Munoz FJ (2005) The physiology and pathophysiology of nitric oxide in the brain. Prog Neurobiol 76:126-152.

Guo H, Albrecht S, Bourdeau M, Petzke T, Bergeron C, LeBlanc AC (2004) Active caspase-6 and caspase-6-cleaved tau in neuropil threads, neuritic plaques, and neurofibrillary tangles of Alzheimer's disease. Am J Pathol 165:523-531.

Hanger DP, Byers HL, Wray S, Leung KY, Saxton MJ, Seereeram A, Reynolds CH, Ward MA, Anderton BH (2007) Novel phosphorylation sites in tau from Alzheimer brain support a role for casein kinase 1 in disease pathogenesis. J Biol Chem 282:23645-23654.

Harper JD, Wong SS, Lieber CM, Lansbury PT (1997) Observation of metastable Abeta amyloid protofibrils by atomic force microscopy. Chem Biol 4:119-125.

Harper JD, Wong SS, Lieber CM, Lansbury PT, Jr. (1999) Assembly of A beta amyloid protofibrils: an in vitro model for a possible early event in Alzheimer's disease. Biochemistry 38:8972-8980.

Harrington CR, Colaco CA (1994) Alzheimer's disease. A glycation connection. Nature 370:247-248.

Hartley DM, Walsh DM, Ye CP, Diehl T, Vasquez S, Vassilev PM, Teplow DB, Selkoe DJ (1999) Protofibrillar intermediates of amyloid beta-protein induce acute electrophysiological changes and progressive neurotoxicity in cortical neurons. J Neurosci 19:8876-8884.

Hartmann D, De Stooper B, Serneels L, Craessaerts K, Herreman A, Annaert W, Umans L, Lubke T, Lena IA, von FK, Saftig P (2002) The disintegrin/metalloprotease ADAM 10 is essential for Notch signalling but not for alpha-secretase activity in fibroblasts. Hum Mol Genet 11:2615-2624.

Harwood DG, Sultzer DL, Feil D, Monserratt L, Freedman E, Mandelkern MA (2005) Frontal lobe hypometabolism and impaired insight in Alzheimer disease. Am J Geriatr Psychiatry 13:934-941.

Head E (2008) Oxidative Damage and Cognitive Dysfunction: Antioxidant Treatments to Promote Healthy Brain Aging. Neurochem Res.
Hebert SS, Godin C, Levesque G (2003) Oligomerization of human presenilin-1 fragments. FEBS Lett 550:30-34.

Hensley K, Carney JM, Mattson MP, Aksenova M, Harris M, Wu JF, Floyd RA, Butterfield DA (1994) A model for beta-amyloid aggregation and neurotoxicity based on free radical generation by the peptide: relevance to Alzheimer disease. Proc Natl Acad Sci U S A 91:3270-3274.

Hensley K, Maidt ML, Yu Z, Sang H, Markesbery WR, Floyd RA (1998) Electrochemical analysis of protein nitrotyrosine and dityrosine in the Alzheimer brain indicates region-specific accumulation. J Neurosci 18:8126-8132.

Heutink P (2000) Untangling tau-related dementia. Hum Mol Genet 9:979-986.

Hink U, Oelze M, Kolb P, Bachschmid M, Zou MH, Daiber A, Mollnau H, August M, Baldus S, Tsilimingas N, Walter U, Ullrich V, Munzel T (2003) Role for peroxynitrite in the inhibition of prostacyclin synthase in nitrate tolerance. J Am Coll Cardiol 42:1826-1834.

Huang TH, Yang DS, Plaskos NP, Go S, Yip CM, Fraser PE, Chakrabartty A (2000) Structural studies of soluble oligomers of the Alzheimer beta-amyloid peptide. J Mol Biol 297:73-87.

Huang X, Atwood CS, Hartshorn MA, Multhaup G, Goldstein LE, Scarpa RC, Cuajungco MP, Gray DN, Lim J, Moir RD, Tanzi RE, Bush AI (1999) The A beta peptide of Alzheimer's disease directly produces hydrogen peroxide through metal ion reduction. Biochemistry 38:7609-7616.

Huie RE, Padmaja S (1993) The reaction of no with superoxide. Free Radic Res Commun 18:195-199.

Ignarro LJ (1989) Endothelium-derived nitric oxide: actions and properties. FASEB J 3:31-36.

Iijima K, Liu HP, Chiang AS, Hearn SA, Konsolaki M, Zhong Y (2004) Dissecting the pathological effects of human Abeta40 and Abeta42 in Drosophila: a potential model for Alzheimer's disease. Proc Natl Acad Sci U S A 101:6623-6628.

Imahori K, Uchida T (1997) Physiology and pathology of tau protein kinases in relation to Alzheimer's disease. J Biochem 121:179-188.

Inestrosa NC, Reyes AE, Chacon MA, Cerpa W, Villalon A, Montiel J, Merabachvili G, Aldunate R, Bozinovic F, Aboitiz F (2005) Human-like rodent amyloid-beta-peptide determines Alzheimer pathology in aged wild-type Octodon degu. Neurobiol Aging 26:1023-1028.

Irie Y, Saeki M, Kamisaki Y, Martin E, Murad F (2003) Histone H1.2 is a substrate for denitrase, an activity that reduces nitrotyrosine immunoreactivity in proteins. Proc Natl Acad Sci U S A 100:5634-5639.

Irizarry MC, Soriano F, McNamara M, Page KJ, Schenk D, Games D, Hyman BT (1997) Abeta deposition is associated with neuropil changes, but not with overt neuronal loss in the human amyloid precursor protein V717F (PDAPP) transgenic mouse. J Neurosci 17:7053-7059.

Ischiropoulos H (2003) Biological selectivity and functional aspects of protein tyrosine nitration. Biochem Biophys Res Commun 305:776-783.

Ischiropoulos H, Zhu L, Chen J, Tsai M, Martin JC, Smith CD, Beckman JS (1992) Peroxynitrite-mediated tyrosine nitration catalyzed by superoxide dismutase. Arch Biochem Biophys 298:431-437.

Ito K, Hanazawa T, Tomita K, Barnes PJ, Adcock IM (2004) Oxidative stress reduces histone deacetylase 2 activity and enhances IL-8 gene expression: role of tyrosine nitration. Biochem Biophys Res Commun 315:240-245.

Janue A, Olive M, Ferrer I (2007) Oxidative stress in desminopathies and myotilinopathies: a link between oxidative damage and abnormal protein aggregation. Brain Pathol 17:377-388.

Ji Y, Bennett BM (2003) Activation of microsomal glutathione s-transferase by peroxynitrite. Mol Pharmacol 63:136-146.

Jo DG, Arumugam TV, Woo HN, Park JS, Tang SC, Mughal M, Hyun DH, Park JH, Choi YH, Gwon AR, Camandola S, Cheng A, Cai H, Song W, Markesbery WR, Mattson MP (2008) Evidence that gamma-secretase mediates oxidative stress-induced beta-secretase expression in Alzheimer's disease. Neurobiol Aging.

Kamisaki Y, Wada K, Bian K, Balabanli B, Davis K, Martin E, Behbod F, Lee YC, Kanai AJ, Pearce LL, Clemens PR, Birder LA, VanBibber MM, Choi SY, de Groat WC, Peterson J (2001) Identification of a neuronal nitric oxide synthase in isolated cardiac mitochondria using electrochemical detection. Proc Natl Acad Sci U S A 98:14126-14131.

Kang J, Muller-Hill B (1990) Differential splicing of Alzheimer's disease amyloid A4 precursor RNA in rat tissues: PreA4(695) mRNA is predominantly produced in rat and human brain. Biochem Biophys Res Commun 166:1192-1200.

Kanski J, Alterman MA, Schoneich C (2003) Proteomic identification of age-dependent protein nitration in rat skeletal muscle. Free Radic Biol Med 35:1229-1239.

Kauwe JS, Wang J, Chakraverty S, Goate AM, Henao-Martinez AF (2008) Novel presenilin 1 variant (P117A) causing Alzheimer's disease in the fourth decade of life. Neurosci Lett 438:257-259.

Kawarabayashi T, Younkin LH, Saido TC, Shoji M, Ashe KH, Younkin SG (2001) Age-dependent changes in brain, CSF, and plasma amyloid (beta) protein in the Tg2576 transgenic mouse model of Alzheimer's disease. J Neurosci 21:372-381.

Kayed R, Head E, Thompson JL, McIntire TM, Milton SC, Cotman CW, Glabe CG (2003) Common structure of soluble amyloid oligomers implies common mechanism of pathogenesis. Science 300:486-489.

Kim SH, Yin YI, Li YM, Sisodia SS (2004) Evidence that assembly of an active gamma-secretase complex occurs in the early compartments of the secretory pathway. J Biol Chem 279:48615-48619.

Kinobe R, Ji Y, Nakatsu K (2004) Peroxynitrite-mediated inactivation of heme oxygenases. BMC Pharmacol 4:26.

Kirschner DA, Abraham C, Selkoe DJ (1986) X-ray diffraction from intraneuronal paired helical filaments and extraneuronal amyloid fibers in Alzheimer disease indicates cross-beta conformation. Proc Natl Acad Sci U S A 83:503-507.

Kirschner DA, Inouye H, Duffy LK, Sinclair A, Lind M, Selkoe DJ (1987) Synthetic peptide homologous to beta protein from Alzheimer disease forms amyloid-like fibrils in vitro. Proc Natl Acad Sci U S A 84:6953-6957.

Kishida KT, Klann E (2007) Sources and targets of reactive oxygen species in synaptic plasticity and memory. Antioxid Redox Signal 9:233-244.

Kishida KT, Pao M, Holland SM, Klann E (2005) NADPH oxidase is required for NMDA receptor-dependent activation of ERK in hippocampal area CA1. J Neurochem 94:299-306.

Knappenberger KS, Tian G, Ye X, Sobotka-Briner C, Ghanekar SV, Greenberg BD, Scott CW (2004) Mechanism of gamma-secretase cleavage activation: is gamma-secretase regulated through autoinhibition involving the presenilin-1 exon 9 loop? Biochemistry 43:6208-6218.

Knops J, Suomensaari S, Lee M, McConlogue L, Seubert P, Sinha S (1995) Cell-type and amyloid precursor protein-type specific inhibition of A beta release by bafilomycin A1, a selective inhibitor of vacuolar ATPases. J Biol Chem 270:2419-2422.

Knowles RB, Wyart C, Buldyrev SV, Cruz L, Urbanc B, Hasselmo ME, Stanley HE, Hyman BT (1999) Plaque-induced neurite abnormalities: implications for disruption of neural networks in Alzheimer's disease. Proc Natl Acad Sci U S A 96:5274-5279.

Koeck T, Levison B, Hazen SL, Crabb JW, Stuehr DJ, Aulak KS (2004) Tyrosine nitration impairs mammalian aldolase A activity. Mol Cell Proteomics 3:548-557.

Koike H, Tomioka S, Sorimachi H, Saido TC, Maruyama K, Okuyama A, Fujisawa-Sehara A, Ohno S, Suzuki K, Ishiura S (1999) Membrane-anchored metalloprotease MDC9 has an alpha-secretase activity responsible for processing the amyloid precursor protein. Biochem J 343 Pt 2:371-375.

Kojro E, Fahrenholz F (2005) The non-amyloidogenic pathway: structure and function of alpha-secretases. Subcell Biochem 38:105-127.

Koppal T, Subramaniam R, Drake J, Prasad MR, Dhillon H, Butterfield DA (1998) Vitamin E protects against Alzheimer's amyloid peptide (25-35)-induced changes in neocortical synaptosomal membrane lipid structure and composition. Brain Res 786:270-273.

Kuhla B, Haase C, Flach K, Luth HJ, Arendt T, Munch G (2007) Effect of pseudophosphorylation and cross-linking by lipid peroxidation and advanced glycation end product precursors on tau aggregation and filament formation. J Biol Chem 282:6984-6991.

Kuhla B, Luth HJ, Haferburg D, Boeck K, Arendt T, Munch G (2005) Methylglyoxal, glyoxal, and their detoxification in Alzheimer's disease. Ann N Y Acad Sci 1043:211-216.

Kumar-Singh S, Theuns J, Van BB, Pirici D, Vennekens K, Corsmit E, Cruts M, Dermaut B, Wang R, Van BC (2006) Mean age-of-onset of familial alzheimer disease caused by presenilin mutations correlates with both increased Abeta42 and decreased Abeta40. Hum Mutat 27:686-695.

Kuo WN, Kanadia RN, Shanbhag VP (1999a) Denitration of peroxynitrite-treated proteins by "protein nitratases" from dog prostate. Biochem Mol Biol Int 47:1061-1067.

Kuo WN, Kanadia RN, Shanbhag VP, Toro R (1999b) Denitration of peroxynitrite-treated proteins by 'protein nitratases' from rat brain and heart. Mol Cell Biochem 201:11-16.

Kuret J, Congdon EE, Li G, Yin H, Yu X, Zhong Q (2005) Evaluating triggers and enhancers of tau fibrillization. Microsc Res Tech 67:141-155.

Kuzuya A, Uemura K, Kitagawa N, Aoyagi N, Kihara T, Ninomiya H, Ishiura S, Takahashi R, Shimohama S (2007) Presenilin 1 is involved in the maturation of beta-site amyloid precursor protein-cleaving enzyme 1 (BACE1). J Neurosci Res 85:153-165.

Lambert JC, Amouyel P (2007) Genetic heterogeneity of Alzheimer's disease: complexity and advances. Psychoneuroendocrinology 32 Suppl 1:S62-S70.

Lambert MP, Barlow AK, Chromy BA, Edwards C, Freed R, Liosatos M, Morgan TE, Rozovsky I, Trommer B, Viola KL, Wals P, Zhang C, Finch CE, Krafft GA, Klein WL (1998) Diffusible, nonfibrillar ligands derived from Abeta1-42 are potent central nervous system neurotoxins. Proc Natl Acad Sci U S A 95:6448-6453.

Lammich S, Kojro E, Postina R, Gilbert S, Pfeiffer R, Jasionowski M, Haass C, Fahrenholz F (1999) Constitutive and regulated alpha-secretase cleavage of Alzheimer's amyloid precursor protein by a disintegrin metalloprotease. Proc Natl Acad Sci U S A 96:3922-3927.

Laporte V, Lombard Y, Levy-Benezra R, Tranchant C, Poindron P, Warter JM (2004) Uptake of Abeta 1-40- and Abeta 1-42-coated yeast by microglial cells: a role for LRP. J Leukoc Biol 76:451-461.

Lavie L, Reznick AZ, Gershon D (1982) Decreased protein and puromycinyl-peptide degradation in livers of senescent mice. Biochem J 202:47-51.

Leger CL, Torres-Rasgado E, Fouret G, Carbonneau MA (2008) First evidence for an LDL- and HDL-associated nitratase activity that denitrates albumin-bound nitrotyrosine--physiological consequences. IUBMB Life 60:73-78.

LeVine H, III (1993) Thioflavine T interaction with synthetic Alzheimer's disease beta-amyloid peptides: detection of amyloid aggregation in solution. Protein Sci 2:404-410.

Levites Y, Das P, Price RW, Rochette MJ, Kostura LA, McGowan EM, Murphy MP, Golde TE (2006) Anti-Abeta42- and anti-Abeta40-specific mAbs attenuate amyloid deposition in an Alzheimer disease mouse model. J Clin Invest 116:193-201.

Levy E, Carman MD, Fernandez-Madrid IJ, Power MD, Lieberburg I, van Duinen SG, Bots GT, Luyendijk W, Frangione B (1990) Mutation of the Alzheimer's disease amyloid gene in hereditary cerebral hemorrhage, Dutch type. Science 248:1124-1126.

Levy-Lahad E, Wasco W, Poorkaj P, Romano DM, Oshima J, Pettingell WH, Yu CE, Jondro PD, Schmidt SD, Wang K, . (1995) Candidate gene for the chromosome 1 familial Alzheimer's disease locus. Science 269:973-977.

Lewczuk P, Esselmann H, Otto M, Maler JM, Henkel AW, Henkel MK, Eikenberg O, Antz C, Krause WR, Reulbach U, Kornhuber J, Wiltfang J (2004) Neurochemical diagnosis of Alzheimer's dementia by CSF Abeta42, Abeta42/Abeta40 ratio and total tau. Neurobiol Aging 25:273-281.

Lewis J, Dickson DW, Lin WL, Chisholm L, Corral A, Jones G, Yen SH, Sahara N, Skipper L, Yager D, Eckman C, Hardy J, Hutton M, McGowan E (2001) Enhanced neurofibrillary degeneration in transgenic mice expressing mutant tau and APP. Science 293:1487-1491.

Lewko B, Stepinski J (2002) Cyclic GMP signaling in podocytes. Microsc Res Tech 57:232-235.

Li Y, Grupe A (2007) Genetics of late-onset Alzheimer's disease: progress and prospect. Pharmacogenomics 8:1747-1755.

Liang WS, Reiman EM, Valla J, Dunckley T, Beach TG, Grover A, Niedzielko TL, Schneider LE, Mastroeni D, Caselli R, Kukull W, Morris JC, Hulette CM, Schmechel D, Rogers J, Stephan DA (2008) Alzheimer's disease is associated with reduced expression of energy metabolism genes in posterior cingulate neurons. Proc Natl Acad Sci U S A 105:4441-4446.

Liu SJ, Zhang JY, Li HL, Fang ZY, Wang Q, Deng HM, Gong CX, Grundke-Iqbal I, Iqbal K, Wang JZ (2004) Tau becomes a more favorable substrate for GSK-3 when it is prephosphorylated by PKA in rat brain. J Biol Chem 279:50078-50088.

Lovell MA, Robertson JD, Teesdale WJ, Campbell JL, Markesbery WR (1998) Copper, iron and zinc in Alzheimer's disease senile plaques. J Neurol Sci 158:47-52.

Lovestone S, Reynolds CH (1997) The phosphorylation of tau: a critical stage in neurodevelopment and neurodegenerative processes. Neuroscience 78:309-324.

Luth HJ, Holzer M, Gartner U, Staufenbiel M, Arendt T (2001) Expression of endothelial and inducible NOS-isoforms is increased in Alzheimer's disease, in APP23 transgenic mice and after experimental brain lesion in rat: evidence for an induction by amyloid pathology. Brain Res 913:57-67.

Luth HJ, Ogunlade V, Kuhla B, Kientsch-Engel R, Stahl P, Webster J, Arendt T, Munch G (2005) Age- and stage-dependent accumulation of advanced glycation end products in intracellular deposits in normal and Alzheimer's disease brains. Cereb Cortex 15:211-220.

Lyles GA, Chalmers J (1995) Aminoacetone metabolism by semicarbazide-sensitive amine oxidase in rat aorta. Biochem Pharmacol 49:416-419.

Mandelkow E, von BM, Biernat J, Mandelkow EM (2007) Structural principles of tau and the paired helical filaments of Alzheimer's disease. Brain Pathol 17:83-90.

Mannervik B (2008) Molecular enzymology of the glyoxalase system. Drug Metabol Drug Interact 23:13-27.

Mark RJ, Fuson KS, May PC (1999) Characterization of 8-epiprostaglandin F2alpha as a marker of amyloid beta-peptide-induced oxidative damage. J Neurochem 72:1146-1153.

Masoro EJ, Katz MS, McMahan CA (1989) Evidence for the glycation hypothesis of aging from the food-restricted rodent model. J Gerontol 44:B20-B22.
Mathews C.K., Van Hole K.E. (1999) Biochemistry.

Mattson MP (1995) Degenerative and protective signaling mechanisms in the neurofibrillary pathology of AD. Neurobiol Aging 16:447-457.

McNulty S, Fonfria E (2005) The role of TRPM channels in cell death. Pflugers Arch 451:235-242.

Mena R, Edwards PC, Harrington CR, Mukaetova-Ladinska EB, Wischik CM (1996) Staging the pathological assembly of truncated tau protein into paired helical filaments in Alzheimer's disease. Acta Neuropathol 91:633-641.

Millan-Crow LA, Crow JP, Kerby JD, Beckman JS, Thompson JA (1996) Nitration and inactivation of manganese superoxide dismutase in chronic rejection of human renal allografts. Proc Natl Acad Sci U S A 93:11853-11858.

Miranda S, Opazo C, Larrondo LF, Munoz FJ, Ruiz F, Leighton F, Inestrosa NC (2000) The role of oxidative stress in the toxicity induced by amyloid beta-peptide in Alzheimer's disease. Prog Neurobiol 62:633-648.

Monti JM, Jantos H (2004) Effects of L-arginine and SIN-1 on sleep and waking in the rat during both phases of the light-dark cycle. Life Sci 75:2027-2034.

Morais VA, Leight S, Pijak DS, Lee VM, Costa J (2008) Cellular localization of Nicastrin affects amyloid beta species production. FEBS Lett 582:427-433.

Mosconi L, Brys M, Switalski R, Mistur R, Glodzik L, Pirraglia E, Tsui W, De SS, de Leon MJ (2007) Maternal family history of Alzheimer's disease predisposes to reduced brain glucose metabolism. Proc Natl Acad Sci U S A 104:19067-19072.

Mosconi L, Tsui WH, De SS, Li J, Rusinek H, Convit A, Li Y, Boppana M, de Leon MJ (2005) Reduced hippocampal metabolism in MCI and AD: automated FDG-PET image analysis. Neurology 64:1860-1867.

Mudher A, Lovestone S (2002) Alzheimer's disease-do tauists and baptists finally shake hands? Trends Neurosci 25:22-26.

Mullan M, Crawford F, Axelman K, Houlden H, Lilius L, Winblad B, Lannfelt L (1992) A pathogenic mutation for probable Alzheimer's disease in the APP gene at the N-terminus of beta-amyloid. Nat Genet 1:345-347.

Multhaup G, Schlicksupp A, Hesse L, Beher D, Ruppert T, Masters CL, Beyreuther K (1996) The amyloid precursor protein of Alzheimer's disease in the reduction of copper(II) to copper(I). Science 271:1406-1409.

Munch G, Thome J, Foley P, Schinzel R, Riederer P (1997) Advanced glycation endproducts in ageing and Alzheimer's disease. Brain Res Brain Res Rev 23:134-143.

Mungrue IN, Bredt DS, Stewart DJ, Husain M (2003) From molecules to mammals: what's NOS got to do with it? Acta Physiol Scand 179:123-135.

Muñoz FJ, Inestrosa NC. (1999) Neurotoxicity of acetylcholinesterase amyloid beta-peptide aggregates is dependent on the type of Abeta peptide and the AChE concentration present in the complexes. FEBS Lett. 450:205-9.

Munoz FJ, Opazo C, Gil-Gomez G, Tapia G, Fernandez V, Valverde MA, Inestrosa NC (2002) Vitamin E but not 17beta-estradiol protects against vascular toxicity induced by beta-amyloid wild type and the Dutch amyloid variant. J Neurosci 22:3081-3089.

Murad F (1998) An activity in rat tissues that modifies nitrotyrosine-containing proteins. Proc Natl Acad Sci U S A 95:11584-11589.
Newman DK, Hoffman S, Kotamraju S, Zhao T, Wakim B, Kalyanaraman B, Newman PJ (2002) Nitration of PECAM-1 ITIM tyrosines abrogates phosphorylation and SHP-2 binding. Biochem Biophys Res Commun 296:1171-1179.

Nowicky AV, Bindman LJ (1993) The nitric oxide synthase inhibitor, N-monomethyl-L-arginine blocks induction of a long-term potentiation-like phenomenon in rat medial frontal cortical neurons in vitro. J Neurophysiol 70:1255-1259.

Ntais C, Polycarpou A (2005) Association of the endothelial nitric oxide synthase (NOS3) Glu298Asp gene polymorphism with the risk of Alzheimer's disease-- a meta-analysis. J Neurol 252:1276-1278.

Olah J, Orosz F, Keseru GM, Kovari Z, Kovacs J, Hollan S, Ovadi J (2002) Triosephosphate isomerase deficiency: a neurodegenerative misfolding disease. Biochem Soc Trans 30:30-38.

Olah J, Orosz F, Puskas LG, Hackler L, Jr., Horanyi M, Polgar L, Hollan S, Ovadi J (2005) Triosephosphate isomerase deficiency: consequences of an inherited mutation at mRNA, protein and metabolic levels. Biochem J 392:675-683.

Orosz F, Wagner G, Liliom K, Kovacs J, Baroti K, Horanyi M, Farkas T, Hollan S, Ovadi J (2000) Enhanced association of mutant triosephosphate isomerase to red cell membranes and to brain microtubules. Proc Natl Acad Sci U S A 97:1026-1031.

Ovadi J, Orosz F, Hollan S (2004) Functional aspects of cellular microcompartmentation in the development of neurodegeneration: mutation induced aberrant protein-protein associations. Mol Cell Biochem 256-257:83-93.

Paivio A, Nordling E, Kallberg Y, Thyberg J, Johansson J (2004) Stabilization of discordant helices in amyloid fibril-forming proteins. Protein Sci 13:1251-1259.

Paravastu AK, Petkova AT, Tycko R (2006) Polymorphic fibril formation by residues 10-40 of the Alzheimer's beta-amyloid peptide. Biophys J 90:4618-4629.

Pei JJ, Braak H, Gong CX, Grundke-Iqbal I, Iqbal K, Winblad B, Cowburn RF (2002) Up-regulation of cell division cycle (cdc) 2 kinase in neurons with early stage Alzheimer's disease neurofibrillary degeneration. Acta Neuropathol 104:369-376.

Peiretti F, Canault M, prez-Beauclair P, Berthet V, Bonardo B, Juhan-Vague I, Nalbone G (2003) Intracellular maturation and transport of tumor necrosis factor alpha converting enzyme. Exp Cell Res 285:278-285.

Peppa M, Uribarri J, Vlassara H (2008) Aging and glycoxidant stress. Hormones (Athens) 7:123-132.

Petkova AT, Leapman RD, Guo Z, Yau WM, Mattson MP, Tycko R (2005) Self-propagating, molecular-level polymorphism in Alzheimer's beta-amyloid fibrils. Science 307:262-265.

Pfeiffer S, Lass A, Schmidt K, Mayer B (2001) Protein tyrosine nitration in cytokine-activated murine macrophages. Involvement of a peroxidase/nitrite pathway rather than peroxynitrite. J Biol Chem 276:34051-34058.

Pinhel MA, Nakazone MA, Cacao JC, Piteri RC, Dantas RT, Godoy MF, Godoy MR, Tognola WA, Conforti-Froes ND, Souza D (2008) Glutathione S-transferase variants

increase susceptibility for late-onset Alzheimer's disease: association study and relationship with apolipoprotein E epsilon4 allele. Clin Chem Lab Med 46:439-445.
Poll-The BT, Aicardi J, Girot R, Rosa R (1985) Neurological findings in triosephosphate isomerase deficiency. Ann Neurol 17:439-443.

Pompliano DL, Peyman A, Knowles JR (1990) Stabilization of a reaction intermediate as a catalytic device: definition of the functional role of the flexible loop in triosephosphate isomerase. Biochemistry 29:3186-3194.

Prast H, Philippu A (2001) Nitric oxide as modulator of neuronal function. Prog Neurobiol 64:51-68.

Precious E, Gunn CE, Lyles GA (1988) Deamination of methylamine by semicarbazide-sensitive amine oxidase in human umbilical artery and rat aorta. Biochem Pharmacol 37:707-713.

Preuss U, Doring F, Illenberger S, Mandelkow EM (1995) Cell cycle-dependent phosphorylation and microtubule binding of tau protein stably transfected into Chinese hamster ovary cells. Mol Biol Cell 6:1397-1410.

Primakoff P, Myles DG (2000) The ADAM gene family: surface proteins with adhesion and protease activity. Trends Genet 16:83-87.

Puig B, Gomez-Isla T, Ribe E, Cuadrado M, Torrejon-Escribano B, Dalfo E, Ferrer I (2004) Expression of stress-activated kinases c-Jun N-terminal kinase (SAPK/JNK-P) and p38 kinase (p38-P), and tau hyperphosphorylation in neurites surrounding betaA plaques in APP Tg2576 mice. Neuropathol Appl Neurobiol 30:491-502.

Quinn J, Davis F, Woodward WR, Eckenstein F (2001) Beta-amyloid plaques induce neuritic dystrophy of nitric oxide-producing neurons in a transgenic mouse model of Alzheimer's disease. Exp Neurol 168:203-212.

Radtke-Schuller S (2001) Neuroarchitecture of the auditory cortex in the rufous horseshoe bat (Rhinolophus rouxi). Anat Embryol (Berl) 204:81-100.

Ralser M, Heeren G, Breitenbach M, Lehrach H, Krobitsch S (2006) Triose phosphate isomerase deficiency is caused by altered dimerization--not catalytic inactivity--of the mutant enzymes. PLoS ONE 1:e30.

Ramalho RM, Viana RJ, Castro RE, Steer CJ, Low WC, Rodrigues CM (2008) Apoptosis in transgenic mice expressing the P301L mutated form of human tau. Mol Med 14:309-317.

Reed TT, Pierce WM, Jr., Turner DM, Markesbery WR, Butterfield DA (2008) Proteomic identification of nitrated brain proteins in early Alzheimer's disease inferior parietal lobule. J Cell Mol Med.

Resende R, Moreira PI, Proenca T, Deshpande A, Busciglio J, Pereira C, Oliveira CR (2008) Brain oxidative stress in a triple-transgenic mouse model of Alzheimer disease. Free Radic Biol Med 44:2051-2057.

Reynolds MR, Berry RW, Binder LI (2005a) Site-specific nitration differentially influences tau assembly in vitro. Biochemistry 44:13997-14009.
Richardson JS (1993) Free radicals in the genesis of Alzheimer's disease. Ann N Y Acad Sci 695:73-76.

Rogaev EI, Sherrington R, Rogaeva EA, Levesque G, Ikeda M, Liang Y, Chi H, Lin C, Holman K, Tsuda T, . (1995) Familial Alzheimer's disease in kindreds with missense mutations in a gene on chromosome 1 related to the Alzheimer's disease type 3 gene. Nature 376:775-778.

Ryberg H, Soderling AS, Davidsson P, Blennow K, Caidahl K, Persson LI (2004) Cerebrospinal fluid levels of free 3-nitrotyrosine are not elevated in the majority of patients with amyotrophic lateral sclerosis or Alzheimer's disease. Neurochem Int 45:57-62.

Sahasrabudhe SR, Spruyt MA, Muenkel HA, Blume AJ, Vitek MP, Jacobsen JS (1992) Release of amino-terminal fragments from amyloid precursor protein reporter and mutated derivatives in cultured cells. J Biol Chem 267:25602-25608.

Sambamurti K, Kinsey R, Maloney B, Ge YW, Lahiri DK (2004) Gene structure and organization of the human beta-secretase (BACE) promoter. FASEB J 18:1034-1036.

Sampson JB, Ye Y, Rosen H, Beckman JS (1998) Myeloperoxidase and horseradish peroxidase catalyze tyrosine nitration in proteins from nitrite and hydrogen peroxide. Arch Biochem Biophys 356:207-213.

Sando SB, Melquist S, Cannon A, Hutton ML, Sletvold O, Saltvedt I, White LR, Lydersen S, Aasly JO (2008) APOE epsilon 4 lowers age at onset and is a high risk factor for Alzheimer's disease; a case control study from central Norway. BMC Neurol 8:9.

Sano M, Grossman H, Van DK (2008) Preventing Alzheimer's disease : separating fact from fiction. CNS Drugs 22:887-902.

Saran M, Michel C, Bors W (1990) Reaction of NO with O2-. implications for the action of endothelium-derived relaxing factor (EDRF). Free Radic Res Commun 10:221-226.

Sato T, Diehl TS, Narayanan S, Funamoto S, Ihara Y, De Strooper B, Steiner H, Haass C, Wolfe MS (2007) Active gamma-secretase complexes contain only one of each component. J Biol Chem 282:33985-33993.

Schneider A, Biernat J, von BM, Mandelkow E, Mandelkow EM (1999) Phosphorylation that detaches tau protein from microtubules (Ser262, Ser214) also protects it against aggregation into Alzheimer paired helical filaments. Biochemistry 38:3549-3558.

Schubert D, Behl C, Lesley R, Brack A, Dargusch R, Sagara Y, Kimura H (1995) Amyloid peptides are toxic via a common oxidative mechanism. Proc Natl Acad Sci U S A 92:1989-1993.

Selkoe DJ (2008) Soluble oligomers of the amyloid beta-protein impair synaptic plasticity and behavior. Behav Brain Res 192:106-113.

Sell DR, Lane MA, Johnson WA, Masoro EJ, Mock OB, Reiser KM, Fogarty JF, Cutler RG, Ingram DK, Roth GS, Monnier VM (1996) Longevity and the genetic determination of collagen glycoxidation kinetics in mammalian senescence. Proc Natl Acad Sci U S A 93:485-490.

Serpell LC, Blake CC, Fraser PE (2000) Molecular structure of a fibrillar Alzheimer's A beta fragment. Biochemistry 39:13269-13275.

Shankar GM, Li S, Mehta TH, Garcia-Munoz A, Shepardson NE, Smith I, Brett FM, Farrell MA, Rowan MJ, Lemere CA, Regan CM, Walsh DM, Sabatini BL, Selkoe DJ (2008) Amyloid-beta protein dimers isolated directly from Alzheimer's brains impair synaptic plasticity and memory. Nat Med 14:837-842.

Shelat PB, Chalimoniuk M, Wang JH, Strosznajder JB, Lee JC, Sun AY, Simonyi A, Sun GY (2008) Amyloid beta peptide and NMDA induce ROS from NADPH oxidase and AA release from cytosolic phospholipase A2 in cortical neurons. J Neurochem 106:45-55.

Sherrington R, Rogaev EI, Liang Y, Rogaeva EA, Levesque G, Ikeda M, Chi H, Lin C, Li G, Holman K, . (1995) Cloning of a gene bearing missense mutations in early-onset familial Alzheimer's disease. Nature 375:754-760.

Shi XP, Chen E, Yin KC, Na S, Garsky VM, Lai MT, Li YM, Platchek M, Register RB, Sardana MK, Tang MJ, Thiebeau J, Wood T, Shafer JA, Gardell SJ (2001) The pro domain of beta-secretase does not confer strict zymogen-like properties but does assist proper folding of the protease domain. J Biol Chem 276:10366-10373.

Shoffner JM (1997) Oxidative phosphorylation defects and Alzheimer's disease. Neurogenetics 1:13-19.

Shoji M, Kanai M, Matsubara E, Tomidokoro Y, Shizuka M, Ikeda Y, Ikeda M, Harigaya Y, Okamoto K, Hirai S (2001) The levels of cerebrospinal fluid Abeta40 and Abeta42(43) are regulated age-dependently. Neurobiol Aging 22:209-215.

Sibille N, Sillen A, Leroy A, Wieruszeski JM, Mulloy B, Landrieu I, Lippens G (2006) Structural impact of heparin binding to full-length Tau as studied by NMR spectroscopy. Biochemistry 45:12560-12572.

Simic G, Lucassen PJ, Krsnik Z, Kruslin B, Kostovic I, Winblad B, Bogdanovi (2000) nNOS expression in reactive astrocytes correlates with increased cell death related DNA damage in the hippocampus and entorhinal cortex in Alzheimer's disease. Exp Neurol 165:12-26.

Singh IN, Sullivan PG, Deng Y, Mbye LH, Hall ED (2006) Time course of post-traumatic mitochondrial oxidative damage and dysfunction in a mouse model of focal traumatic brain injury: implications for neuroprotective therapy. J Cereb Blood Flow Metab 26:1407-1418.

Sinha S, et al. (1999) Purification and cloning of amyloid precursor protein beta-secretase from human brain. Nature 402:537-540.

Sinha S, Lieberburg I (1999) Cellular mechanisms of beta-amyloid production and secretion. Proc Natl Acad Sci U S A 96:11049-11053.

Sisodia SS (1992) Beta-amyloid precursor protein cleavage by a membrane-bound protease. Proc Natl Acad Sci U S A 89:6075-6079.

Sisodia SS, Koo EH, Hoffman PN, Perry G, Price DL (1993) Identification and transport of full-length amyloid precursor proteins in rat peripheral nervous system. J Neurosci 13:3136-3142.

Slack BE, Ma LK, Seah CC (2001) Constitutive shedding of the amyloid precursor protein ectodomain is up-regulated by tumour necrosis factor-alpha converting enzyme. Biochem J 357:787-794.

Smallwood HS, Lourette NM, Boschek CB, Bigelow DJ, Smith RD, Pasa-Tolic L, Squier TC (2007) Identification of a denitrase activity against calmodulin in activated macrophages using high-field liquid chromatography--FTICR mass spectrometry. Biochemistry 46:10498-10505.

Smith DG, Cappai R, Barnham KJ (2007) The redox chemistry of the Alzheimer's disease amyloid beta peptide. Biochim Biophys Acta 1768:1976-1990.

Smith MA, Richey Harris PL, Sayre LM, Beckman JS, Perry G (1997) Widespread peroxynitrite-mediated damage in Alzheimer's disease. J Neurosci 17:2653-2657.

Sompol P, Ittarat W, Tangpong J, Chen Y, Doubinskaia I, Batinic-Haberle I, Abdul HM, Butterfield DA, St Clair DK (2008) A neuronal model of Alzheimer's disease: an insight into the mechanisms of oxidative stress-mediated mitochondrial injury. Neuroscience 153:120-130.

Song Y, Zweier JL, Xia Y (2001) Heat-shock protein 90 augments neuronal nitric oxide synthase activity by enhancing Ca2+/calmodulin binding. Biochem J 355:357-360.

Soto C, Branes MC, Alvarez J, Inestrosa NC (1994) Structural determinants of the Alzheimer's amyloid beta-peptide. J Neurochem 63:1191-1198.

Souza JM, Daikhin E, Yudkoff M, Raman CS, Ischiropoulos H (1999) Factors determining the selectivity of protein tyrosine nitration. Arch Biochem Biophys 371:169-178.

Stamler JS, Singel DJ, Loscalzo J (1992) Biochemistry of nitric oxide and its redox-activated forms. Science 258:1898-1902.

Stepanichev MY, Onufriev MV, Yakovlev AA, Khrenov AI, Peregud DI, Vorontsova ON, Lazareva NA, Gulyaeva NV (2008) Amyloid-beta (25-35) increases activity of neuronal NO-synthase in rat brain. Neurochem Int 52:1114-1124.

Tabaton M, Gambetti P (2006) Soluble amyloid-beta in the brain: the scarlet pimpernel. J Alzheimers Dis 9:127-132.

Tabaton M, Tamagno E (2007) The molecular link between beta- and gamma-secretase activity on the amyloid beta precursor protein. Cell Mol Life Sci 64:2211-2218.

Takeuchi M, Yamagishi S (2008) Possible involvement of advanced glycation end-products (AGEs) in the pathogenesis of Alzheimer's disease. Curr Pharm Des 14:973-978.

Tamagno E, Bardini P, Obbili A, Vitali A, Borghi R, Zaccheo D, Pronzato MA, Danni O, Smith MA, Perry G, Tabaton M (2002) Oxidative stress increases expression and activity of BACE in NT2 neurons. Neurobiol Dis 10:279-288.

Tellez LA, Blancas-Mejia LM, Carrillo-Nava E, Mendoza-Hernandez G, Cisneros DA, Fernandez-Velasco DA (2008) Thermal unfolding of triosephosphate isomerase from Entamoeba histolytica: dimer dissociation leads to extensive unfolding. Biochemistry 47:11665-11673.

Thomas DD, Espey MG, Vitek MP, Miranda KM, Wink DA (2002) Protein nitration is mediated by heme and free metals through Fenton-type chemistry: an alternative to the NO/O2- reaction. Proc Natl Acad Sci U S A 99:12691-12696.

Thornalley PJ (2003) Glyoxalase I--structure, function and a critical role in the enzymatic defence against glycation. Biochem Soc Trans 31:1343-1348.

Thorns V, Hansen L, Masliah E (1998) nNOS expressing neurons in the entorhinal cortex and hippocampus are affected in patients with Alzheimer's disease. Exp Neurol 150:14-20.

Tohgi H, Abe T, Yamazaki K, Murata T, Ishizaki E, Isobe C (1999) Alterations of 3-nitrotyrosine concentration in the cerebrospinal fluid during aging and in patients with Alzheimer's disease. Neurosci Lett 269:52-54.

Tong Y, Zhou W, Fung V, Christensen MA, Qing H, Sun X, Song W (2005) Oxidative stress potentiates BACE1 gene expression and Abeta generation. J Neural Transm 112:455-469.

Torok M, Milton S, Kayed R, Wu P, McIntire T, Glabe CG, Langen R (2002) Structural and dynamic features of Alzheimer's Abeta peptide in amyloid fibrils studied by site-directed spin labeling. J Biol Chem 277:40810-40815.

Trabace L, Kendrick KM (2000) Nitric oxide can differentially modulate striatal neurotransmitter concentrations via soluble guanylate cyclase and peroxynitrite formation. J Neurochem 75:1664-1674.

Tran MH, Yamada K, Nakajima A, Mizuno M, He J, Kamei H, Nabeshima T (2003) Tyrosine nitration of a synaptic protein synaptophysin contributes to amyloid beta-peptide-induced cholinergic dysfunction. Mol Psychiatry 8:407-412.

Tucek S, Ricny J, Dolezal V (1990) Advances in the biology of cholinergic neurons. Adv Neurol 51:109-115.

Unzeta M, Sole M, Boada M, Hernandez M (2007) Semicarbazide-sensitive amine oxidase (SSAO) and its possible contribution to vascular damage in Alzheimer's disease. J Neural Transm 114:857-862.

Vadseth C, Souza JM, Thomson L, Seagraves A, Nagaswami C, Scheiner T, Torbet J, Vilaire G, Bennett JS, Murciano JC, Muzykantov V, Penn MS, Hazen SL, Weisel JW, Ischiropoulos H (2004) Pro-thrombotic state induced by post-translational modification of fibrinogen by reactive nitrogen species. J Biol Chem 279:8820-8826.

Van der Vliet, V, Eiserich JP, Halliwell B, Cross CE (1997) Formation of reactive nitrogen species during peroxidase-catalyzed oxidation of nitrite. A potential additional mechanism of nitric oxide-dependent toxicity. J Biol Chem 272:7617-7625.

Vasan S, Foiles P, Founds H (2003) Therapeutic potential of breakers of advanced glycation end product-protein crosslinks. Arch Biochem Biophys 419:89-96.

Vassar R, et al. (1999) Beta-secretase cleavage of Alzheimer's amyloid precursor protein by the transmembrane aspartic protease BACE. Science 286:735-741.

Vetrivel KS, Zhang YW, Xu H, Thinakaran G (2006) Pathological and physiological functions of presenilins. Mol Neurodegener 1:4.

Vitek MP, Bhattacharya K, Glendening JM, Stopa E, Vlassara H, Bucala R, Manogue K, Cerami A (1994) Advanced glycation end products contribute to amyloidosis in Alzheimer disease. Proc Natl Acad Sci U S A 91:4766-4770.

Wakabayashi T, De Stooper B (2008) Presenilins: members of the gamma-secretase quartets, but part-time soloists too. Physiology (Bethesda) 23:194-204.

Wang B, Tan S, Yang Z, Xie YC, Wang J, Zhou S, Li S, Zheng C, Ma X (2008) Association between Alzheimer's disease and the NOS3 gene Glu298Asp polymorphism in Chinese. J Mol Neurosci 34:173-176.

Wang Y, Ha Y (2004) The X-ray structure of an antiparallel dimer of the human amyloid precursor protein E2 domain. Mol Cell 15:343-353.

Ward RV, Jennings KH, Jepras R, Neville W, Owen DE, Hawkins J, Christie G, Davis JB, George A, Karran EH, Howlett DR (2000) Fractionation and characterization of oligomeric, protofibrillar and fibrillar forms of beta-amyloid peptide. Biochem J 348 Pt 1:137-144.

Weinshenker D (2008) Functional consequences of locus coeruleus degeneration in Alzheimer's disease. Curr Alzheimer Res 5:342-345.

Weldon DT, Rogers SD, Ghilardi JR, Finke MP, Cleary JP, O'Hare E, Esler WP, Maggio JE, Mantyh PW (1998) Fibrillar beta-amyloid induces microglial phagocytosis, expression of inducible nitric oxide synthase, and loss of a select population of neurons in the rat CNS in vivo. J Neurosci 18:2161-2173.

Weskamp G, Cai H, Brodie TA, Higashyama S, Manova K, Ludwig T, Blobel CP (2002) Mice lacking the metalloprotease-disintegrin MDC9 (ADAM9) have no evident major abnormalities during development or adult life. Mol Cell Biol 22:1537-1544.

Whiteman M, Ketsawatsakul U, Halliwell B (2002) A reassessment of the peroxynitrite scavenging activity of uric acid. Ann N Y Acad Sci 962:242-259.

Wiener HW, Perry RT, Chen Z, Harrell LE, Go RC (2007) A polymorphism in SOD2 is associated with development of Alzheimer's disease. Genes Brain Behav 6:770-775.
Wiesinger H (2001) Arginine metabolism and the synthesis of nitric oxide in the nervous system. Prog Neurobiol 64:365-391.

Wilkinson BL, Landreth GE (2006) The microglial NADPH oxidase complex as a source of oxidative stress in Alzheimer's disease. J Neuroinflammation 3:30.
Wolfe MS, Xia W, Ostaszewski BL, Diehl TS, Kimberly WT, Selkoe DJ (1999) Two transmembrane aspartates in presenilin-1 required for presenilin endoproteolysis and gamma-secretase activity. Nature 398:513-517.

Wolfe MS, Xia W, Ostaszewski BL, Diehl TS, Kimberly WT, Selkoe DJ (1999) Two transmembrane aspartates in presenilin-1 required for presenilin endoproteolysis and gamma-secretase activity. Nature 398:513-517.

Wrigley JD, Nunn EJ, Nyabi O, Clarke EE, Hunt P, Nadin A, De Strooper B, Shearman MS, Beher D (2004) Conserved residues within the putative active site of gamma-secretase differentially influence enzyme activity and inhibitor binding. J Neurochem 90:1312-1320.

Wu G, Morris SM, Jr. (1998) Arginine metabolism: nitric oxide and beyond. Biochem J 336 (Pt 1):1-17.

Wu J, Basha MR, Zawia NH (2008) The environment, epigenetics and amyloidogenesis. J Mol Neurosci 34:1-7.

Xia W, Zhang J, Ostaszewski BL, Kimberly WT, Seubert P, Koo EH, Shen J, Selkoe DJ (1998) Presenilin 1 regulates the processing of beta-amyloid precursor protein C-terminal fragments and the generation of amyloid beta-protein in endoplasmic reticulum and Golgi. Biochemistry 37:16465-16471.

Yamamoto T, Shimoyama N, Mizuguchi T (1993) Nitric oxide synthase inhibitor blocks spinal sensitization induced by formalin injection into the rat paw. Anesth Analg 77:886-890.

Yan SD, Chen X, Schmidt AM, Brett J, Godman G, Zou YS, Scott CW, Caputo C, Frappier T, Smith MA, . (1994) Glycated tau protein in Alzheimer disease: a mechanism for induction of oxidant stress. Proc Natl Acad Sci U S A 91:7787-7791.

Zekry D, Epperson TK, Krause KH (2003) A role for NOX NADPH oxidases in Alzheimer's disease and other types of dementia? IUBMB Life 55:307-313.

Zhang X (2004) Cholinergic activity and amyloid precursor protein processing in aging and Alzheimer's disease. Curr Drug Targets CNS Neurol Disord 3:137-152.

Zhang YJ, Xu YF, Chen XQ, Wang XC, Wang JZ (2005) Nitration and oligomerization of tau induced by peroxynitrite inhibit its microtubule-binding activity. FEBS Lett 579:2421-2427.

Zhang YJ, Xu YF, Liu YH, Yin J, Li HL, Wang Q, Wang JZ (2006) Peroxynitrite induces Alzheimer-like tau modifications and accumulation in rat brain and its underlying mechanisms. FASEB J 20:1431-1442.

Zhuo JM, Prakasam A, Murray ME, Zhang HY, Baxter MG, Sambamurti K, Nicolle MM (2008) An increase in Abeta42 in the prefrontal cortex is associated with a reversal-learning impairment in Alzheimer's disease model Tg2576 APPsw mice. Curr Alzheimer Res 5:385-391.

VII. APPENDIX

Appendix I

“Protein nitrotyrosination in Alzheimer’s Disease”

Francesc X. Guix, Mireia Coma, Gerard Ill-Raga

and Francisco J. Muñoz

Guix FX, Coma M, Ill-Raga G, Muñoz FJ.
Protein Nitrtyrosination in Alzheimer's disease.
In Von Bernhardi R, Inestrosa NC, editors.
Neurodegenerative Diseases: From Molecular Concepts to Therapeutic Targets. Hauppauge NY:
Nova Science Publishers, inc; 2008. p.133-43.

Appendix II

“The physiology and pathophysiology of nitric oxide in the brain”

F.X. Guix, I. Uribesalgo, M. Coma, F.J. Muñoz

Guix FX, Uribesalgo I, Coma M, Muñoz FJ.
The physiology and pathophysiology of nitric oxide in the brain.
Prog Neurobiol. 2005 Jun;76(2):126-52.

Appendix III

“Oxidative stress triggers the amyloidogenic pathway in human vascular smooth muscle cells”

Mireia Coma, Francesc X. Guix, Gerard Ill-Raga, Iris Uribesalgo, Francesc Alameda, Miguel A. Valverde, Francisco J. Muñoz

Coma M, Guix FX, Ill-Raga G, Uribesalgo I, Alameda F, Valverde MA, Muñoz FJ.
Oxidative stress triggers the amyloidogenic pathway in human vascular smooth muscle cells.
Neurobiol Aging. 2008 Jul;29(7):969-80. Epub 2007 Feb 15.

Appendix IV

“Lack of oestrogen protection in amyloid mediated endothelial damage due to protein nitrotyrosination”

M. Coma, F. X. Guix, I. Uribesalgo, G. Espuña, M. Solé, D. Andreu

and F. J. Muñoz

Coma M, Guix FX, Uribesalgo I, Espuña G, Solé M, Andreu D, Muñoz FJ.
Lack of oestrogen protection in amyloid-mediated endothelial damage due to protein nitrotyrosination.
Brain. 2005 Jul;128(Pt 7):1613-21. Epub 2005 Apr 7.